Technical Report 214

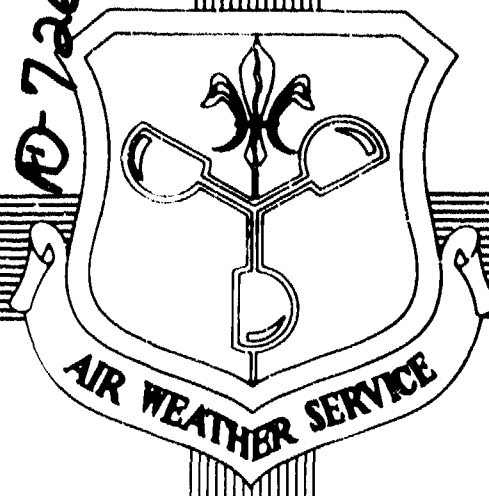

GUIDE TO LOCAL DIFFUSION OF AIR POLLUTANTS

By
Gordon A. Beals, Maj USAF
USAF ETAC

Approved For Public Release;
Distribution Unlimited

PUBLISHED BY
AIR WEATHER SERVICE (MAC)
UNITED STATES AIR FORCE
SCOTT AFB, ILLINOIS
MAY 1971

PREFACE

One of the most pressing problems of Air Force installation planners in the 1970's is minimizing environmental pollution. Air Weather Service personnel can give valuable assistance to these planners by providing realistic estimates of atmospheric diffusion. This Technical Report has been prepared as an aid to making diffusion estimates. The scope of this report is limited to calculating pollution concentrations from on-base sources.

GORDON A. BEALS, Major, USAF
Chief Scientist
USAF Environmental Technical Applications Center
Washington, D. C.
30 April 1971

TABLE OF CONTENTS

LIST OF ILLUSTRATIONS

LIST OF TABLES

Chapter 1

INTRODUCTION

1. General.

Air pollution is not a new phenomenon and has been the concern of many notable individuals and scientists for years. Nevertheless, air pollution, along with water pollution, has suddenly become a subject of national importance. In the last few years several Presidential Executive Orders have been issued with the aim of reducing sources of air pollution at Federal installations. Thus, the Air Force is deeply concerned with reducing air pollution around their installations and has embodied this concern in AFR 161-22. Provisions of this regulation task Air Weather Service with providing meteorological support to air-pollution control and abatement personnel. As a consequence, detachment commanders and staff weather officers can expect an increasing number of inquiries from civil engineering and environmental health personnel about the meteorological aspects of air pollution. Intense interest in air pollution, however, is not limited to these two activities only. All aspects of operations and training within the Air Force must operate with an awareness of the pollution problem. For example, Headquarters USAF has recently instructed the major air commands to conduct fire-fighting training during periods of good atmospheric dispersion.

Historically, military interests in atmospheric dispersion dates back to the use of toxic gases in World War I. Much of the early work on atmospheric dispersion was conducted by British scientists in connection with chemical warfare research. Later American researchers also recognized the importance of such investigations. The emphasis placed by Air Weather Service on atmospheric dispersion began in earnest with the recognition that liquid fuels for Titan missiles were toxic and that a potential safety hazard existed with respect to storage and transfer of these potentially dangerous fuels. The assistance required of Air Weather Service personnel by the operational aspects of the Titan missile complexes intensified the research for knowledge of dispersion within the free atmosphere next to the earth's surface.

In order to ably fulfill their new responsibilities as advisors to the anti-pollution effort, AWS forecasters, and especially DETCOs and STAFFMETS, should become familiar with the natural processes that control the dispersion of contaminants. This technical report is intended to give the field forecaster an appreciation of atmospheric dispersion processes and practical methods for assessing the ability of the air to dilute and carry away contaminants. A comprehension of such processes entails a knowledge of the very lower layers of

the atmosphere.

2. Various Scales of Air Pollution.

There are three broad scales of air pollution which can be defined on the basis of geographical extent and degree of dependence on local meteorological conditions. In order of decreasing geographical scale, they are global pollution, area pollution, and local pollution.

a. Global Air Pollution. On this scale, while local effects are of little importance, the general circulation imposes some restriction on the ultimate spread of pollutants. The principal factors controlling the concentration of pollutants on this scale are the rate at which the pollutants are being introduced into the atmosphere worldwide and the "residence time," i.e., the length of time it takes for a pollutant to settle out as particles, be washed out by precipitation, to diffuse upward and eventually into space, or to be converted through some chemical process into an invisible, harmless gas.

b. Area Pollution. A second scale of air pollution is typified by the Los Angeles "smog" problem. Here, existing meteorological conditions combined with unique terrain features act to confine the pollutants in a localized region. The meteorological parameters of importance on this scale are dealt with routinely in forecasting, viz., wind speed and temperature inversions. Again, as on the global scale, the details of diffusion from individual sources are not too important. This is the type and scale of air pollution considered in the air pollution potential forecasts that are relayed to AWS detachments in the continental United States on the communication circuits.

c. Local Pollution. On the smallest scale the concentration of pollutants mostly depends on the details of the processes of atmospheric diffusion. An example of this type of pollution is the zone of acrid fumes that often exists downwind from pulp mills. This type of local phenomenon could also be contributing to both of the other scales of air pollution but at levels that would not be readily noticed. An air pollution source on the local scale is usually considered serious only if it produces concentrations of contaminants that exceed certain limits within populated areas. However, as will be explained in the next section, the limits on concentration apply to the total concentration, i.e., the sum of all local and area sources.

3. Air Pollution Limits and the Concept of Air Quality.

Most of the state and local air pollution laws express their limits in terms of parts of contaminant per million parts of contaminated air at 1013-mb pressure and 25°C. The general concept of enforcement is to evaluate the concentration at the downwind property line. In general, this concentration will be the sum of the local pollution introduced at the installation (diluted in the distance from release point to the property line), plus whatever pollution is present in the area due to other sources. This residual pollution from other

sources is known as the background level.

It should be apparent now that the background pollution level is as important as the local diffusion characteristics in determining and controlling the amount of pollutants that can safely be emitted. When the background is high, only a small amount of pollutant can be released before a critical condition is reached, even if diffusion conditions are locally good.

Air-quality standards fall into two general types — long term and short term. The long-term limits apply to average concentrations measured over periods of several hours to a month. Short-term limits, which apply to situations lasting an hour or less, have not yet been adopted. However, the Environmental Protection Agency will begin issuing short-term guidelines in 1971. State and local agencies can be expected to adopt short-term limits very soon thereafter.

Air Weather Service personnel normally would not become involved in setting air-quality standards. However, it is within the framework of these standards or limits that the staff meteorologist must make his pollution forecasts. The situation is very similar to setting critical crosswind components for aircraft landings. Two similarities are apparent. First, the limits are different for each pollutant just as different crosswind components apply to each aircraft type. Second, the setting of the pollution limits is a subjective process in which medical or industrial hygiene personnel evaluate past data on exposures to pollutants just as flying safety personnel use their judgment and the accumulated data on accidents to set critical crosswinds. In both cases, the operational impact may be considered in balancing the requirements of health and safety against the requirements of mission accomplishment. However, in the case of air pollution, the balance must be made at a higher level of government since the health and safety of the general public, not just military personnel and equipment, are involved.

4. The Relationship Between Meteorology and the Concentration of Air Pollutants.

Meteorology and air pollution have a direct relationship. The occurrence of air pollution in any degree depends on the presence or absence of dilution and diffusion processes. In the free atmosphere, both of these processes depend almost entirely on familiar meteorological parameters, viz., turbulence, wind, temperature, precipitation, atmospheric stability, inversions, etc. This relationship can best be illustrated by two examples. For instance, consider the warning found on the containers of many kinds of cleaning fluids or solvents: "Caution — Avoid excessive breathing of fumes. Use only in a well-ventilated place." Why is the ventilated place less dangerous than a closed room? The reason is the presence of the dilution process. The ventilated area allows fresh air to mix with and dilute the toxic fumes of the cleaning fluid so that the remaining concentration is not harmful. The property of dilution is economically one of the most useful properties of the atmosphere. In our daily living countless tons of waste products annually are disposed of simply by

discharging the material into the atmosphere and letting the winds carry it away. As the waste material is transported, it is also mixed through larger and larger volumes of air by the action of turbulent eddies with the concentration becoming weaker and weaker. This is an example of the way in which the natural environment makes the handling of toxic chemicals safer.

A second example, however, shows how these same atmospheric processes, previously shown to be so advantageous, can make other situations more dangerous. Suppose a railroad tank-car full of chlorine is derailed and ruptures. Police and Civil Defense officials rush to evacuate people from the area immediately downwind from the wreck. Why? Because the wind will carry the deadly chlorine fumes from the spot of the accident to other places as much as several miles away. With insufficient diffusion this brings danger where none previously existed. Suppose the air were absolutely still. With no wind there would be no spread of dangerous fumes except by the comparatively slow process of molecular diffusion and thus no other area would be dangerously contaminated by the chlorine.

In every real situation, the good and the bad are both represented. For, as in the example of the last paragraph, the same moving atmosphere that created a danger by transporting the chlorine also helps reduce the danger by diluting the concentration of the gas as it moves. The essence of the relationship between the atmosphere and the release of toxic substances can be found in the following question. Will the mixing action of the atmosphere dilute the material to a tolerable level fast enough to keep the spread from being a danger? This question is indeed a challenging one because the cleansing efficiency of the atmosphere varies from place-to-place, day-to-day, or even hour-to-hour.

The same principles apply to nontoxic air pollution. That is, the winds carry pollution from the source to other places while diluting it along the way.

Chapter 2

FUNDAMENTALS OF MICROMETEOROLOGY

1. General.

The term micrometeorology is used in this report in its broadest sense; that is, as the meteorology of the layer from the earth's surface to an altitude where the effects of the immediate underlying surface on the temperature and motion of the atmosphere become negligible. This definition of micrometeorology includes a considerable portion of what is often considered as mesometeorology.

Most Air Weather Service meteorologists have received the bulk of their meteorology experience as synoptic meteorologists. As such, they were trained to ignore or "filter out" of their analyses any local irregularities that existed on a scale of less than 50 miles or so, except for incorporating local effects in terminal forecasts. This "filtering" is quite appropriate for depicting the general state of the weather and for predicting those aspects of weather that change according to the movement of major pressure systems. On the other hand, the air motions that affect the transport and diffusion of air pollutants are much more local and depend on atmospheric conditions a few hundred feet in vertical extent and hundreds of yards to a few miles in the horizontal. When one is considering the transport and dilution of pollutants, the most important variables are wind direction and temperature lapse rate. In that near-ground layer both the temperature lapse rate and the air movements exhibit characteristic variations from day to night and from season to season. Furthermore, small-scale differences in the temperature and wind fields can be attributed to local irregularities in the underlying terrain. This chapter will review the physical basis for the normal variation of wind and temperature near the ground.

2. The Physical Basis of Meteorological Variation Near the Ground.

Over level terrain, both the normal diurnal variation and the local irregularities of the temperature and wind fields can be explained primarily in terms of the response of the underlying surface to incoming solar radiation by day and outgoing infrared radiation at night.

a. The Balance of Energy at the Surface. The balance of energy at the earth's surface in the daytime is roughly shown in Figure 1a. The wide arrow labeled "net incoming solar radiation" is the resultant of all radiation processes (absorption, reflection, reradiation) acting at the ground surface. About half of the net incoming radiant energy is conducted downward into the ground during the morning as the ground warms. This point will be elaborated later. The remaining half of the energy is split between evaporation and upward heat transport. The relative magnitudes of these two processes depends mostly on the

moisture available for evaporation.

The energy flow at the surface during the nighttime is depicted in Figure 1b. At night, heat flows from the ground to supply much of the energy that is lost from the ground surface as effective outgoing radiation. The relative magnitudes of the heat flows are roughly indicated by the width of the arrows, which are also scaled to show magnitudes as compared with Figure 1a. The main difference between day and night energy transfer is that heat flows into the ground and into the lowest layers of the air by day and the flow is reversed by night. These flow directions result in substantial changes from day to night in the temperature of the ground surface and the air layer nearest it. The amount of temperature change depends on the physical characteristics of the underlying surface and on the operation of all three modes of heat transfer within the atmosphere.

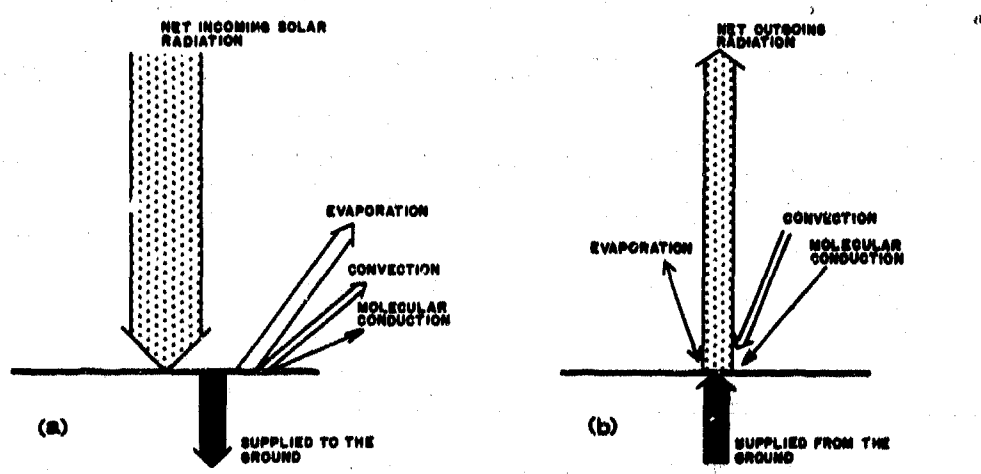

Figure 1. Energy Balance at the Ground
(a) Middle of the Day, (b) At Night.

b. Physical Characteristics Affecting the Response of the Underlying Surface. One factor affecting the energy balance at the ground surface is the albedo, or reflectivity, of the underlying surface. Those surfaces with low albedo will absorb more of the incoming solar radiation. For example, the high midday temperature of a black-top road (low albedo) compared to a nearby field (higher albedo) is primarily due to this albedo difference. However, the albedo is not too often the controlling parameter. Concrete pavement even with its higher albedo will often become hotter than black-top. In this case the difference is found primarily in the heat conductivity and the heat capacity (the amount of heat required to raise the temperature of a substance) per unit volume of the particular surface. The heat capacity per unit volume is the product of specific heat and density. If the density and specific heat of the

underlying surface are large, a great amount of energy must be absorbed or given off at the surface in order to change the temperature appreciably. If the heat conductivity of the surface is high, the heat energy will flow rapidly into or out of the ground. This rapid heat flow will result in a small temperature change occurring over a large depth, while a low heat conductivity would result in large temperature changes through a shallow depth.

c. Physical Processes Affecting the Response of the Air Layer Near the Ground. We learn in elementary physics courses that there are three processes that transfer heat: radiation, conduction, and convection. The first two have already been mentioned in connection with the variation of the ground temperature. Both radiation and conduction contribute to heat transfer in the atmosphere, but, except for a very thin layer next to the ground, both of these processes are less effective for heat interchange than convection in its broadest sense. In this instance, convection means transport of heat due to any motion of fluid particles other than molecular. Thus, convection includes stirring and mixing by all causes as well as thermally-forced convection, which we associate with dust devils or cumulus clouds. The total heat transferred to or from the ground surface by all of these processes acting in the air is less than the heat transferred by any one of the various processes affecting the temperature of the ground. Therefore, heat transfer within the atmosphere has only a minor influence on the range of temperature at the ground or the temperature of the air immediately next to the ground. Instead, heat transfer within the atmosphere determines how deep a layer will respond to changes of ground temperature and the speed of that response. As an extreme case, if there were no heat transfer of any kind in the air, the air molecules right next to the ground would acquire the temperature of the ground and the temperature of the rest of the atmosphere would not change. In reality, there is considerable heat transport, enough that at least several hundred feet of the atmosphere experiences a very noticeable change of temperature from day to night. In the middle of the day and late at night, when the air and ground temperatures are changing only slowly, the temperature gradients will be inversely proportional to the effectiveness of the heat transfer.

As noted, the principal mode of heat transfer in the atmospheric surface layer is turbulent mixing. The term "turbulent," as used here, refers only to the randomness of the motions and does not imply the violent motion that a forecaster normally visualizes when he considers aircraft-type turbulence. Random motions of the air are present nearly everywhere. The curling, irregular wisp of smoke from a cigarette testifies to the presence of some turbulence even indoors. As gentle as the random mixing may be, however, it is still 10 to 100 times more efficient in transferring heat than is molecular conduction. Outdoors, where the mixing is more vigorous, turbulent transfer is 100 to 100,000 times more efficient. The intensity of the mixing depends on the speed of the wind, the roughness of the terrain, and the vertical gradient of temperature.

The effect of the temperature lapse rate depends on whether it is greater or less than the adiabatic lapse rate. If the lapse rate is stable, energy will be consumed in turbulent mixing, while an unstable atmosphere will feed energy into the turbulent motions. This characteristic gives the atmosphere a preferred direction of heat flow – upward. If the atmosphere is extremely unstable, the intensity of turbulence is great and a large amount of heat is transferred, which, in turn, tends to reduce the lapse rate. On the other hand, the sharper the nocturnal inversion the weaker is the mixing action, tending to intensify the inversion when radiation processes more than offset the weak mixing.

3. Local Temperature Structure.

The preceding discussion provides a basis for understanding both the normal variations of temperature near the earth's surface and the differences that arise because of the inhomogenieties of that surface.

a. Diurnal and Annual Variations. Figure 2 shows the daily cycle of temperature at three different heights over a desert area for summer and winter. The difference between the amplitude of the January and July temperature curves show the specific effect of solar radiation on the ground temperature. The influence of cloud cover on the daily range of temperature is depicted in Figure 3. Both figures clearly show that the ground temperature responds to the incoming and outgoing radiation and that the air temperature follows the ground

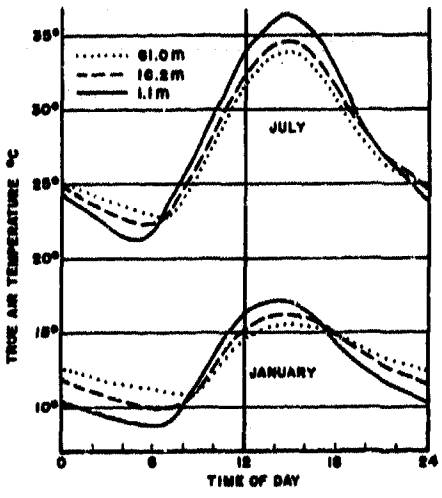

Figure 2. The Daily Cycle of Temperature at Three Heights (from R. Geiger, The Climate Near the Ground, Figure 32, Harvard University Press, Cambridge, Mass. 1950).

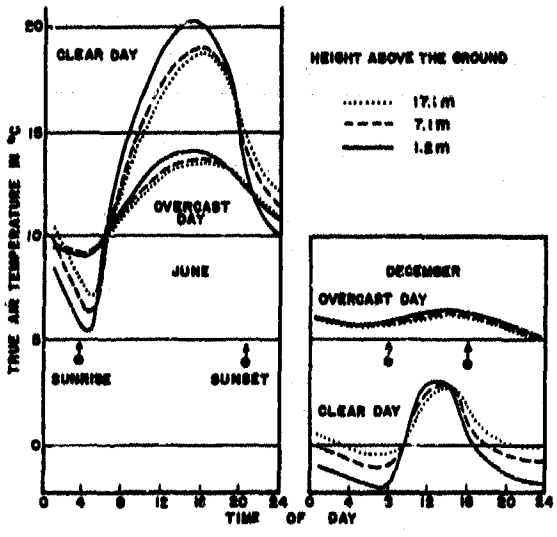

Figure 3. The Dependence of the Diurnal Temperature Range on Cloudiness (from R. Geiger, The Climate Near the Ground, Figure 36, Harvard University Press, Cambridge, Mass. 1950).

temperature. The diurnal range of temperature is smaller as the distance from the ground increases. Needless to say, these patterns are familiar to the practicing meteorologist in the weather station. However, it is important to be not only aware of the general behavior of the temperature at a given level, but to understand the physical basis for the variation and its implications on the variation of the temperature gradient, which is the most important single atmospheric variable affecting the dilution of air pollution.

Typical vertical temperature profiles of a land station of the mid-latitudes are shown for specific hours in Figure 4. The diurnal variation of the all-important temperature gradient is illustrated by Figure 5. The three sections of this figure also include the effect of cloudiness at three wind-speed ranges. The seasonal variation of lapse rates at a southern Idaho station is presented in Figure 6, showing the temperature difference between heights of 1.5 and 120 meters. Predictably, the steepest lapse rates occur in the middle of the day in summer. The maximum average inversions also occur in the summer months. This might seem surprising, but it is a direct consequence of the greater diurnal range of ground temperature which occurs in the summer. The wintertime inversions are more persistent than those of the summer, frequently lasting for days,

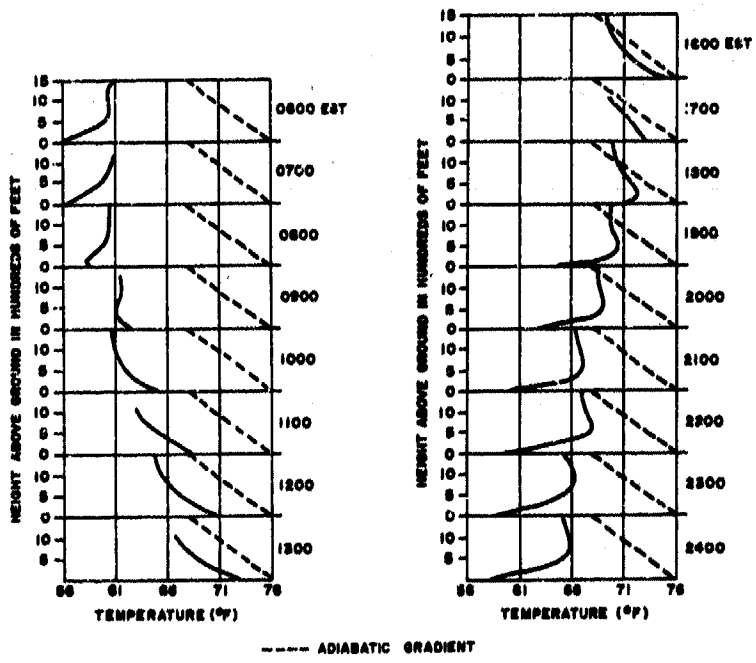

Figure 4. Typical Profiles of Temperature in the Lowest 1500 Feet for Various Times of Day (from Holland [12]).

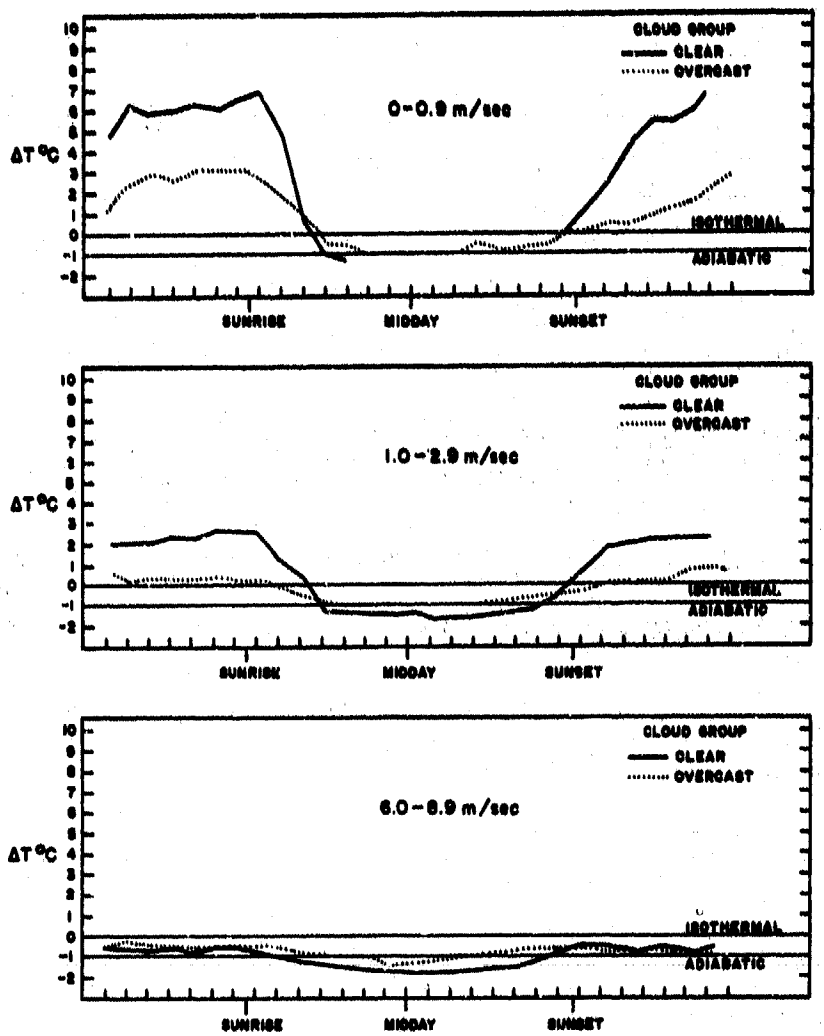

Figure 5. Diurnal Variation of Temperature Difference Between 11 m and 110 m for Different Cloudiness and Wind Speed [19].

but their average intensity is less. Because of the effect of the lapse rate on eddy conduction of heat, it is the prolonged slight inversions associated with strong winds in winter that actually result in the greatest downward net transport of heat in the atmosphere near the ground.

b. The Influence of the Underlying Surface. So far we have discussed the features of the temperature pattern that would be present over flat, uniform terrain. In paragraph 2.b, we discussed factors that would influence the response of the ground layer to the radiation balance. Because turbulent mixing in the atmosphere is so dependent on the local temperature gradient, we must now examine the effects on the local temperature structure produced by variations in the response of the underlying surface. We will consider specifically the effects of soil type, including snow cover as a special case, and the markedly

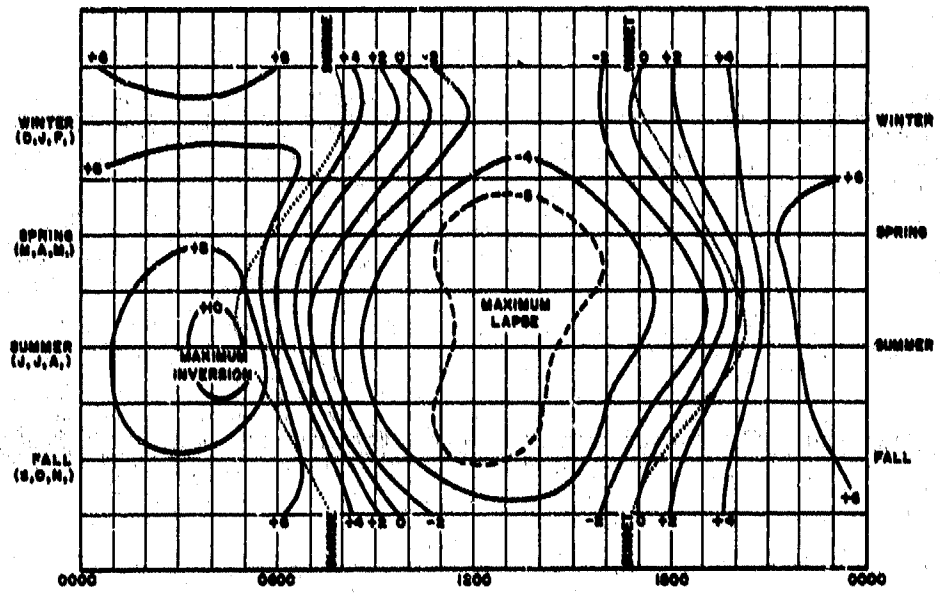

Figure 6. Seasonal Variation in the Vertical Temperature Difference Between 1.5 m and 120 m (southern Idaho) [5].

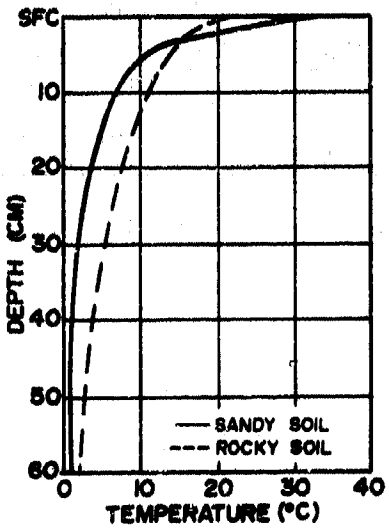

Figure 7. Diurnal Range of Temperature in Scandinavian Summer for Two Kinds of Ground.

different response properties of bodies of water.

The most important differences in the underlying surface are its density and heat conductivity. The way these properties influence the ground temperature is illustrated in Figure 7. The solid curves show the diurnal variation of temperature in a dry, sandy soil. The density and thermal conductivity of this type of soil are both low because the "dead air" trapped in spaces between the grains of sand reduces both of these properties. The dotted curves show the temperature range expected for a densely-packed, rocky soil. The heat penetrates farther into this denser type of soil so that the range of temperature at the surface is smaller. The dampness of the ground surface also influences the thermal properties considerably. If water is trapped within the spaces instead of "dead air," conductivity, density, and specific heat are all increased.

The low temperatures experienced at night over a snow surface are well-known. They occur because the snow, especially if it is fresh, has a much lower

density and conductivity than any type of bare soil. The most extreme inversions in the lower atmosphere in winter are, therefore, found over snow cover. The ability of a snow cover to reject the heating effect of the sun's rays in the daytime is generally overrated. A moment's reflection will bring to mind the fact that, barring unusually strong cold advection, there is a substantial rise of temperature on clear days even when there is a complete cover of fresh snow. This rise is due to the fact that some 10 or 15% of the incoming solar radiation does penetrate into the top few inches of the snow cover and thereby is able to warm the top layers noticeably because of the previously-mentioned low density and conductivity of the snow cover. The effect of a snow cover may then be summarized as follows. At night, a snow cover produces extreme inversions. By day, a snow cover reduces, but does not completely eliminate, the superadiabatic lapse rate that normally occurs near the ground.

Snow cover represents something near the extreme condition of low conductivity. Open bodies of water represent the opposite extreme. The one property of water that distinguishes it most from solid surfaces is that water, being a fluid, can transfer heat in the convective mode, which is usually much more efficient than heat transfer in solids. Any body of water that is more than a puddle will have currents set up in it by the stress of the wind and these currents result in very effective mixing so that any temperature changes occurring are distributed through a deep layer. Of secondary importance, but still significant, is the fact that incoming radiation from the sun penetrates into a fairly deep layer of water instead of all being absorbed at the surface. These two differences result in smaller seasonal and much smaller diurnal changes of the air temperature at the surface over water than over land. The result is that over water bodies there is very little diurnal air temperature change unless it is caused by advection from a nearby land area. Over an inland body of unfrozen water, the temperature gradients are the opposite of the patterns shown in Figure 6; the most unstable periods are at night during the winter and the most stable, by day in summer.

c. The Influence of Topography on Temperature. There are two main types of topographic effects on air temperature and lapse rates. The first is due simply to differences in elevation and the second due to differences in the slope of the ground surface.

Considering the second type first, the fact that the ground is sloping changes the hour of the day at which the ground surface is most nearly perpendicular to the sun's rays and, thus, the time of maximum temperature and maximum lapse rate. For example, the west side of a valley will warm and also cool earlier than the east side since the sun travels from east to west. Similarly, in the mid-latitudes a valley that opens toward the south will generally have a better-developed thermal wind system by day than one that opens toward the north.

The diurnal range of temperature at the floor of a valley is larger than on

its sloping sides. This is not particularly surprising since frequently superadiabatic lapse rates prevail by day and inversions by night. However, the situation is not quite that simple. The fact that the ground is not level means that, at a fixed level, the air closer to the sides of the valley cools more at night than the air above the middle of the valley floor. This establishes a pressure gradient which causes the air to flow down the slopes toward the valley floor. This air movement as a type of wind, will be discussed later; however, its effect on the temperature is to cause the whole valley to fill with cold air. Thus, the temperature inversion at the floor of the valley is not nearly as intense as are those on an open plain. On the other hand, the inversion near the top of the valley is steeper than it would be if this drainage flow was not present. The resulting distribution of temperature in this situation is shown in Figure 8. Even with the valley circulation effect, however, the changes caused by the proximity to the ground surface are not completely masked. The nighttime and daytime isotherm patterns are very similar but, by day, the warmer air is on the valley floor.

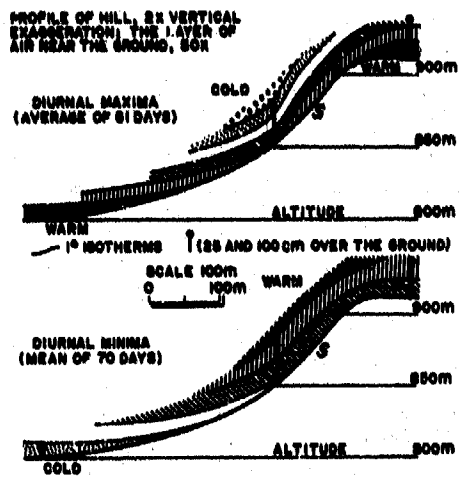

Figure 8. Patterns of Temperature on a Hillside (from R. Geiger, The Climate Near the Ground, Figure 110, Harvard University Press, Cambridge, Mass. 1950)

4. Local Wind Structure:

a. The Mean Vertical Variation of the Horizontal Wind Speed. It is readily noted that the wind speed one foot or less above the ground is quite a bit weaker than the wind at the same time near shoulder height. This decrease of the wind speed near the ground is, of course, a direct consequence of frictional drag of the atmosphere against the earth's surface. Well above the surface, the steady-state wind speed is determined by the balance of pressure forces and the Coriolis force. The level above which the friction of the ground no longer influences the wind speed in direction is usually termed the "gradient wind level." At heights between the ground and the gradient wind level, the vertical distribution of wind speed is determined by the action of molecular viscosity at the ground level and by "eddy viscosity" at higher levels in a manner completely analogous to the way the distribution of temperature is controlled by the three processes of heat transfer.

The diurnal pattern of wind speed is controlled largely by the effect of temperature gradient on the intensity of turbulent mixing and, hence, on the "eddy viscosity." During the day, buoyancy effects greatly enhance the turbulent mixing with height so the gradient of the wind speed is rapidly reduced to

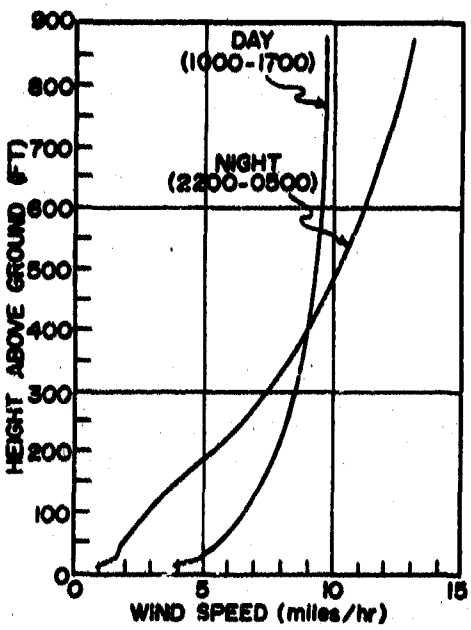

Figure 9. Average Wind-Speed Profiles Constructed from Measurements Made During a 1-Year Period at the Oak Ridge National Laboratory [12].

a small value. At night the effect of buoyancy tends to oppose the increase of turbulent mixing with height so that the gradient of the wind speed is more uniform. Figure 9 shows typical changes of the wind speed distribution between day and night at a mid-latitude station. The most obvious difference is the well-known decrease of wind at night in the layers close to the ground, but equally pronounced is the increase of wind at night at heights from a few hundred feet to about 3000 feet.

Another parameter affecting the distribution of wind speed is the roughness of the ground surface. A rough surface causes more turbulence near the ground than does a smooth surface so that vertical mixing is more effective. This enhanced mixing results in a smaller value for the gradient of the wind speed near the ground. This smaller gradient, when combined with the no-wind condition at the ground surface, results in a lower wind speed near the ground than over a smoother surface, and a more rapid increase of wind with height in the layer above the anemometer level over the rough surface. These effects are illustrated in Figure 10.

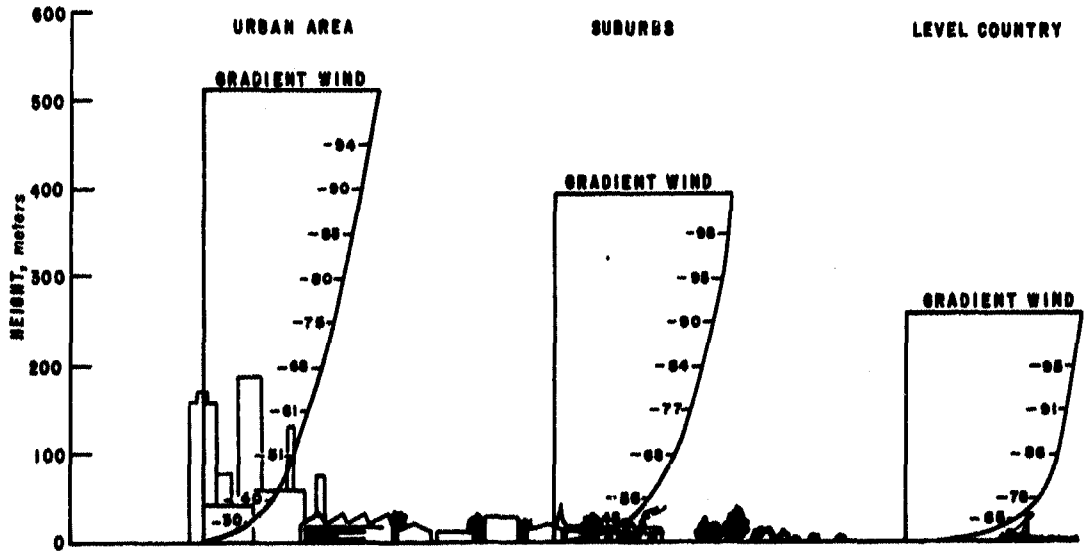

Figure 10. Examples of Variation of Wind with Height Over Different Size Roughness Elements (figures are percentages of gradient wind) [4].

b. Variation with Height of the Horizontal Wind Direction. Another feature of the winds in the surface layer is well-known to the meteorologist. That is that the winds in the surface layer do not blow parallel to the isobars, but cross the isobars at an angle from high pressure toward low pressure. Farther from the ground, as the "gradient wind level" is approached, the wind direction becomes more nearly parallel to the direction of the geostrophic or gradient wind. The importance of this turning of the wind with altitude is that the net drift of a cloud of pollutants will be in a direction between that of the geostrophic wind and that of the actual surface wind, provided the pollutants are being mixed through a fairly deep layer.

c. The Influence of Geographical Features on the Local Wind. There are two primary ways in which the topography can modify the local wind regime. The first of these is through the thermal effects of different surfaces. The second is the dynamic effect of hills or mountain ranges on the general flow pattern.

A common example of the first type is the "sea breeze." Because of its high conductivity and specific heat, a body of water changes temperature during the day much less than nearby land areas. This difference of temperature of the surface in turn causes a difference in the density of the air over the surface such that the pressure over water is higher by day and lower by night than that of adjacent land areas. This pressure difference causes the wind to have a component directed from the water toward the land during the day and from the land toward the water at night.

Another example of a thermally-induced wind system develops in mountainous terrain. As discussed previously, when the atmosphere cools at night, the air next to the sloping sides of the valley is more dense than the air in the center of the valley at the same elevation, this causes the air on the slopes to drain toward the valley center. This drainage ultimately results in a general flow toward the mouth of the valley. Gravity-flow systems of this type will usually extend to the height of the adjacent ridge tops. Figure 11 depicts the wind regime that results from a typical combination of valley wind with a light prevailing wind. The opposite thermal pattern develops during the daytime and there is a tendency for upslope and up-valley winds. However, up-valley winds are not usually as distinct because the greater turbulent mixing during daytime destroys the small local density gradients that maintain these local circulations.

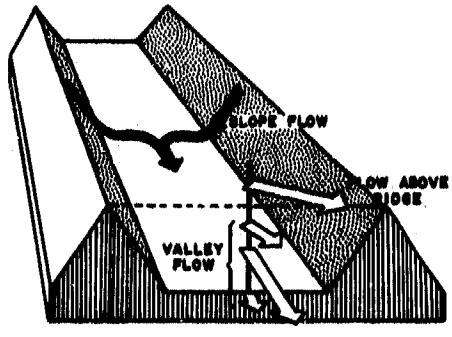

Figure 11. Combination of Valley Wind with a Light Prevailing Wind [20].

We turn now to the strictly dynamic influences of topography. Perhaps the most dramatic example of the influence of topography on the general flow is the mountain-wave phenomenon, which often produces severe updrafts and downdrafts on

Figure 12. Flow Perpendicular to a Set of Ridgelines.

the lee side of mountain ranges. The same phenomenon, in miniature, occurs in the vicinity of any ridge-valley system. While these local circulations on the smaller scale do not often constitute a hazard to aircraft, they can drastically alter the pattern of spreading of any concentration of airborne material. It is not too uncommon for the local wind in a valley to be completely reversed from the prevailing flow (see Figure 12). However, if the prevailing winds are not exactly perpendicular to an elongated valley, a similar phenomenon known as channeling results. This is illustrated by Figure 13.

Of all the local wind circulations, only the sea breeze has been successfully analyzed in a quantitative fashion that permits accurate predictions. Yet the micrometeorologist must be aware of the qualitative changes that are caused by the other topographical influences so he can visualize the diffusion and transport patterns that result from topographical modification of the broad-scale wind patterns.

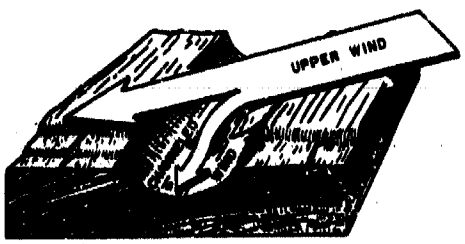

Figure 13. Channeling of Wind by a Valley [20].

Chapter 3

BASIC CONCEPTS IN DIFFUSION

1. General.

In Chapter 1 we mentioned turbulent mixing as a means of diluting the concentration of pollutants or toxic matter in the atmosphere. This turbulent mixing was called eddy conductivity in Chapter 2 when explaining the distribution of temperature near the ground. In the present chapter we return to the process of diffusion of matter in the atmosphere. The fundamental theoretical problem of diffusion is to relate the spread of a cloud of material, and the consequent reduction in concentration of the suspended matter, to the turbulence of the wind. The practical problem is to find means of estimating the rate of diffusion from simultaneous measurements of purely meteorological variables, such as wind, temperature, and their fluctuations. In this chapter we also present some fundamental definitions and elaborate somewhat on the mechanism of diffusion so that the relationship between diffusion and the more directly measurable meteorological parameters becomes clearer.

2. Basic Concepts and Definitions.

Some of the basic characteristics of the diffusion problem can best be illustrated in the context of the effect of specific types of sources of contamination. We will assume that the toxic or harmful material is in the form of gases or very small particles that faithfully follow all of the complex motions of the atmospheric whirls and eddies.

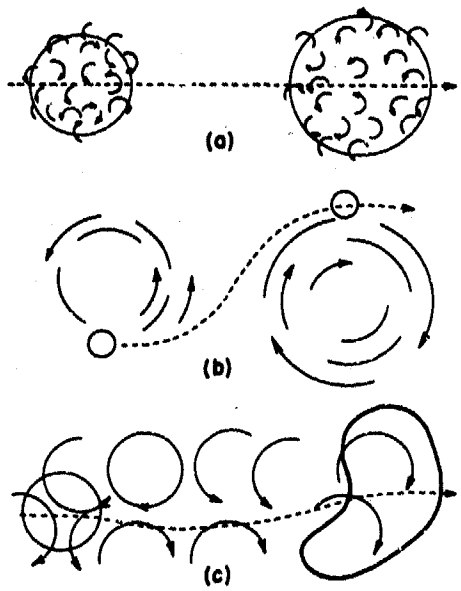

Figure 14. Idealized Diffusion of a "Puff" [20].

a. Instantaneous Point Source. No source is completely instantaneous and the point source concept is an idealization, but this definition is a useful approximation to the release of harmful toxic matter in a short "puff" or an explosion. A small spill of highly volatile material would also be classed as an instantaneous point source. One can easily imagine three different types of effects of atmospheric turbulence depending on the relative sizes of the initial cloud and the eddies in the atmosphere. These are illustrated in Figure 14. If the motions in the atmosphere consisted only of a mean wind and turbulence on a

scale much smaller than the size of the "puff," the situation might appear as in Figure 14a; the cloud drifting with the wind, but being enlarged by the turbulence (small arrows). On the other hand, if all the eddies were larger than the cloud, the situation would be more like Figure 14b. The third possibility, eddies of the same size as the cloud, would produce the complex result of Figure 14c. Actually, turbulence in the actual atmosphere consists of eddies of all different sizes so that, in reality, all three effects are combined. For an instantaneous point source the amount of material injected into the atmosphere is usually given as the total quantity of material released (grams or milligrams), and the distribution is usually given in terms of exposure, which is the integral of the concentration as the cloud passes a point.

b. Continuous Point Source. This idealization has received the greatest amount of attention in the literature. Good approximations of it are releases from stacks and accidental releases caused by pipeline cracks or spills that do not quickly evaporate. The quantity of material released by a continuous point source is expressed in terms of rate (e.g., kilograms per hour). If the release is prolonged and the character of the mean wind and turbulence do not change, it is appropriate to talk about the average concentration of the contaminating material at a given point downwind from the source. The concentration will fluctuate, but a mean concentration over a chosen sampling period is meaningful. Figure 15 shows how the irregular fluctuations smooth out with time to form predictable average concentrations.

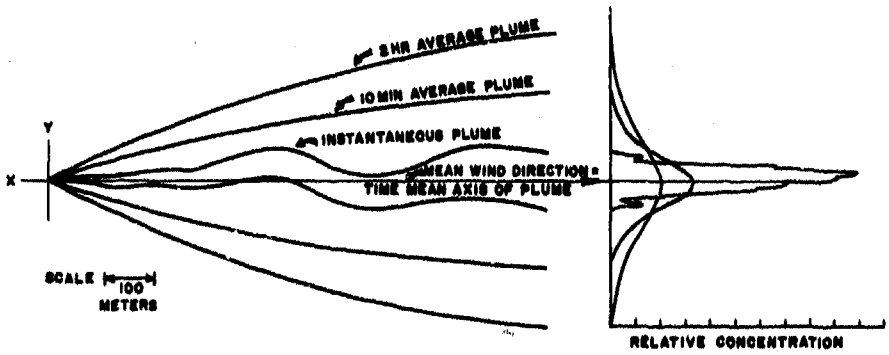

Figure 15. Instantaneous and Average Aspects of a Smoke Plume [20].

c. Continuous Horizontal Line Source. This problem received considerable attention by early British researchers (e.g., Sutton) in connection with chemical warfare developments. This type of model is now finding use in the analysis of urban air pollution. Any consideration of this source type by AWS meteorologists will probably be limited to supporting the use of incapacitating gases.

d. Continuous Area Source. This source configuration is usually modeled by considering the area as a series of continuous line sources oriented perpendicular to the prevailing wind. It is of considerable interest in urban air pollution. The main application for AWS meteorologists would be for a detailed analysis of the hazard associated with large spills of slowly-evaporating liquids.

e. Instantaneous Horizontal Line Source. This possibility corresponds to an aircraft spray source. It has been studied by the Army in connection with CB weapons. The analysis is similar to the instantaneous point source except that the concentration in the crosswind direction is uniform.

f. Instantaneous Area Source. This case is also of interest mainly for Army support. The analysis consists of superimposing the effects of a large number of parallel line sources.

g. Instantaneous Vertical Line Source. This case corresponds to the trail of exhaust fumes from a rocket launching and is therefore of considerable importance to AWS staff meteorologists at the missile ranges. However, the associated diffusion analysis is theoretically the most complex, so only the diffusion of the ground-level portion of the trail has been studied.

3. Theoretical Analysis of Diffusion.

There is no single physical model capable of explaining all the features of turbulent diffusion. There are two basic approaches, each of which has merits not possessed by the other. One relates the transport to the gradient of the concentration by an exchange coefficient. For example, in the case of heat transport, the exchange coefficient is the same thing as the eddy conductivity discussed earlier. The second approach considers the statistics of the air motions.

a. The Gradient or "K" Theory. The basic hypothesis is that the rate of diffusion depends in a linear fashion on the gradient of pollution. This approach was first proposed by the German physiologist Adolph Fick to explain the diffusion of salt in a liquid. For the simplest case of a gradient in one direction and uniform concentrations in the other directions, the differential equation describing the process is

$$(1) \qquad \frac{d\bar{q}}{dt} = K \frac{\partial^2 \bar{q}}{\partial x^2}$$

Here, $\bar{q}$ represents average concentration, t is elapsed time, and x is distance in one direction. K is the coefficient of diffusivity. The solution of Equation (1) is

$$(2) \qquad \bar{q} = \frac{Q}{\sqrt{4\pi Kt}} \exp\left(-\frac{x^2}{4Kt}\right)$$

Here Q represents the source strength (total release of pollutant). For three-

dimensional diffusion from a point, the equivalent equation is

$$(3) \qquad \bar{q} = \frac{Q}{(4\pi Kt)^{3/2}} \exp\left(-\frac{x^2+y^2+z^2}{4Kt}\right)$$

Here, x, y, and z are the distances from the point along the axes of a conventional right-handed coordinate system. These equations are straightforward in application, and evaluation of air pollution would be comparatively easy if a single value of K applied to the whole atmosphere. As we shall see in the next two subparagraphs, the actual values of K are dependent on the temperature gradient; therefore, they change with time and also with height. Furthermore, they also depend on the roughness of the underlying terrain and the wind speed. The completely general differential equation would be:

$$(4) \qquad \frac{d\bar{q}}{dt} = \frac{\partial}{\partial x}\left(K_x \frac{\partial \bar{q}}{\partial x}\right) + \frac{\partial}{\partial y}\left(K_y \frac{\partial \bar{q}}{\partial y}\right) + \frac{\partial}{\partial z}\left(K_z \frac{\partial \bar{q}}{\partial z}\right)$$

Completely general solutions to this equation do not exist in analytical (mathematical function) form. Solutions can be worked out on electronic computers for particular initial concentrations of contaminant and particular sets of assumptions about the K values.

Even if the above equation could be solved in a convenient manner, there would be yet another objection. The K-theory assumes that there is no transport in a given direction unless the concentration has a gradient in that direction. It has been shown, however, (Smith [21]) that if there is a vertical wind shear and a vertical gradient of the contaminant concentration, a significant horizontal diffusion of the contaminant will occur even if there is no horizontal gradient of the concentration. (This is quite separate from the horizontal transport due to the mean wind.) Thus, the complete equation of diffusion would have to contain at least nine additional terms to describe the interactions between wind shears and concentration gradients.

Having expounded on the difficulties of the complete K theory, it is only fair to say that many simplifications are quite plausible. In particular, if the vertical dimensions of the cloud of contaminant are small compared to the distance from the ground, the variations of the K's can safely be neglected, leading to a solution of the form

$$\frac{\bar{q}}{Q} = (4\pi t)^{-3/2} (K_x K_y K_z)^{-1/2} \exp\left[\frac{1}{4t}\left(\frac{x^2}{K_x} + \frac{y^2}{K_y} + \frac{z^2}{K_z}\right)\right]$$

When such simplifications are justified, the K theory gives very useful results.

b. Statistical Theory of Diffusion. A more realistic theory of atmospheric diffusion was published in 1921 by the noted British fluid dynamicist, Sir Geoffrey Taylor [23]. The most useful expression of this theory from the point of view of understanding turbulent diffusion has been given by Pasquill [18]. It relates the mean square distance, $\overline{y^2}$, traveled by a particle during the time

interval, t_1, to the power spectrum of the turbulent velocity fluctuation in that direction. The expression is

$$(5) \qquad \overline{y^2}(t_1) = v'^2 t_1^2 \int_0^\infty s_v(n) \left(\frac{\sin \pi n t_1}{\pi n t_1}\right)^2 dn$$

Here v'^2 is the variance of wind speed in the y direction. The power spectrum $s_v(n)$ tells how much of the turbulent energy v'^2 can be regarded as equivalent to an oscillation at the frequency n. The term

$$\left(\frac{\sin \pi n t_1}{\pi n t_1}\right)^2$$

has a maximum value of unity when $t_1 = 0$ or $n = 0$. It can be seen from this that the value of the integral in Equation (5) depends on the whole spectrum of turbulent energy; but, for the larger values of t_1, the diffusion is dominated by the low-frequency (slowly-varying) components of the turbulent velocity. This dominance by the low-frequency components is in accord with our intuition. If the motions of the particles are mainly at low frequencies, the particles will undergo large excursions before changing direction. On the other hand, a particle whose motion could be described by a high-frequency oscillation might have a large mean kinetic energy, but its excursions could be short. Of course, we cannot identify individual particles of air with particular frequencies of the power spectrum; nevertheless, the analogy helps us visualize the information contained in the statistics.

It can be shown that this statistical theory predicts diffusion equivalent to a "K" that increases linearly with time of travel while close to the source. Thus, the distribution of smoke from a stack or other point source is described at first by a "K" that increases linearly downwind. For values of travel time longer than five or six minutes, the statistical theory gives almost the same result as K-theory.

4. The Dependence of Diffusion on the Temperature Gradient.

Whether the diffusion process is described in terms of an exchange coefficient, a mixing length, or an autocorrelation function, atmospheric diffusion is enhanced by an unstable lapse rate. We were implying K-theory for heat transfer when we discussed the concept of eddy conductivity in Chapter 2 and the dependence of the eddy conductivity on lapse rate. The reason is very simple. When the lapse rate is unstable, a particle displaced vertically will experience a gravitational force tending to move it further in the direction of the displacement. Since the force is exerted along a direction in which the particle is already moving, the kinetic energy of the particle is increased. Since motion in all three directions is linked by the equation of continuity, the increased kinetic energy of the vertical component of turbulence results in an increase of the horizontal turbulence as well. The reverse

situation prevails when the lapse rate is stable. Energy is removed from the vertical component because the buoyancy (gravitational-density) forces are opposed to the direction of motion. Again, the reduction of energy of the vertical component causes a reduction of energy in the horizontal components.

The high degree of correlation between lapse rate and the intensity of turbulence can be seen by comparing Figure 16 with Figure 6. Figure 6 shows the seasonal and diurnal variation of lapse rate, while Figure 16 shows the seasonal and diurnal variation of σ_A, the standard deviation of the horizontal wind direction, an indicator of the intensity of the lateral component of turbulence.

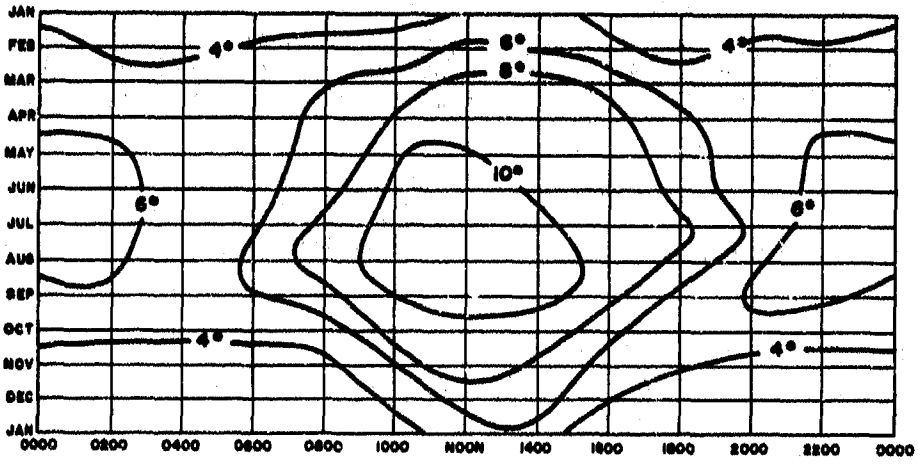

Figure 16. Seasonal and Diurnal Variation of the Standard Diviation of the Horizontal Wind Direction at 75 m. (Estimated from Figure 2.33 [20].)

A slightly more elegant explanation of the effect of lapse rate on diffusion is provided by the statistical theory. As we saw in paragraph 3b, diffusion depends on the energy in the low-frequency portion of the power spectrum. The characteristic time-scale of convective motions in the atmosphere is from one to several minutes. Therefore, convective motions introduce large amounts of energy into the low-frequency portions of the spectrum, and, thus, the integral in Equation (5) will be large. In contrast, at night low-frequency energy is selectively absorbed. Figure 17

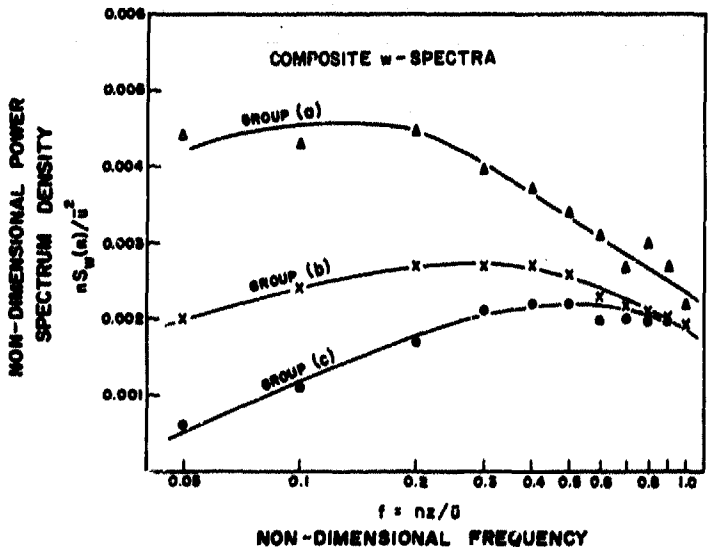

Figure 17. Composite Spectra of Vertical Velocity at Brookhaven, Long Island [16].

shows typical turbulence spectra associated with various lapse rates. The curve labeled "group (a)" is for quite unstable conditions. The curve labeled "group (c)" is for near adiabatic lapse rates.

The effect of lapse rate on diffusion is illustrated by some typical patterns followed by the effluent from a smokestack, which have now become classic in literature of air pollution. These patterns and their relation to stability are illustrated in Figure 18 and discussed below.

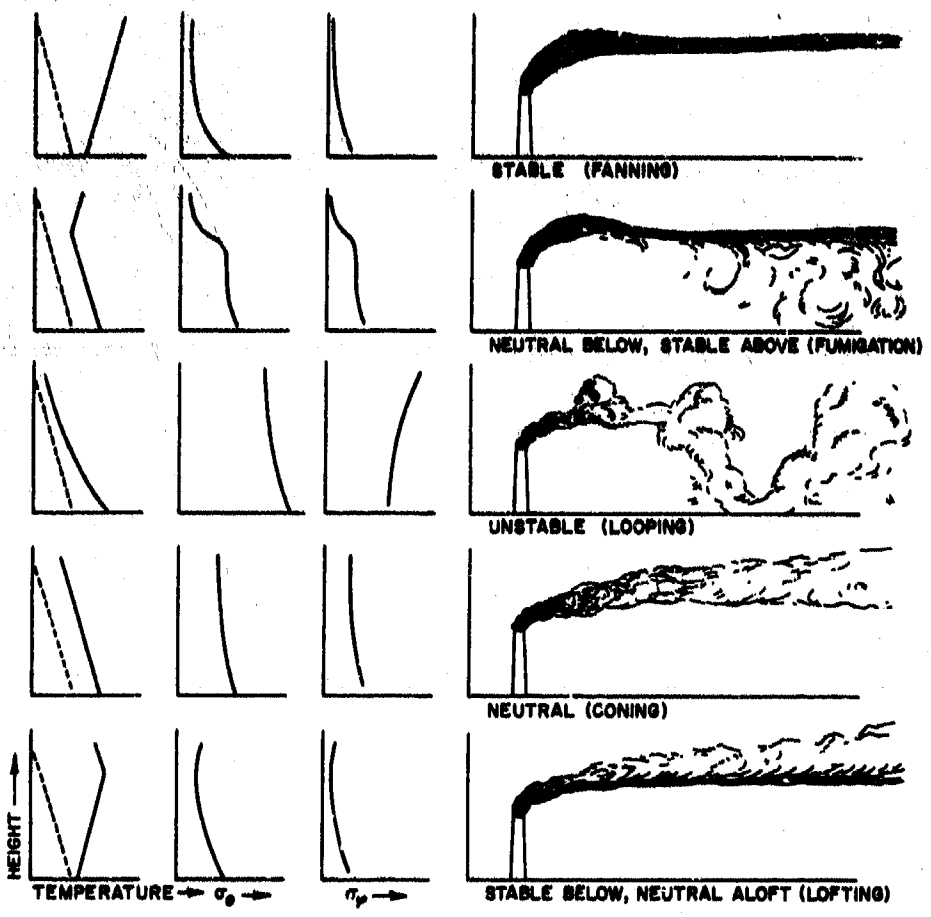

Figure 18. Effect of Lapse Rate on Vertical Diffusion [20].

a. Fanning. This condition occurs with stable conditions. The low-frequency components of the turbulence are suppressed, especially in the vertical, so the vertical spread of the plume is very small. The plume may show a slow meandering of direction. With respect to a long-term mean wind, this meandering produces an effective spreading of the plume which is much greater laterally than vertically.

b. Fumigation. There is a brief period after sunrise when the lapse rate is stable aloft but unstable near the ground. When the top of the unstable

layer reaches the height of the stack, the diffusion toward the ground can be large while the upward diffusion remains small. A high concentration of pollutant can then suddenly be brought to ground level.

c. Looping illustrates the much larger scale of the turbulent eddies under unstable conditions. Diffusion is very rapid so that points away from the axis of the plume, but near the source, experience a greater concentration than under more stable conditions. On the other hand, further downwind, concentrations are smaller than with more stable lapse rates.

d. Coning is characteristic of nearly equal intensities of turbulence in the vertical and horizontal directions. This is characteristic of temperature gradients between isothermal and adiabatic. The scale of the eddies, or the low-frequency energy of the turbulence, is seen to be less than experienced with looping, unstable conditions, but more than in the stable conditions which produce fanning. Coning is characteristic of strong winds and cloudy skies.

e. Lofting is the opposite of fumigation. When an inversion is present below the stack, but not above, the preferred direction of the diffusion is upward. This situation is very desirable from the point of view of avoiding hazardous exposure at the ground. Of course, it applies only to elevated sources of contaminant.

5. Variation of Diffusivity with Height.

Besides being dependent on lapse rate, the diffusing power of the atmosphere also varies with height. Near the ground, the size of any coherent air movement will be limited by the proximity to the ground. It has been found experimentally that, with near-adiabatic lapse rates, the distribution of temperature and wind speed are explained very well by assuming that the exchange coefficient (K) increases linearly with height.

As would be expected, the statistical theory also predicts an increase of the diffusivity with height. Investigations of the spectra of turbulent energy have shown that, near the ground, the spectra are nearly universal functions of the non-dimensional frequency, $f = nz/U$, where U is the mean wind [14]. The formula relating spectra under a change of frequency variable is such that $s_v(n) = z^2/U^2\ s_v(f)$, and $dn = U/z\ df$. For any particular height and atmospheric stability, the turbulent energy is proportional to the mean wind speed, e.g., $\overline{v'^2}/U^2 = \text{constant}$. Therefore,

$$(6) \qquad \overline{y'^2}(t_1) \sim Uzt_1^2 \int_0^\infty s_v(f) \left(\frac{\sin \pi f U t_1}{\pi f U t_1}\right)^2 df$$

Equation (6) shows that, if the turbulent energy is constant with height, the diffusivity will increase linearly with height and wind speed. Actually, such a quantity as $\overline{v'^2}/U^2$ decreases with height in the manner shown by Figure 19.

When the atmosphere is stable, the decrease of turbulent energy with height

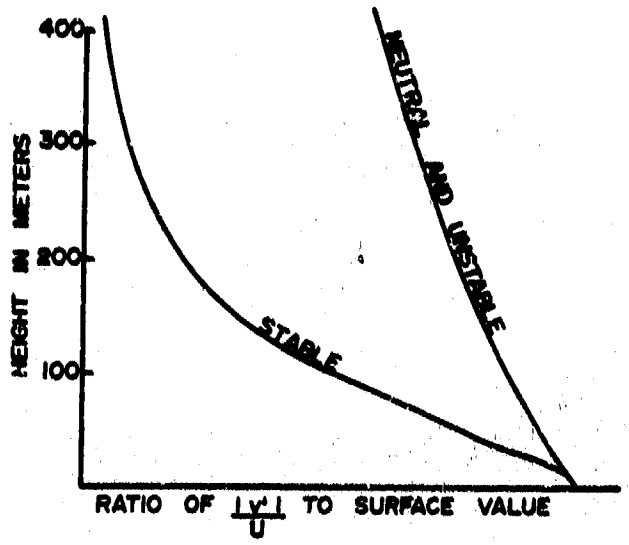

Figure 19. Decrease of Lateral Turbulence with Height for Different Stability Conditions.

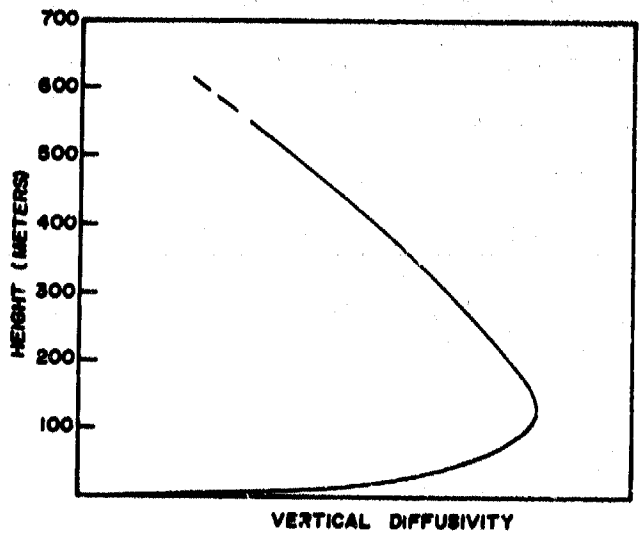

Figure 20. Typical Variation of Vertical Diffusivity (K) with Height (from [2]).

is very marked. In addition, under stable conditions, the influence of the ground surface disappears at heights of only a few hundred feet and the spectra no longer obey the "universal" relationship described in the preceding paragraph. Kaimal and Haugen [14] found that, in stable conditions, the peak of the vertical velocity spectrum becomes constant with height rather than being inversely proportional to height. Thus, in stable conditions, the maximum vertical diffusivity is located quite close to the ground. The decrease of the intensity of turbulence with height under neutral (adiabatic lapse rates) and stable conditions eventually dominates the frequency effect so that the diffusivity decreases with height as the gradient-wind level is approached. This decrease has its counterpart in the more sophisticated K-theories which have been used to explain the wind distribution between the ground and the gradient-wind level. The height dependence of K from one of these theories [2] is shown in Figure 20.

6. The Effect of Variation in the Wind Direction with Height.

In Chapter 2 we mentioned the gradual turning of the wind direction between the ground and the gradient-wind level. When a diffusing cloud is mixed through a deep layer, the net drift of the cloud will be in a direction approximately halfway between the surface wind direction and the geostrophic wind direction.

Chapter 4

ESTIMATING DIFFUSION AND CONCENTRATION FROM METEOROLOGICAL OBSERVATIONS

1. General.

In this chapter we discuss the practical question of using purely meteorological observations to estimate the diffusion and calculate relative concentrations of released toxic material. Estimates of dispersion of toxic matter can be made by two distinct methods, air-tracer surveys and calculation from generalized formulae.

An air-tracer survey consists of releasing known quantities of inert gases or small particles under a variety of weather conditions and then measuring the quantity of tracer material that arrives at various locations. The observed concentrations of tracer material are then correlated with meteorological parameters such as wind speed, temperature lapse rate, wind direction, and the variability of wind direction. From these correlations, equations are developed to express concentration directly in terms of the meteorological parameters. Examples of this approach are diffusion equations developed in the Mountain Iron project [11] and the Ocean Breeze and Dry Gulch projects [9].

Air-tracer surveys are the most direct and accurate method of estimating diffusion. However, this approach is also the most expensive, and is usually not followed until a definite environmental hazard has been recognized and a practical control procedure is required. Since the diffusion equations developed through tracer sampling are peculiar to the location where the survey was conducted, they will not be discussed further. The balance of this chapter will present more general methods which can be used to make preliminary estimates of diffusion without resorting to tracer surveys.

2. Diffusion Formulae that Assume a Gaussian Distribution.

Almost all of the formulae commonly used to describe the behavior of atmospheric contaminants assume that the spatial distribution of the contaminant can be described by the bell-shaped Gaussian curve used in statistics. This distribution is appropriate for two independent reasons. First, a distribution of the Gaussian form is a fundamental solution of the differential equation of diffusion, Equations (1) or (4), if the K or K's are constant. Second, a well-known law in statistics states that the distribution of the means of finite samples of random variables will tend to the Gaussian form as the number of such samples tends to infinity. This principle applies to concentration measurements of air pollution which are averages over time of an instantaneously-fluctuating concentration.

a. Sutton's Diffusion Model. One of the most widely-used Gaussian models in earlier years was Sutton's model. While it was first proposed as an application of Taylor's statistical theory of diffusion, the model is stated in terms of parameters that resemble the diffusion coefficients of the K-theory. In Chapter 3, paragraph 3b, we introduced the concept that, after diffusing for a time, t_1, particles would have a mean-square displacement $\overline{y^2}$ from their initial position. Sutton's theory [22] shows that

$$\overline{y^2} = \tfrac{1}{2} C_y^2 (Ut_1)^{2-n}$$

where C_y is a "virtual diffusion coefficient," U is the mean wind speed and n is a number to be derived from the power-law expression for wind profiles. If p is the power-law exponent, i.e.,

$$U(z) = U_1 \left(\frac{z}{z_1}\right)^p$$

then $n = 2p/1+p$. For the commonly-used 1/7 power law, n is 0.25. For an instantaneous point source, the concentration q of a contaminant is given by

$$(7) \qquad q = \frac{Q}{(\pi Ut)^{3/2} C_x C_y C_z} \exp\left[-(Ut)^{n-2}\left(\frac{x^2}{C_x^2} \frac{y^2}{C_y^2} \frac{z^2}{C_z^2}\right)\right]$$

This is identical with the equation at the end of Chapter 3, paragraph 3a, if $n = 1$ and $C_x^2 = 4K_x/U$, $C_y^2 = 4K_y/U$, etc. The parameters C_x, C_y, and C_z are thus generalized K-values. In the formula, t is measured from the time of release and n is a parameter associated with stability; x, y, and z denote distances from the center of the cloud. The values of the parameters C_x, C_y, and C_z are to be determined from turbulence statistics by the formulae

$$C_x^2 = \frac{4}{(1-n)(2-n)} \left(\frac{N}{U}\right)^n \left(\frac{\overline{U'^2}}{U^2}\right)^{1-n}$$

etc. The ratio N/U depends on height above the ground and the roughness of the ground but is almost independent of wind speed. N is a parameter Sutton calls "macroviscosity." The parameter $\overline{U'^2}$ is the variance of the x-component of air velocity. As mentioned in Chapter 3, paragraph 5, the ratio $\overline{U'^2}/U^2$ is nearly constant for a given site, height, and stability.

The steady-state formula for a continuously-emitting point source at ground level is

$$(8) \qquad \overline{q}(x,y,z) = \frac{2Q}{\pi C_y C_z U x^{2-n}} \exp\left[-x^{n-2}\left(\frac{y^2}{C_y^2} + \frac{z^2}{C_z^2}\right)\right]$$

In this equation the x-y-z coordinate system remains centered on the source, rather than moving with the mean wind. Two other parameters derived from

Sutton's method are the maximum concentration at the ground from a source at height h above the ground.

$$(9) \qquad \bar{q}_{max} = \frac{0.234\ Q}{Uh^2} \frac{C_z}{C_y}$$

and the value of x where the maximum ground concentration occurs,

$$x_{max} = \left(\frac{h^2}{C_z^2}\right)^{1/n}$$

The Sutton method is most useful for nearly-adiabatic lapse rates and releases from elevated sources where the vertical variations of the coefficients are small.

b. More Recent Gaussian Models. While Sutton's model has considerable theoretical validity, it is necessary to specify four parameters n, C_x, C_y, and C_z, in order to use the formula, all of which are dependent on height and stability. Actually, a Gaussian distribution is completely determined by its mean and its standard deviation. The modern tendency, therefore, is to omit the theoretical considerations and to simply relate the standard deviations of the contaminant distribution directly to the meteorological parameters. Under this concept, the form of the distribution for a continuous source located at ground level is:

$$(10) \qquad \bar{q} = \frac{Q}{\pi U \sigma_y \sigma_z} \exp\left[-\tfrac{1}{2}\left(\frac{y^2}{\sigma_y^2} + \frac{z^2}{\sigma_z^2}\right)\right]$$

In this equation, as in Sutton's, the diffusion along the mean wind axis by turbulence has been neglected in comparison with the transport due to the mean wind. The parameters σ_y and σ_z are the standard deviations of the Gaussian distributions in the y and z directions. The equivalent equation for an instantaneous point source at ground level would be:

$$(11) \qquad q = \frac{Q}{\sqrt{2\pi^3}\ \sigma_x^2 \sigma_y^2 \sigma_z^2} \exp\left[-\tfrac{1}{2}\left(\frac{x^2}{\sigma_x^2} + \frac{y^2}{\sigma_y^2} + \frac{z^2}{\sigma_z^2}\right)\right]$$

where the x, y, and z follow the cloud. In both of these formulae the values of σ_x, σ_y, and σ_z are not constant, but increase downwind from the point of release. The peak concentration at the center of the cloud decreases downwind while the curve representing the distribution of concentration gets broader. On the centerline of the cloud, the values of y and z are zero; therefore, the formula for the peak concentration C_p becomes

$$(12) \qquad C_p = \frac{Q}{\pi U \sigma_y \sigma_z}$$

The maximum ground-level concentration from an elevated release is

$$(13) \qquad \bar{q}_{max} = \frac{0.234\, Q}{Uh^2} \frac{\sigma_z}{\sigma_y}$$

These formulae are quite practical when the values of σ_x, σ_y, and σ_z are determined. Methods for estimating these are presented in the following paragraph.

3. Estimating Diffusion Parameters from Ordinary Meteorological Data.

In order to apply equations such as (10) and (12), it is necessary to know σ_y and σ_z as a function of distance from the source. Over the past several years there has been a continuing effort on the part of several meteorological agencies to determine functional relations of σ_y and σ_z to distance. In spite of this continuing effort, there is no agreement on a single "best formula" for the growth of σ_y and σ_z downwind as a function of normally-available meteorological information. The most recent studies [25] show that σ_A, the standard deviation of the horizontal wind direction, is the best single meteorological parameter for estimating diffusion from continuous sources. This parameter is a direct measure of crosswind turbulence and is also highly correlated with the intensity of vertical turbulence. One of the earliest systems for relating diffusion to meteorological measurements, and still one of the best systems, was developed by Cramer [3] based on measurements of σ_A and σ_φ, the standard deviation of the vertical wind angle. These parameters are difficult to calculate without the use of analog or digital computers, so other systems have been developed which require less sophisticated information.

The system used by meteorologists supporting the Atomic Energy Commission and the National Air Pollution Control Administration was originally devised by Pasquill [17]. It was stated originally in terms of the height and angular spread of a cloud of smoke. The relations for the height and angular spread were redefined in terms of σ_y and σ_z by Gifford [7]. With this redefinition, the predictions of Pasquill agree with Cramer within a factor of two. Pasquill's graphs (as modified by Gifford) relating σ_y and σ_z to distance are presented as Figures 21 and 22. Six stability categories, A through F, were defined by Pasquill in terms of wind speed and a qualitative assessment of the strength of the incoming or outgoing radiation. A summary of rules for selecting the appropriate category is presented in Tables 1 and 2. For concentrations on the plume axis, Equation (12) indicates that C_p/Q is inversely proportioned to $U\sigma_y\sigma_z$. Figure 23 depicts C_pU/Q as a function of distance for the six categories.

If information on the standard deviation of horizontal wind direction is available, the following table of equivalence (Table 3) is recommended. The values in the table are based on approximately 200 diffusion trials conducted in the Green Glow, Prairie Grass, Ocean Breeze, and Dry Gulch projects sponsored by AFCRL, and projects in support of the AEC at Idaho Falls, Idaho and Hanford, Washington. As with Table 2, if two letter-categories are indicated, one should choose a value halfway between the two curves.

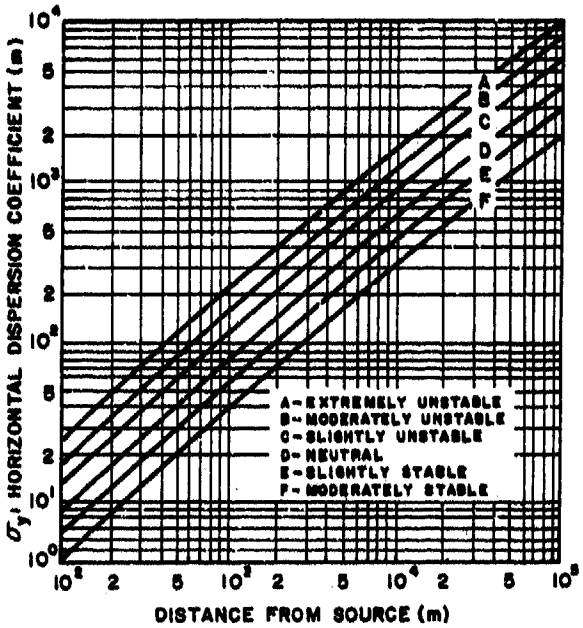

Figure 21. Lateral Standard Deviation of Diffusing Plumes as a Function of Downwind Distance and Stability Category [20].

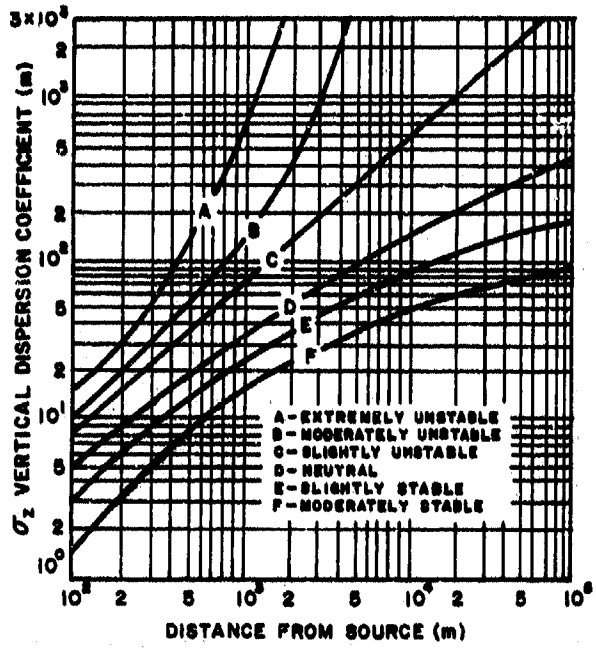

Figure 22. Vertical Standard Deviation of Diffusing Plumes as a Function of Downwind Distance and Stability Category [20].

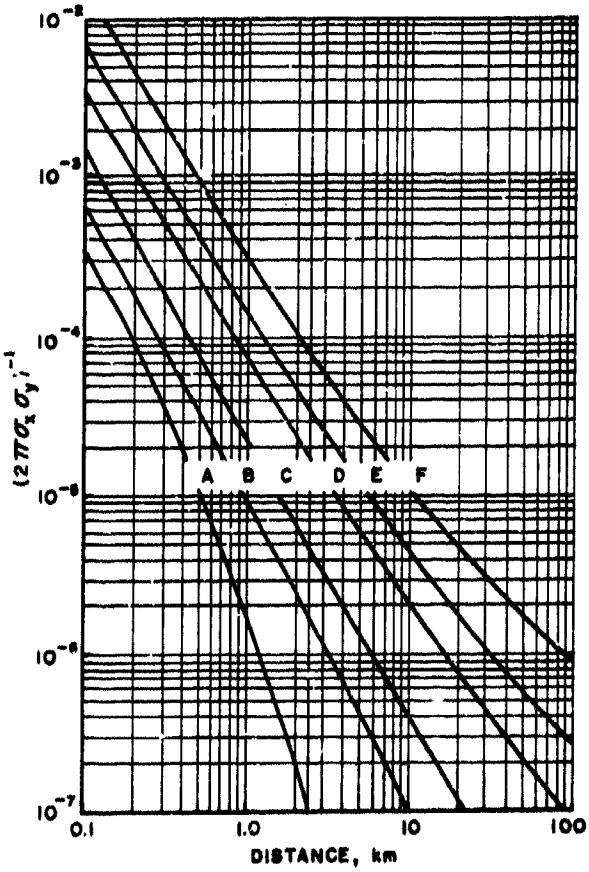

Figure 23. Reduction in Centerline Concentration Due to Crosswind Expansion.

A rough measure of σ_A can be obtained from the trace of wind direction from the RO2 wind recorder or a similar instrument. The technique consists of finding the extreme range of wind directions during a 30-minute period and dividing by eight [15]. The method is very crude and some workers prefer to divide by only five or six instead of eight. But crude as it is, the method is more accurate than assigning the Pasquill category purely on the basis of the information in Tables 1 and 2.

CAUTION: Categories A and B should never be used for nighttime peak concentrations, and category C would be appropriate at night only when strong gusty winds persist following a cold front passage. Values of σ_A at night larger than about 8° over flat ground or 14° over rough ground indicate fanning. Short-term peak concentrations will then be as large as those given by curve F, or even larger.

Equation (10) can be evaluated for off-axis points using Figures 23 and 24. For the Pasquill categories, use Figure 23 to get the centerline concentration appropriate to the stability category. Figure 24 gives the value of the exponential term for lateral distances 1 to 1000 meters and σ_y of 1 to 2000 meters. Figure 24 is labeled in terms of general numbers, a and b, because it can also be used with vertical distances and σ_z to get concentrations away from the ground. Graphs of $U\bar{q}/Q$ for all points on the ground-level plane have been presented in [26] based also on the Pasquill σ_y and σ_z values. These plots are reproduced as Figures 25 through 30.

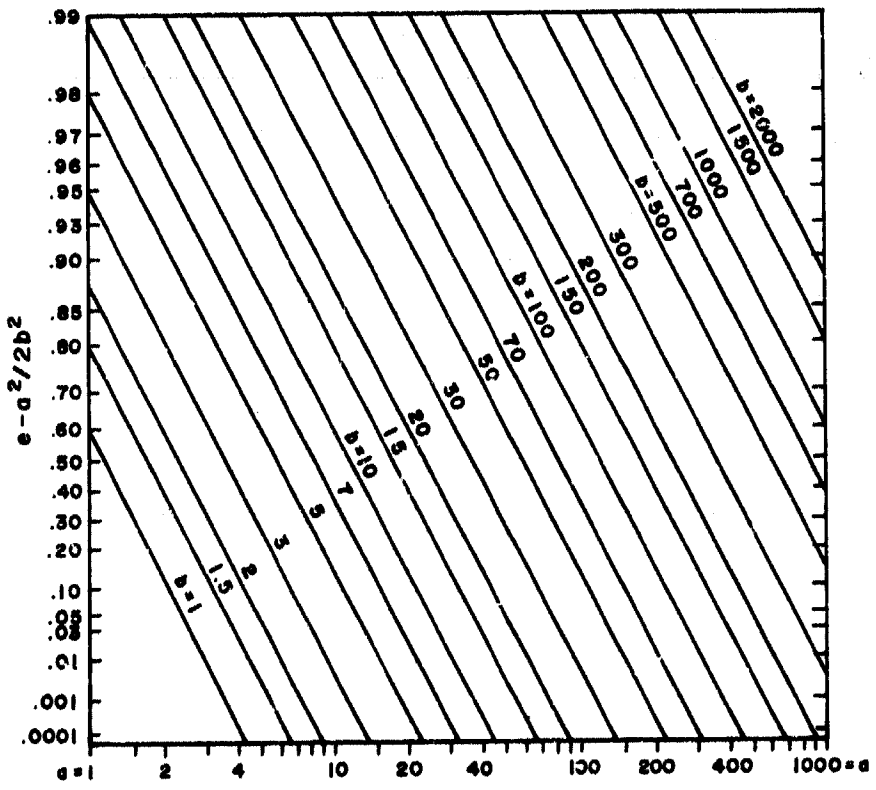

Figure 24. Graphical Aid for Computing $e^{-(a^2/2b^2)}$.

TABLE 1

Net Radiation Classes

Cloud Cover	Night	Elevation of Sun			
		≤ 15°	> 15° but ≤ 35°	> 35° but ≤ 65°	> 65°
< 3/8	-2	-1	+1	+2	+3
3/8 or 4/8 at any hgt or broken abv 16000 ft (incl. -⊕)	-1	0	+1	+2	+3
⊕ abv 16000 ft or ⊖ between 7000 ft and 16000 ft	-1	0	0	+1	+1
⊖ below 7000 ft	0	0	0	0	+1
⊕ below 7000 ft	0	0	0	0	0

TABLE 2

Stability Category Based On Wind Speed and Net Radiation

Surface Wind Speed		Net Radiation Class (see Table 1)					
m/sec	knots	+3	+2	+1	0	-1	-2
< 2	< 4	A	A-B	B	D	E	F
2-3	4-6	A-B	B	C	D	E	F
3-5	6-10	B	B-C	C	D	D	E
5-6	10-12	C	C-D	D	D	D	D
> 6	> 12	C	D	D	D	D	D

TABLE 3

Pasquill-Type Classification Bases on Standard Deviation of Wind Direction

σ_A	At 1/2 Mile or Less, Use Type	At 1.25 Miles, Use Type	At 5 Miles or More, Use Type
≤ 2.5°	E-F	E	D-E
5°	D-E	D	C-D*
10°	C-D*	C*	C*
15°	B*	B-C*	B-C*
20°	A-B*	B*	B-C*
≥ 25°	A*	A-B*	B*

* See Caution in text.

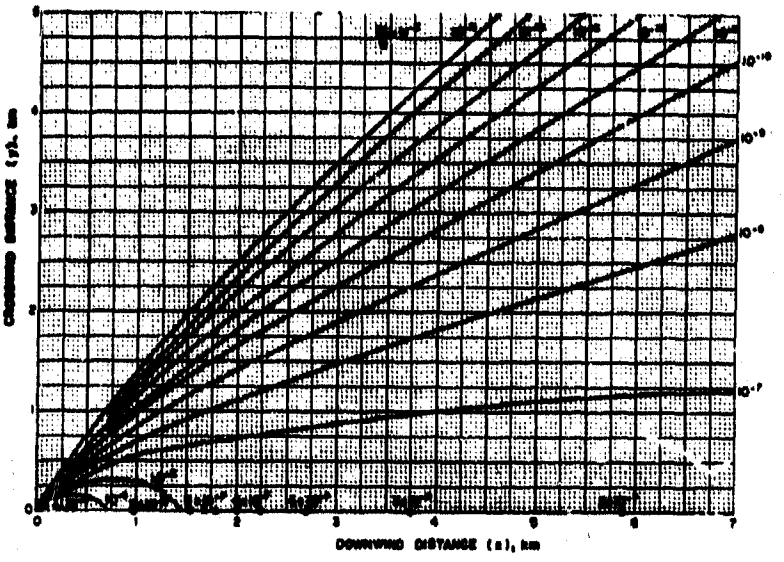

Figure 25. Isopleths of qU/Q on the Ground for a Ground-Level Source, A Stability.

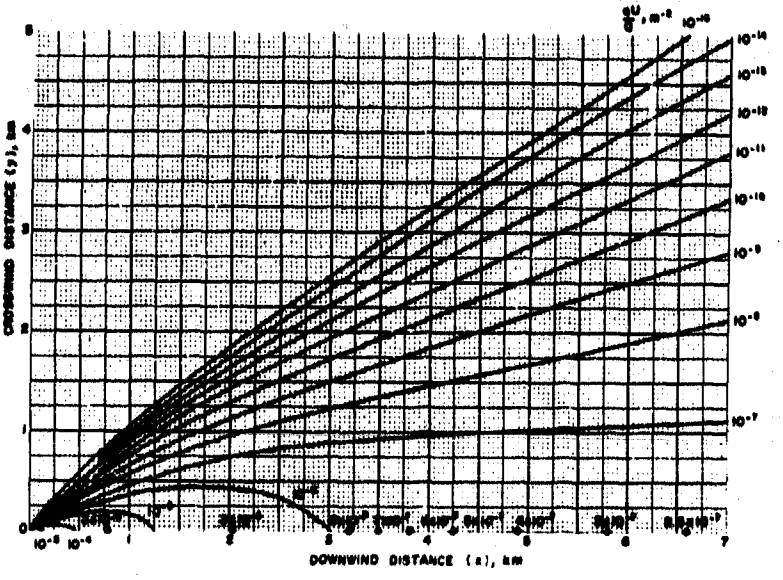

Figure 26. Isopleths of qU/Q on the Ground for a Ground-Level Source, B Stability.

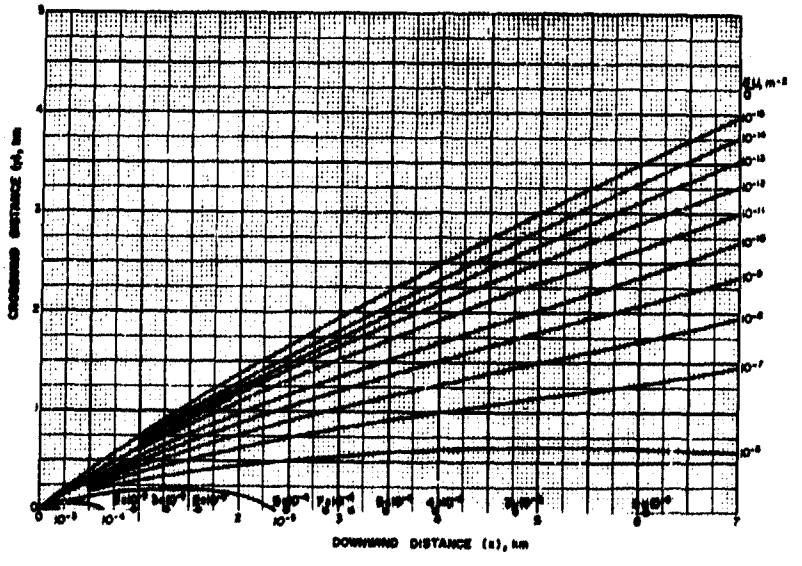

Figure 27. Isopleths of qU/Q on the Ground for a Ground-Level Source, C Stability.

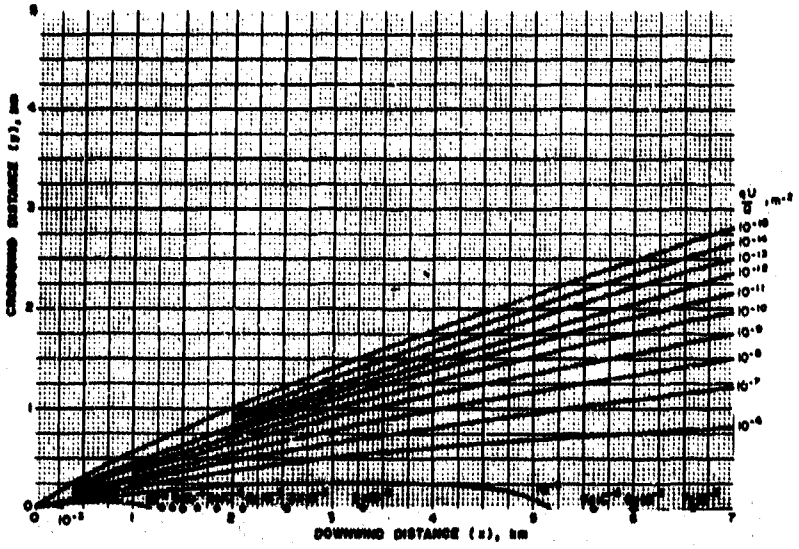

Figure 28. Isopleths of $\overline{qU}/Q$ on the Ground for a Ground-Level Source, D Stability.

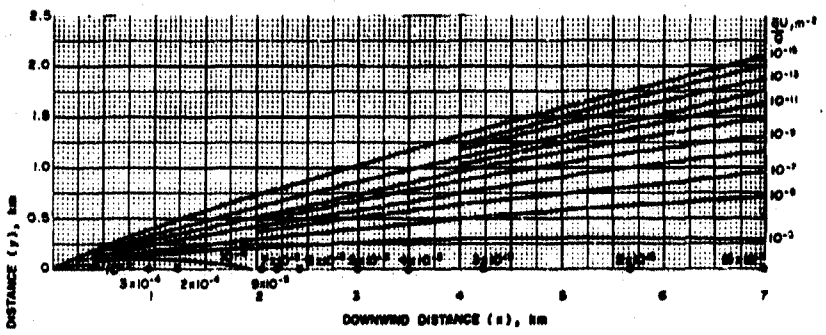

Figure 29. Isopleths of $\overline{qU}/Q$ on the Ground for a Ground-Level Source, E Stability.

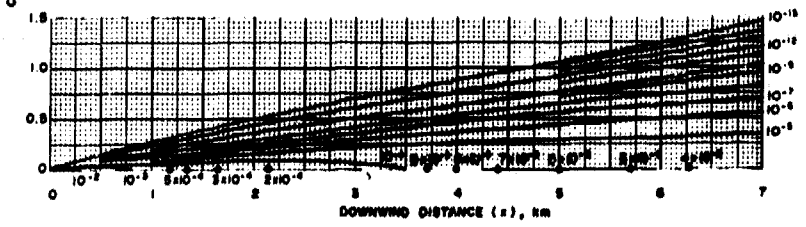

Figure 30. Isopleths of $\overline{qU}/Q$ on the Ground for a Ground-Level Source, F Stability.

4. Non-Gaussian Equations.

The Gaussian assumption is usually retained whenever the distribution in more than one direction is desired. If only the downwind peak concentration is needed, it is possible to drop the a priori functional form and adopt a completely general approach in relating concentration of contaminants to meteorological parameters. An example of the general approach is the technique developed at the Air Force Cambridge Research Laboratories in connection with the Ocean Breeze and Dry Gulch diffusion programs [9]. The relevant meteorological parameters were assumed to be: the mean wind speed U, the downwind distance x, the RMS wind-direction fluctuations σ_A, and the temperature difference ΔT in degrees Farenheit between six feet and 54 feet (negative, if the 54-ft temperature

was colder). A completely general equation of the type

$$C_p/Q = Kx^a U^b \sigma_\theta{}^c (\Delta T + \text{const})^d$$

was fitted to the C_p/Q data by taking logarithms of both sides and using multiple regression techniques to determine best-fitting values of K, a, b, c, and d. C_p is the peak concentration which theoretically corresponds to the value of $\overline{q}$ on the centerline of the Gaussian model. It was found that C_p/Q was independently correlated with the mean wind speed U, but there was no significant improvement when U was included in a multiple correlation. The resulting equation was

$$(14) \qquad C_p Q = 0.00211x^{-1.96} \sigma_A{}^{-0.506} (\Delta T + 10)^{4.33}$$

ΔT and σ_A are strongly correlated with each other as indicated in Chapter 3, paragraph 4. Therefore, the loss of accuracy by omitting one or the other would be small. Since σ_A is hard to compute accurately without digital or analog computers, a simplified equation using only x and ΔT was developed for use at the Titan II launch sites [15]. The simplified equation is

$$(15) \qquad C_p/Q = 0.000175x^{-1.95} (\Delta T + 10)^{4.92}$$

When this equation was tested with a set of independent data for the same locations, the predicted concentrations agreed with the observed concentrations 65% of the time within a factor of two and within a factor of four, 94% of the time. This equation is graphed as Figure 31.

Most applications of diffusion theory to safety require an estimate of the distance beyond which the concentration will be less than a specified level. For this purpose, Equation (15) can be converted to the form

(16)

$$x = 0.0388 (C_p/Q)^{-0.513} (\Delta T+10)^{2.53}$$

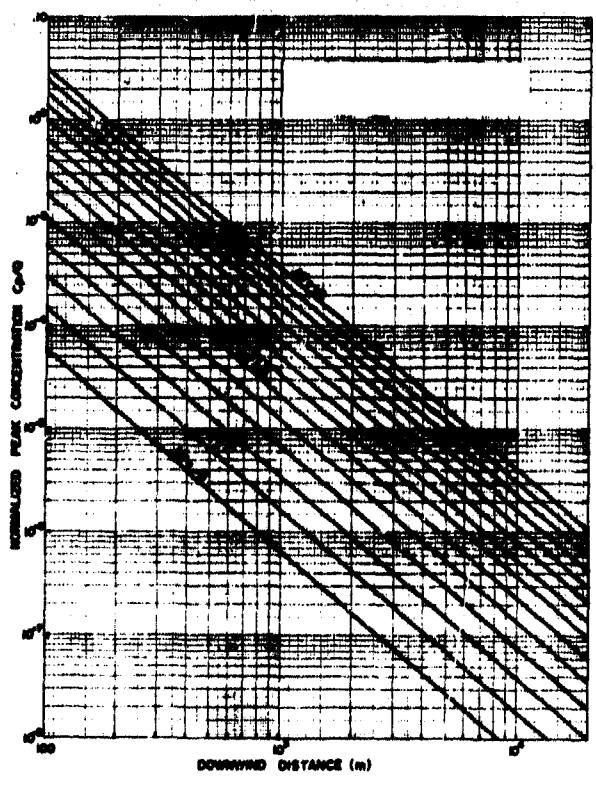

Figure 31. Peak Concentration vs Downwind Distance from Equation (15).

In deriving these equations, data from three different sites were used, one on the West Coast, one on the East Coast, and one in the Great Plains. The data from the three different sites are all scattered about the same regression lines; therefore, the relations expressed by Equations (14) through (16) can be considered fairly universal.

5. Instantaneous Sources.

The Gaussian equation for diffusion from an instantaneous source was given as Equation (11). This equation requires a value for σ_x as a function of downwind distance; such values are shown in Figure 32 for three broad stability categories, as derived by the US Army Munitions Command Operations Research Group [27]. The values of σ_x are larger in stable conditions because true downwind diffusion depends on wind shear, which is largest in stable conditions. The best values of σ_y also differ from their values for continuous sources. The most important differences are that σ_y is smaller and increases less rapidly with distance for instantaneous sources than for continuous sources. Values of σ_y for instantaneous sources are given in Figure 33. These are a compromise between results of tests conducted at Dugway Proving Ground [25] and values recommended in [20]. The confidence in these σ_y values is less than for continuous sources.

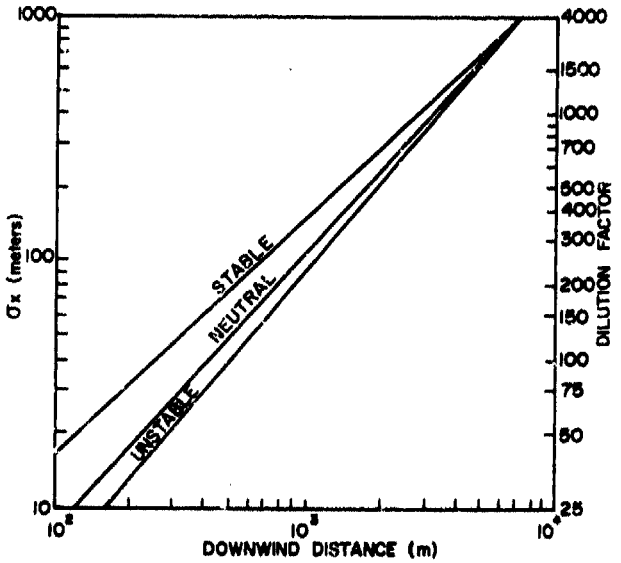

Figure 32. σ_x vs Downwind Distance for Instantaneous Source [27].

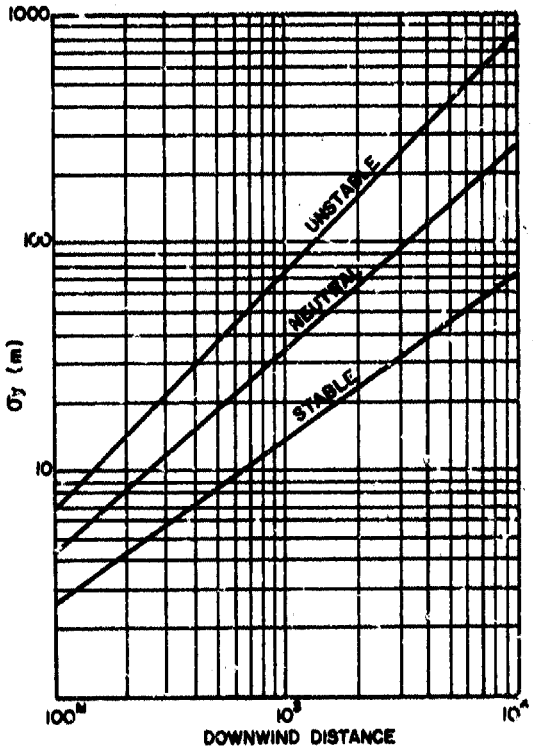

Figure 33. σ_y vs Downwind Distance for Instantaneous Source.

The data on σ_z from instantaneous sources are even fewer. Data taken from chemical-munitions trials at Dugway Proving Ground [25] yield σ_z estimates for truly ground-level releases that agree very well with the values shown in Figure 22 for continuous sources. For elevated sources, σ_z values given in [20] suggest that a curve between C and D of Figure 22 be used for unstable conditions, a curve between D and E for neutral conditions, and a curve slightly below F for stable conditions. Values of the factor $(2\pi\,\sigma_y\sigma_z)^{-1}$ for instantaneous ground-level releases are shown in Figure 34.

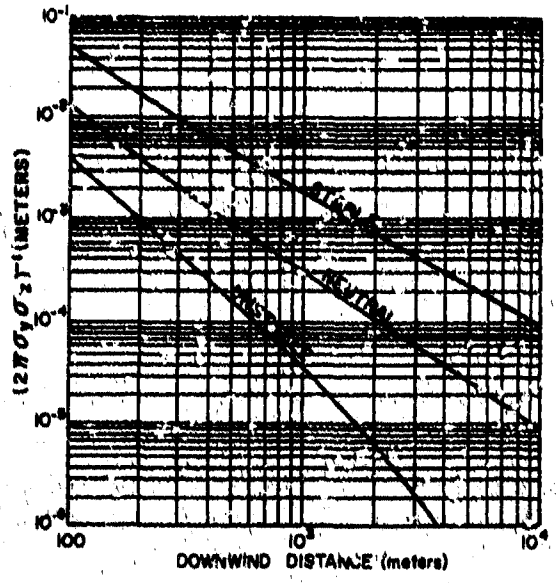

Figure 34. $(2\pi\,\sigma_y\sigma_z)^{-1}$ for Instantaneous Release.

6. Comparison of Equations.

So far, we have mentioned two different systems for relating air-pollution concentrations to more readily-available meteorological data. Neither of these systems can be considered really superior to the other. Both give very similar answers at short distances, where most of the data have been gathered. Unfortunately, there has never been a diffusion test with a simultaneous measurement of the parameters needed to test both systems. In most cases, the choice of systems is dictated by the type of data available.

Actual vertical temperature difference measurements are seldom available except at the Air Force test ranges, Titan II sites, and a few Army installations. Nor is there any widely-accepted system for predicting these vertical temperature differences from other meteorological variables. Thus, for most locations the only available tool is the Pasquill-Gifford system outlined in paragraph 3 of this chapter for which the required meteorological data, cloud cover, wind speed, and sun angle. Examples of calculations with this system will be given in the Appendix.

7. Mixing Depth: The Role of Elevated Inversions.

All of the diffusion equations described so far consider only the effect of the lapse rate near the ground in determining the diffusion (or dilution) from sources at or near the ground.

In many cases the lapse rate near the ground will be isothermal or even adiabatic with a pronounced inversion a few hundred or few thousand feet above the ground. In these situations the diffusion near the source behaves as if there were no inversion present. But because the inversion is present, the cloud or pollutant cannot grow indefinitely in the vertical direction. At

distances far enough downwind the pollutant is uniformly mixed through the layer below the inversion and no further dilution can take place due to vertical mixing. The cloud does continue to expand horizontally unless the lateral spread is also confined by hills parallel to the flow.

Some rules of thumb for the effect of an elevated inversion can be stated as follows:

a. If σ_z is known as a function of downwind distance, x, determine the distances where $\sigma_z = H/2$ and where $\sigma_z = 2H$, H being the height of the inversion. For distances such that $\sigma_z < H/2$, the elevated inversion can be ignored.

b. For distances such that σ_z would be greater than 2H, assume a uniform distribution in the vertical and use the formula

$$(17) \qquad \bar{q} = \frac{Q}{\sqrt{2\pi}\, HU\, \sigma_y} \exp\left(-y^2/2\sigma_y^2\right)$$

c. For values of x such that σ_z would have been between $\frac{1}{2}$H and 2H, the concentration can be estimated by drawing a straight line on log-log paper between the concentration at the value of x where σ_z would be $\frac{1}{2}$H and the concentration at the distance where σ_z would be 2H.

Unfortunately, the application of mixing-depth relations is limited to the Gaussian models described in paragraphs 2 and 3 of this chapter. The statistical methods of paragraph 4 of this chapter cannot be used because σ_z is not known independently as a function of distance. The inability to account for mixing depth has not really affected safety calculations for liquid-propellant spills at the test ranges. The mixing-depth concept is important for air-pollution problems of urban areas where there are numerous sources of pollution and concentrations at the "annoyance" level are significant. Spills of liquid propellants of the magnitude considered in test-range safety problems would normally be diluted to safe levels in less distance than required for elevated inversions to be significant.

Chapter 5

PROCESSES OTHER THAN TURBULENT MIXING THAT AFFECT THE DISTRIBUTION OF TOXIC MATERIAL

1. General.

The methods presented in Chapter 4 assume that nothing happens to the material other than dilution by turbulent mixing. This is not entirely the case as some liquid propellants used in missiles (also some CB agents) have a reaction with air that tends to diminish their concentration. There are also other processes related to atmospheric dynamics, but not to turbulence, which alter the distribution of released matter. The reaction with air will be of substantial importance for some missile propellants soon to be tested. This type of depletion will be considered first.

2. Concentration Changes Resulting from a Reaction with Air.

Most missile liquid propellants of the hydrazine family react with air. This reaction has been recognized for quite a while and was considered when determining the requirements for storage facilities but, no attention has been paid to the effect such a reaction would have on the concentrations in the atmosphere following an accidental release. In some cases, as with unsymmetrical dimethyl hydrazine (UDMH), the reaction is slow. In other cases, notably monomethylhydrazine (MMH), the reaction is faster. Within half an hour after mixing with adequate amounts of air, almost half of the MMH is converted to harmless by-products, which substantially reduces the downwind-hazard distance. The reaction may be even faster in the presence of certain catalysts. MMH will probably not present much of a problem for the AWS staff meteorologist because there are no current USAF plans to use it for anything except small rocket motors in deep-space probes. However, the reaction of MMH provides an excellent example to illustrate the technique of calculating modified concentrations for reacting fuels.

An investigation of the reaction rate of MMH [29] shows that, for concentrations of MMH less than about 10% by volume, the rate of conversion of MMH depends on the amount of MMH still present. That is, the process can be described by the first-order differential equation

$$\frac{dC_{MMH}}{dt} = - kC_{MMH} \tag{18}$$

in which C_{MMH} is the concentration of MMH and k is the proportionality factor. The solution of this equation is

$$C_{MMH} = C_o e^{-kt}$$

in which C_o is the concentration at time, t = 0. A typical plot of the concentration of a function of time is shown in Figure 35.

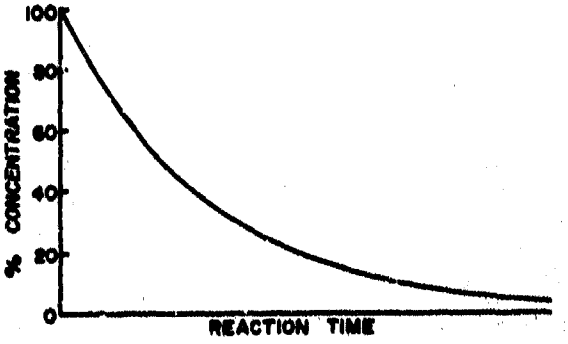

Figure 35. Typical Concentration of Toxic Substance when an Initially Toxic Substance Decays in Air to Form a Harmless Compound.

It is clear that this behavior will affect the pattern of diffusion because the fundamental concept of the statistical theory of diffusion is that the average position of a particle at some time, t, after it is released results from the properties of the ensembled functions. Accounting for the details of the diffusion is made somewhat more complicated by having to account for the changing concentration of toxic material in each "blob" of air, but the most important type of calculation, the peak concentration downwind, can be corrected very simply. As a first approximation, the process of dilution due to the chemical reaction can be considered as independent of the dilution due to mixing. In that case, the concentration is obtained by multiplying $e^{-kx/U}$ times the concentration that would have been obtained for a nonreacting substance. Two graphs will assist in making this calculation.

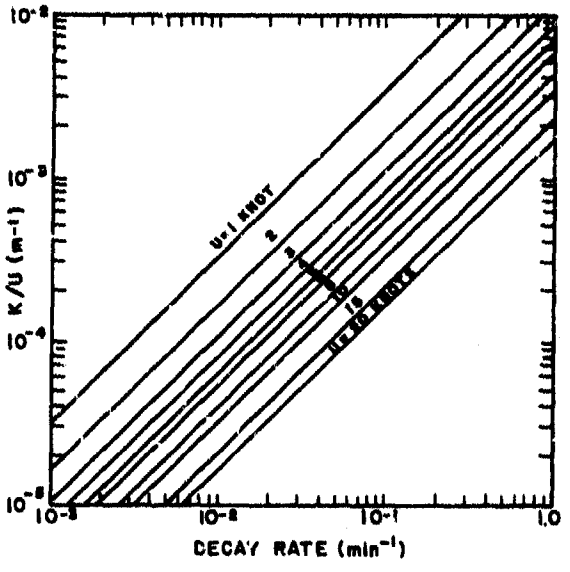

Figure 36. Graph for Converting Decay Rate and Wind Speed to K/U.

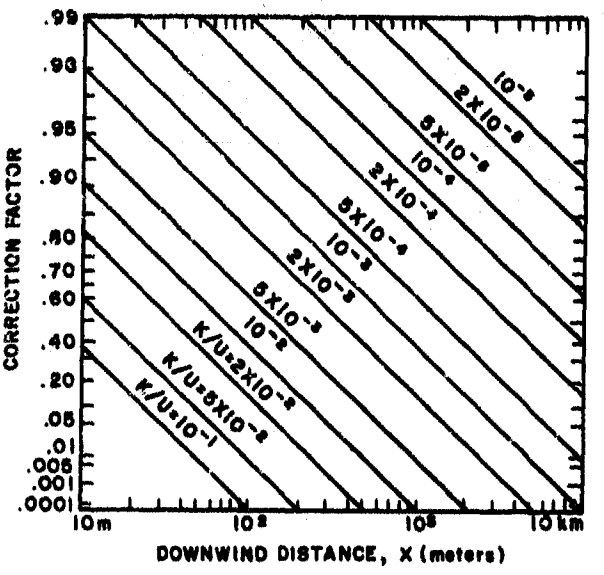

Figure 37. Correction Factor for Concentration of Decaying Pollutants.

Figure 36 converts values of the decay constant k(min^{-1}) and the wind speed in knots to values of K/U for different values of x and k/U. Figure 37 gives the

correction factor, $e^{-kx/U}$, for different values of x and k/U. These graphs can be used to correct the estimates of C_p/Q obtained from Pasquill's curves, or from Equations (14) or (15). Paragraph 4, Chapter 4 also contains an equation, Equation (16), for estimating the distance beyond which the peak concentration would be less than a prescribed value. The corresponding equation for a substance of decaying toxicity would be

$$(19) \qquad xe^{0.513kx/U} = 0.0388(C_p/Q)^{-0.513} (\Delta T + 10)^{2.53}$$

This is simply Equation (16) with x replaced by $xe^{0.513kx/U}$. The value of x which is a solution of Equation (19) is naturally smaller than the value obtained from Equation (16). Figure 38 furnishes the solution for Equation (19) in terms of the solution of Equation (16) and the value of k/U determined from Figure 35.

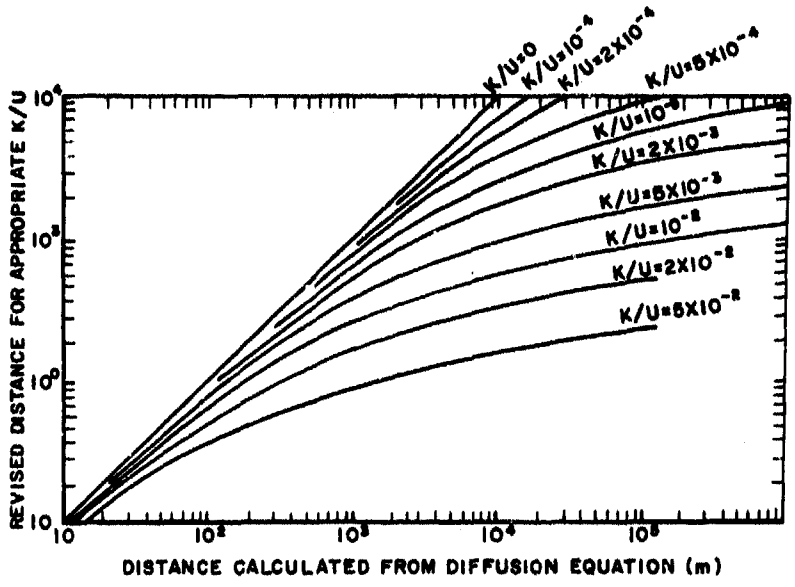

Figure 38. Revised Hazard Distances for Decaying Pollutants.

So far we have discussed the case of a toxic chemical that reacts with air to form harmless products. The reverse possibility exists, i.e., a vapor that would be harmless in the pure state, but toxic after reacting with atmospheric oxygen or nitrogen. The equation for the concentration of such a toxic material in a closed chamber would be:

$$(20) \qquad C = C_f (1 - e^{-kt})$$

where C is the concentration of the new toxic compound at a given time and C_f is

the concentration that would result from the conversion of all of the original chemical to the new compound. A typical plot of concentration versus time for such a reaction is shown in Figure 39.

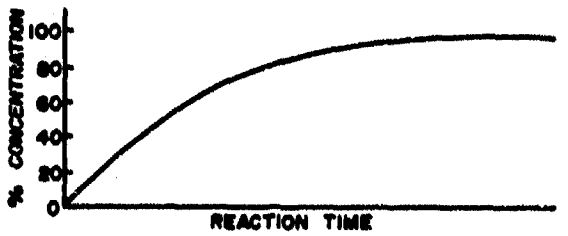

Figure 39. Typical Concentration of Toxic Substance when an Initially Harmless Substance Reacts with Air to Form a Toxic Substance.

Invoking the same assumption of independence of the diffusion and the reaction rate which we used previously, the downwind peak concentration would behave as indicated in Figure 40. This behavior is qualitatively the same as the peak concentration from an elevated source; it has a maximum value a short distance downwind from the release point.

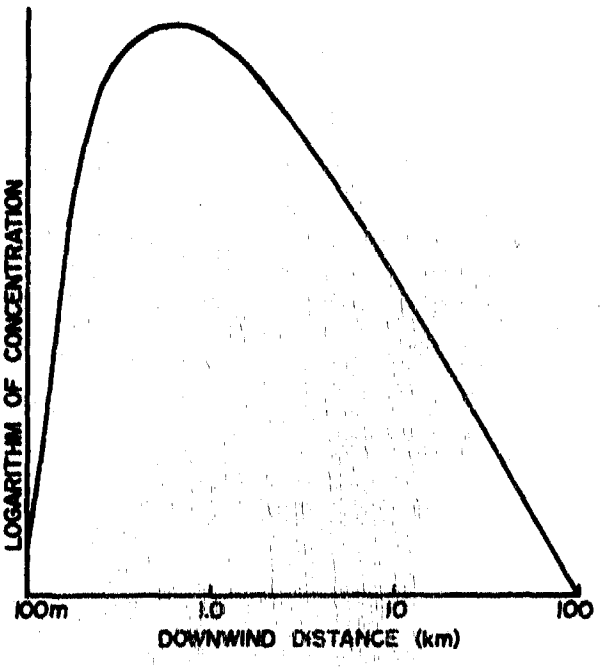

Figure 40. Generalized Plot of Concentration Versus Distance for a Substance Having Characteristics Shown in Figure 39.

The first-order modification to the downwind concentration can be found with the aid of Figure 37. For the case we are now considering, use Figure 36 to obtain k/U. The required correction factor will be obtained by subtracting from one the value of the ordinate from Figure 37. That is, if the value from Figure 37 is 0.30, the required correction factor is 0.70. There is not as much point in calculating a correction for the downwind safe distance in this case because the large distances would be least affected.

Another possible concern is the fact that some materials, such as hydrochloric acid (HCl) and fluorine compounds, are hygroscopic and could be diluted by the condensation of water vapor. There is some disagreement about whether this would actually reduce the toxicity. In such cases, the Staff Surgeon or Staff Bio-environmental Engineer should be responsible for setting the acceptable concentrations for both vapor and aerosol forms. If the aerosol form (as suspended liquid drops) is considered to be less harmful, it would be necessary to estimate the rate at which water vapor will be attracted to the particles of

toxic cloud.

3. Other Depletion Processes:

a. Gravitational Settling and Impacting. The exhaust clouds from solid-propellant rockets contain at least some particles that are large enough to settle under the influence of gravity. If strong acids are present in the exhaust, smaller particles may become very hygroscopic and accumulate enough water to have a definite fall velocity. In general, spherical particles larger than 20 microns [20] will have a tendency to settle if their density is large enough. For liquid water drops up to 500 microns in diameter, the fall velocity of the drops is as small or smaller than the vertical velocities associated with daytime turbulence. The appropriate diffusion model for this case is a combination of normal diffusion and settling. A procedure for revising concentration estimates to account for depletion of the total material in the cloud due to settling is presented in Meteorology and Atomic Energy, 1968 [20]. The correction factors corresponding to the six Pasquill-Gifford stability categories are shown as functions of distance in Figure 41. Fall velocities may be estimated from Figure 42.

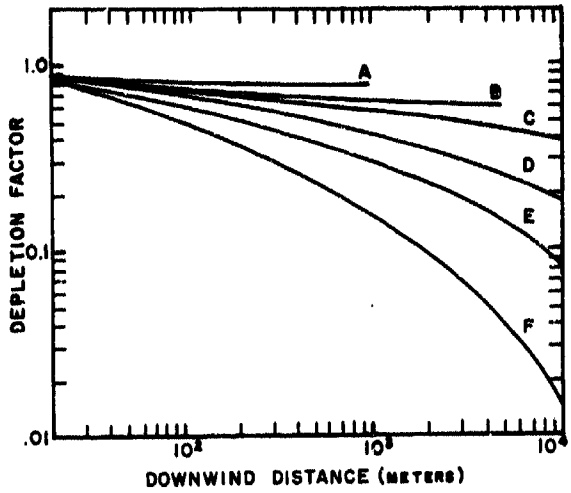

Figure 41. Depletion of Pollution Concentration Due to Gravitational Settling of Particles ($v_f/U = .01$ where the v_f is the deposition velocity).

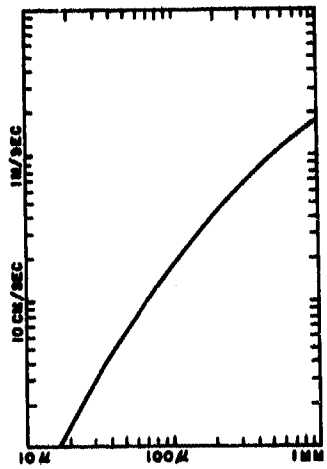

Figure 42. Fall Velocity of Spherical Water Drops as a Function of Size.

b. Washout by Natural Precipitation. Washout of contaminants from the air by precipitation is of considerable importance when considering the concentration of radioactive material in the atmosphere because it represents the only way other than gravitational settling by which radioactive atoms can be removed. For that reason the subject of precipitation washout is important. A useful

first approximation is to consider that the amount of material removed from the toxic cloud per unit time is proportional to the concentration. Then, the reduction in concentration downwind is proportional to $e^{-kx/U}$ as seen in the previous section. All of the graphs required for adjusting the downwind concentrations due to chemical reaction can also be used for computing washout. The real uncertainty is the selection of a proper value of k for washout (Section 5.4 of [20]). The washout problem is relevant to two types of situations involving toxic substances. The first is the case of highly soluble gases and the other is when the toxic material is in the form of solid particles too small to settle out, but larger than one micron in diameter. It is not expected that staff meteorologists will attempt washout calculations. The USAFETAC should be consulted if washout calculations are needed because there are substantial problems in the area of precipitation climatology involved in the selection of the appropriate k values.

4. Characteristics of Real Vapor Releases.

All of the calculation methods presented so far were based on the assumption of an instantaneous point source or a continuous point source. The point-source approximation is generally acceptable for a spill of liquids covering a fairly large area as long as the concentration calculations are not needed for downwind distances less than ten times the diameter of the spill. Nevertheless, the error involved would still exceed 1% for a distance of three kilometers if the diameter of the spill area were 50 feet. The error in the point-source approximation is always on the safe side for locations along the centerline of the cloud if the calculation is made assuming that all of the toxic vapor originates at a point in the center of the spill area.

The most questionable assumption when dealing with actual vapor releases is the assumption that the source strength is constant for 15 minutes or more. This assumption is especially bad in the case of either compressed gases or cryogenic fuels. In both such cases, the source strength decreases rapidly in the first few minutes. In the case of compressed gases, the rate of release is determined by the internal pressure of the holding tank. The tank pressure is reduced with time not only because the gas is escaping, but also, during the first few minutes by adiabatic cooling of the gas. An example, Figure 43 shows the rate of escape of compressed chlorine through a 1 1/3-inch hole in a 55-ton tank car [13].

The rate of evaporation of a spill of cryogenic fuels is determined primarily by the temperature of the ground surface. The evaporation cools the ground just as the temperature of a wet-bulb thermometer is reduced by evaporation. Eventually, an equilibrium temperature is reached at which the heat lost from the surface due to evaporation of the fuel is equal to the upward flow of heat by conduction through the soil. A recent analysis [30] of the evaporation of cryogenic fuels indicates that, during the cool-down period, the evaporation rate is given by

$$(21) \quad Q_A = \frac{T_i - T_o}{\rho_L \Delta H_L} \sqrt{\frac{\rho_s C_s k_s}{\pi t}}$$

where Q_A = evaporation rate per unit area

T_i = initial temperature of soil

T_o = boiling temperature of cryogenic fuel

k_s = thermal conductivity of soil

C_s = specific heat of soil

ρ_s = density of soil

ρ_L = density of fuel in liquid form

ΔH_L = latent heat of evaporation of fuel.

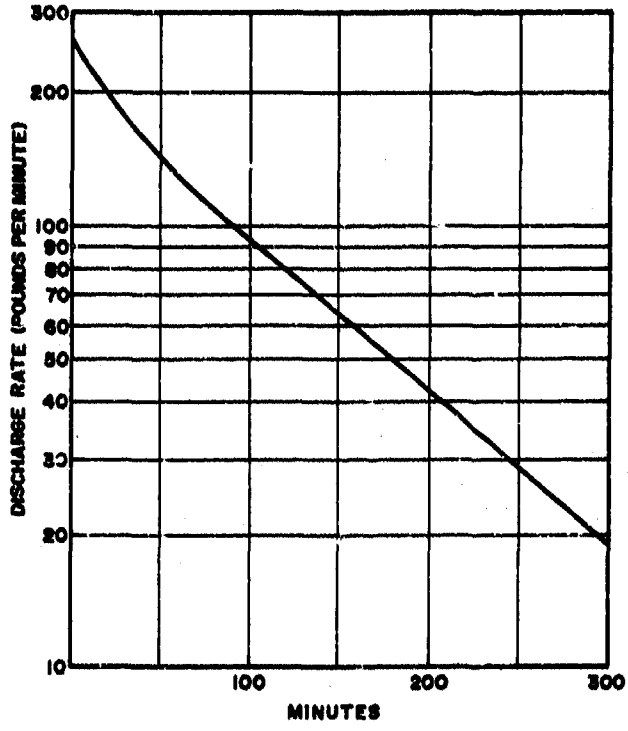

Figure 43. Rate of Escape of Compressed Chlorine Gas [13].

Equation (21) applies from shortly after the spill to the time that an equilibrium ground temperature is reached. The change of evaporation rate with time is illustrated by Figure 44. The slope of the line on a log-log plot is always -1/2 because the denominator of Equation (21) contains the square root of time, but the ordinate value depends on the physical properties of the soil and the fuel involved.

The non-steady source strengths involved with actual vapor releases result

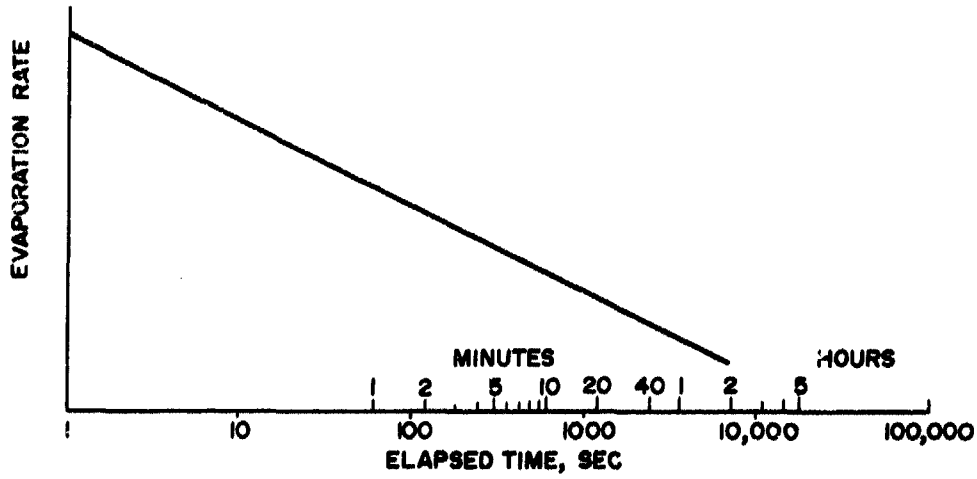

Figure 44. Change of Evaporation Rate with Time.

in a downwind concentration that changes with time. Typical concentration profiles at two different times are shown in Figure 45 for the case where the fuel of Figure 44 is spilled into a diked enclosure, 400 feet on a side. The concave shape of the curve reflects the decreasing evaporation rate. For any particular time after the spill, there would be two downwind concentration maxima: one close to the spill and the other at the farthest distance downwind.

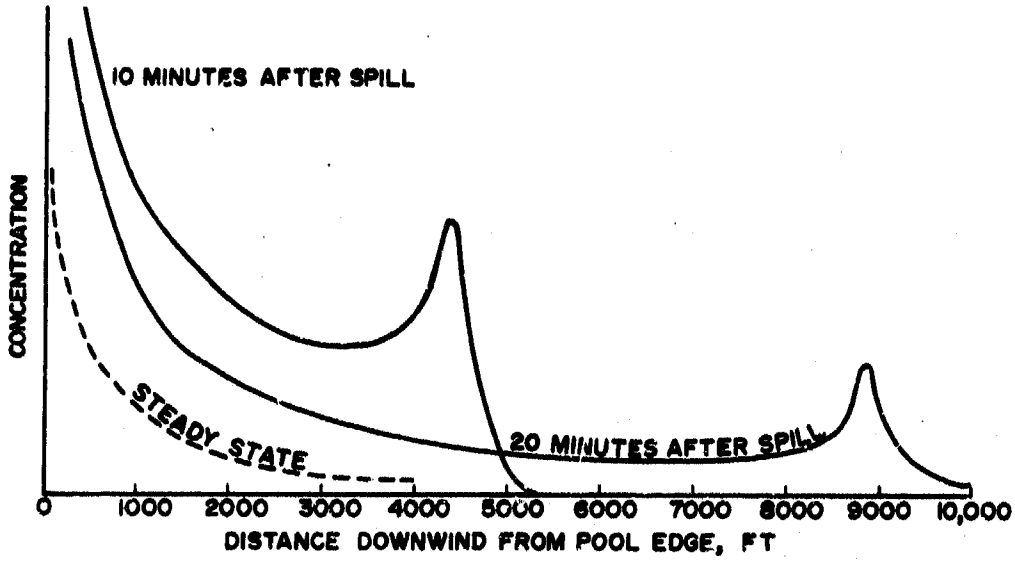

Figure 45. Typical Downwind Profiles of Concentration when Evaporation Rate is Not Steady.

For fuels which have a boiling point near or above normal atmospheric temperatures, the effect of evaporation on the source strength is much less, and it is possible to approximate the source strength by a steady state. There is always an initial wet-bulb effect but, in this case, the change of evaporation rate is less drastic and a steady state is reached sooner. The prevailing wind speed determines the evaporation rate together with the equilibrium temperature. The most appropriate rate of evaporation for a particular fuel should be obtained from operations or environmental safety personnel. For the liquid propellants used in the Titan-series rockets, a classified report by Space Technology Laboratories, Inc. [10] contains a compilation of the data used in specifying the operating-safety distance criteria for toxic sources at the Air Force Eastern Test Range and the Air Force Western Test Range. That report is considered the best currently-available reference on the relation of source strength to wind speed, propellant temperature, area of spill, and density of the liquid. However, since it is not readily available to most AWS personnel, we strongly recommend, if assistance is required in this type of pollutant problem, that units contact USAFETAC through their AWS channels.

5. Diffusion from Buoyant Sources.

So far we have considered only releases at ground level of toxic substances that have nearly the same density as air. This limitation was appropriate in safety analysis for the fuels used in the "core" of the Titan-series missiles. However, there are now rocket motors in which the exhaust products are toxic. The classic example of this type of motor is the solid-propellant motor with beryllium additives.

There is a fundamental difference between the pollution problem of missile liquid propellants and the pollution problem for toxic exhausts. The toxic exhausts are very hot and, therefore, much lighter than the surrounding air, which causes the exhaust to rise initially. Opposing this tendency for the exhaust to rise is the large downward velocity of the gases in a normal missile launching. These opposing tendencies result in the formation of a complex, but nearly spherical, cloud of gases at the launch pad, which then slowly rises. The behavior of this cloud for Titan III boosters has been analyzed by the Aerospace Corporation [8].

a. Traditional Approaches. The toxic hazards associated with these rising clouds are usually evaluated by assuming that the diffusion pattern at any distance downwind is equivalent to the pattern from a non-buoyant elevated source. Near the source this equivalent release height would necessarily become higher and higher with increasing downwind distance as the exhaust cloud continues to rise. Eventually, when a stable layer is reached, the cloud-rise will stop. The equivalent release height would then be constant for calculations further downwind. Fortunately, for most toxic hazard calculations the equilibrium cloud-rise is achieved within a few minutes and, therefore, a constant "effective height" can be used. Only for a detailed analysis of hazards near the pad would it be necessary to consider the change of "effective height" downwind.

The existing data on the rise of instantaneous clouds consist mostly of observation of "fireball" clouds from small nuclear-weapon experiments conducted by the Atomic Energy Commission. Figure 46 shows the height rise as a function

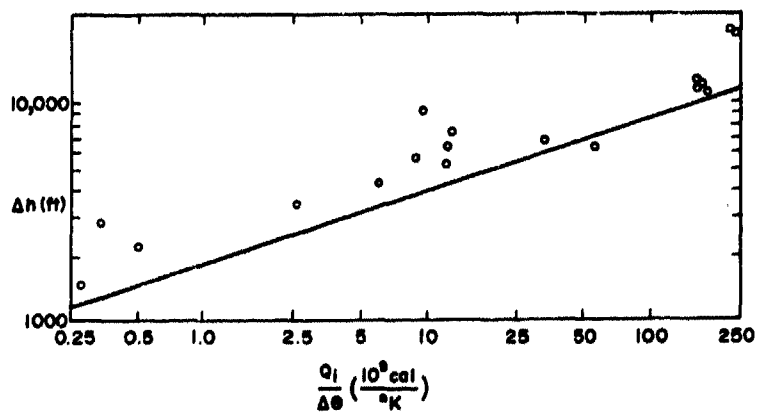

Figure 46. Height Rise of Instantaneous Hot Releases [20].

of $Q_i/\Delta\theta$ where Q_i is the heat energy released and $\Delta\theta$, the difference between the potential temperature at the top of any ground-based inversion and the potential temperature at the equilibrium level. The solid line represents the equation

$$(22) \qquad h = 2.66 \left(\frac{Q_i}{C_p \rho \, \partial\theta/\partial z}\right)^{1/4}$$

which was derived from small-scale laboratory experiments. The height given by Equation (22) may be combined with Equation (9) or (13) to estimate the maximum concentration at ground level. However, the estimates of h from Equation (22) are not too reliable and, therefore, the concentration estimates would be only a first approximation.

If the values of heat released, Q_i, are at all large, it is doubtful whether the maximum ground-level concentration would be obtained before the stability regime changes due to diurnal effects. The real ground-level maximum would occur in connection with a process known as "fumigation," which was mentioned briefly in Chapter 3.

In a typical fumigation situation the toxic products are initially carried aloft by buoyancy into an elevated inversion, where the products remain suspended with little diffusion. After sunrise an adiabatic lapse rate is estimated from the ground up to the base of the stable layer. When the top of the adiabatic layer reaches the height where the contaminants are located, the contaminants are rapidly mixed throughout the adiabatic layer. The concentration would then be uniform through the depth of the remaining inversion.

Unfortunately, there are no tested formulae for predicting the concentration due to buoyant rise and subsequent fumigation. Two formulae have been proposed. One, by Briggs [20] for a steady source is

$$(23) \qquad \bar{q}_{max} = \frac{0.05Q}{F^{1/2} \, s^{-1/4} \, (h_s + 5.1 \, F^{1/4} \, s^{-3/4})}$$

where $\bar{q}_{max}$ = the average concentration at the point of maximum average concentration (g/m^3)

Q = rate of release of toxic material

F = buoyancy flux given by $F = g(\Delta T/T_s) \, V_s r^2$

g = gravitational constant

h_s = height of stack

r = stack radius

s = stability parameter given by $g/T \, \partial\theta/\partial z$

T_s = temperature of stack gases

ΔT = temperature difference between stack and environment

V_s = vertical velocity of stack gases

The other formula, developed at USAFETAC, is applicable to the fumigation from large motors, where the hot exhaust-cloud is expected to be distributed through a fairly deep layer of any inversion. The USAFETAC formula is

$$(24) \qquad \overline{q} = \frac{\Sigma \Delta Q / \Delta t}{\sqrt{2\pi}\, U(h\sigma_y + h^2/8)}$$

where $\overline{q}$ is defined as in Equation (23)

ΔQ = the amount of material that stops rising between any pair of isentropic surfaces, θ_1 and θ_2, within the inversion

Δt = the time interval over which the temperature at the ground rises from θ_1 to θ_2 (minutes)

h = the height above ground of the remaining inversion (meters)

U = mean wind speed at the inversion (meters/minutes)

σ_y = lateral standard deviation of cloud at the point and time where calculation is made

The summation on ΔQ refers to the amounts of material previously "fumigated" from lower levels within the inversion. The equation can be altered to fit the case near a shoreline where the temperature in summer increases inland. In that case, $U\Delta T$ should be replaced by Δx, a distance over which the temperature rises by the required amount.

The formula requires a value for σ_y, the lateral standard deviation of the cloud. An estimate of σ_y for coastal areas which fits data on mesoscale diffusion given by [1] and also those data presented in [20] is $\sigma_y = 25\ t$, where t is the time in minutes since the release and σ_y is in meters. Also fitting the data from the references listed above, the relation $\sigma_y = 70\ x$ can be used, where x is the distance inland in kilometers, for those coastal cases where the temperature change with distance is more significant than the local change with time. These relations probably overestimate the rate of cloud growth with time or distance. The most recent experimental work gives a rate of spreading that is proportional to $x^{0.8}$ or $t^{0.8}$. This is very near unity and substantial differences would be noticed only for very large travel times. Equation (23) contains a measure of the lateral spreading in the numerical coefficient; therefore, no further estimates of spreading are needed to apply that formula.

b. Comment on Statistical Techniques. Completely statistical approaches to the calculation of downwind hazard distances have been very successful for cold ground-level sources. These equations were discussed in Chapter 4. The success of these equations has made it very tempting to try the same techniques for hot sources. However, there are several complications inherent in trying to derive a purely statistical one-step prediction model for buoyant sources.

These difficulties all stem from the fact that a buoyant source is effectively an elevated source, except in the immediate vicinity of the launch pad.

From the discussion in the preceding paragraph, we know that the ground-level concentration will have two maxima and two minima. The primary maximum is on the launch pad itself. The concentration will decrease rapidly away from the launch pad because the exhaust cloud is initially rising much faster than it is diffusing. A short distance downwind the cloud center will have leveled off, and from that point onward, the ground-level concentration increases until a secondary maximum is reached a considerable distance downwind. Finally, beyond the secondary maximum the concentration decreases to zero as the distance becomes very large. From these considerations it is evident that an expression of the form C_p/Q proportional to $x^{-\alpha}$ (a continuously decreasing function of x) could not possibly describe the concentrations for all values of downwind distance. Furthermore, the dependence of C_p/Q on ΔT or σ_A reverses abruptly at the first downwind minimum and again at the secondary maximum. In the zones where concentration decreases with distance, the dependence of C_p/Q on ΔT and σ_A would be qualitatively similar to the cold-source situation. The dependence of C_p/Q on these parameters is reversed in the region between the first downwind minimum and the secondary maximum. Finally, the distances to the first minimum and the secondary maximum are dependent on Q_h (the heat released) and ΔT.

In very unstable conditions the concentration at the secondary maximum may not be much larger than at the first minimum. A scatter diagram of concentration versus distance would show only a general decrease of concentration with distance and no particular correlation with ΔT or σ_A. This is exactly the result obtained in the Sand Storm diffusion program [24], which was carried out only with unstable conditions at Edwards Air Force Base.

The conclusion that prediction equations of the form of Equations (14) or (15) will not work for all possible distances does not mean that the development of statistical one-step diffusion equations is impossible, only that considerably more physical insight is needed. In particular, it may be possible to develop one-step equations for limited portions of the downwind hazard area. Within any zone where the concentration is increasing or decreasing continuously with distance, a simple equation of the type used in Equation (14) would work. If it is possible to identify certain ranges of downwind distance for which the concentration is always in the increasing zone or always in the decreasing zone, separate equations could be developed for each zone.

The only parameter needed in addition to those in Equation (14) is the height of buoyant cloud-rise. This height, in turn, depends on Q_h and ΔT. To include the buoyant rise it is necessary only to put in an additional factor Q_h^e and recalculate the multiple regression. The best-fitting exponent for ΔT will adjust itself to reflect the role that ΔT plays in determining both the cloud-rise and the vertical diffusion.

c. Continuous Buoyant Sources. The same general principles apply to air pollution emitted from smokestacks or longer-burning fires. The initial heat of the effluent causes the plume to rise and become equivalent to a source higher than the actual height of emission. The traditional approach has been to

estimate the final height of the plume and use that height in the formula for diffusion from an elevated source. This procedure is acceptable only for distance downwind such that the plume has nearly reached its final height.

Until recently, this restriction on downwind distance was ignored in most air-pollution calculations. However, G. A. Briggs, a meteorologist at the Oak Ridge National Laboratories, has given a simple formula for "transitional" plume heights [20]. This formula for the change of effective source height, Δh, with distance is

$$\Delta h = 2.0\, F^{1/3}\, x^{2/3}\, U^{-1} \qquad (25)$$

where U = mean wind at stack height

x = downwind distance

The following were defined in connection with Equation (23)

F = buoyancy flux, $F = g(\Delta T/T)\, V_s r^2$

g = gravitational constant

r = inside stack radius

T_s = stack temperature

ΔT = temperature difference between stack and environment

V_s = stack exit velocity

Once the buoyancy flux, F, has been calculated, the calculation of Δh is easily done with graphical aids as follows:

(1) Calculate buoyancy flux.

(2) Estimate wind speed at release level.

(3) Enter Figure 47 with buoyancy flux as the abscissa and go up to the intersection with the wind value. Then, go across to the ordinate to find the value of $2F^{1/3}\, U^{-1}$.

(4) Enter Figure 48 with the downwind distance as the abscissa and go up to the sloping line corresponding to $2F^{1/3}\, U^{-1}$. From this point, go

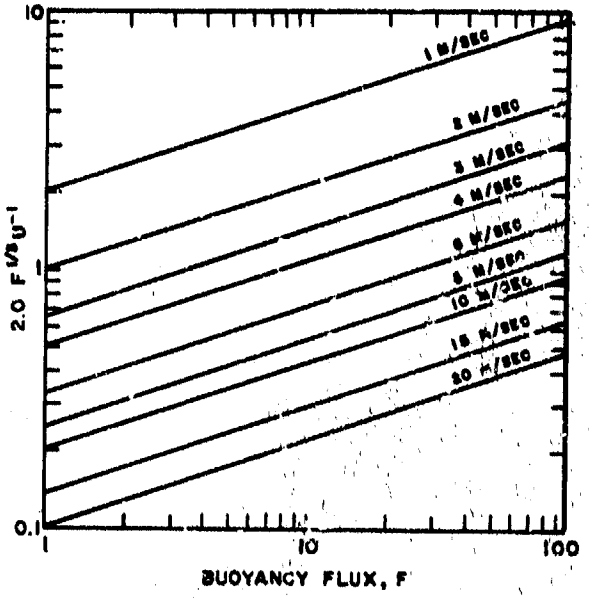

Figure 47. First Step in Evaluating Transitional Plume Rise.

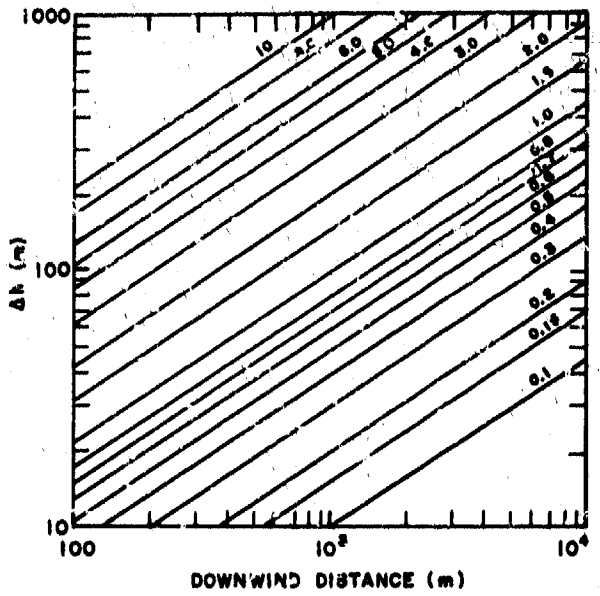

Figure 48. Second Graph for Transitional Plume Rise.

across to the ordinate to get the value Δh.

(5) Check to see that the final plume height has not been reached (see following paragraph).

It is observed that all plumes and buoyant clouds of air pollution eventually lose their buoyancy. The prediction of the final height is especially complicated for smokestacks because the gases start out with some vertical momentum. Consequently, a large number of different formulae have appeared. One of the most successful to date was developed by Holland [12]. It reads

$$\Delta h = \frac{V_s\, d}{U}\left(1.5 + 2.68 \times 10^{-3}\, p\, \frac{T_s - T_a}{T_s}\, d\right) \tag{26}$$

where Δh, U, T_a, T_s, and V_s are defined as before, and:

d = inside stack diameter

p = atmospheric pressure

This formula is now found to underestimate the final height. Better results are obtained by multiplying Δh by three.

Chapter 6

THE ROLE OF THE STAFF METEOROLOGIST IN AIR POLLUTION CONTROL

1. General.

There are two essential steps in air pollution control. They are: (1) reducing emission of pollutants where practical by improved engineering and (2) curtailing operations when atmospheric dispersion is not active enough to produce acceptable pollution levels. A corollary activity is establishing hazard areas in case toxic pollutants are involved. Meteorological support is needed for operational decisions on curtailing operations or setting up potential hazard areas, and for planning purposes in all aspects of air pollution.

2. Meteorological Support for Planning.

Meteorological support for planning purposes is just another kind of climatology — a diffusion climatology. Normally, new facilities will be sited and constructed so as to minimize the possible air pollution effects of any planned or accidental release. If it were possible to find a perfect site, one at which pollution concentrations would never exceed safe levels in populated areas, there would be no need for operationally-oriented meteorological support.

The staff meteorologist normally reviews plans with the goal of determining what sort of meteorological support will be required. The factor of possible air pollution should now be included in this review. It is impossible to emphasize too strongly the importance of examining all aspects of Air Force research and development programs to determine whether a serious environmental hazard may exist routinely or accidentally. While the recognition of environmental hazards is normally the responsibility of bio-environmental engineers, it is often the meteorologist who has the better "feel" for those combinations of emission and meteorological conditions that will produce dangerous concentrations of pollutants. The price of failing to detect environmental hazards until late in the development program is often a costly re-programming of the system. If the environmental hazard is recognized early in the development, meteorological-data networks and control procedures can be developed concurrently.

Much of what has just been said pertains to such pollutants as toxic missile fuels and combustion products. But there is also a need for meteorological support in planning the more routine air-base functions, such as power-plant operations and outdoor burning for incineration or training of fire-fighting crews.

3. Studies of Pollution Potential.

In the air pollution analysis it is necessary to consider the prevailing

winds and the modifications that are caused by topography or diurnal changes. Combined with studies of the mean wind speed and direction should be studies of the diffusive power of the atmosphere. In most cases, the diffusivity would be estimated based on the considerations of Chapters 4 and 5. If a really critical determination of concentrations is required, an air-tracer survey should be conducted at the site in order to provide a reliable system for deciding whether or not to curtail operations at a given time.

The evaluation of potential hazards both for site-selection purposes and for specific releases involves a knowledge of atmospheric behavior on all scales from the highs and lows of the synoptic weather map to the individual eddies that dilute and redistribute the toxic matter and other pollutants within the atmosphere.

Special summaries of hourly weather observations can yield a climatology of diffusion according to the Pasquill-Gifford system. First, the frequency of each category is computed for each wind direction. Next, an estimated median-wind-speed for each category is used together with mathematical representations of Figures 21 and 22 to arrive at average concentrations.

4. Support for Current Operations.

Two types of pollution concentration estimates are required on a more-or-less "real time" basis. One is used for a decision whether or not to curtail operations. The other, pertaining only to toxic substances, is the area to evacuate in case of an accidental release. Preparing a radioactive fallout plot is an example of this type of hazard analysis. Related to this second category of support is operational forecasting for intentional releases of toxic materials such as tests of CW agents or tests of rocket engines using toxic propellants.

Forecasting for intentional releases requires more precision than evaluating the hazard areas for accidents, because the amount of material released is known for the intentional case. It has been said with regard to accidental releases that "by the time you figure out how much material was released, the incident is over except for settling the lawsuits." Therefore, it is important to determine in advance the probable hazard areas for a number of typical situations. The situation which is commonly investigated by the Atomic Energy Commission is the maximum credible accident. A release of this magnitude is then evaluated for hazard distances under a variety of meteorological conditions.

5. Sources of Data and Technical Assistance.

Within the Air Weather Service, expert assistance on diffusion and air pollution problems may be obtained from the USAFETAC. This unit, which has long provided climatological services, has been given the mission of providing micrometeorological services as well. USAFETAC can provide studies based on data from routine meteorological observations taken almost anywhere. There are also limited amounts of micrometeorological data, mostly from existing missile ranges. USAFETAC personnel can assist in interpreting these data as they apply

to the pattern of dispersion of material released into the atmosphere.

In certain cases the site may be so remote that routine meteorological observations do not exist. Also, it has been the experience of many workers in micrometeorology that it is quite difficult to quantitatively predict the magnitude of the local variations even when the qualitative variations are understood. For one or both of these reasons, it may prove necessary to employ mobile meteorological observation teams. Air Weather Service has a capability to provide routine meteorological observations from remote sites through the resources of the 6th Weather Squadron. If the requirement for remote observations is recognized in time to program this support in the normal budgetary cycle, the remote-site observation program can be funded by Air Weather Service. If the requirement is not recognized in time for the normal budgetary processes, the remote-site observation program must be paid for with a transfer of funds to Air Weather Service by the operational agency that needs to use the remote site. Time limitations may dictate that the observational program be handled by a contractor, possibly in connection with an air-tracer survey as outlined below.

In cases where frequent releases of toxic material are contemplated, viz., test ranges, and air-tracer survey should be undertaken in order to provide a reliable system for deciding whether or not to release at a given time. An air-tracer survey might even be justified to fully determine the extent of the hazard associated with the maximum credible accident. An air-tracer survey consists of releasing known quantities of inert material into the atmosphere under a variety of meteorological conditions and sampling the concentration of this material at a variety of downwind and crosswind distances. The staff meteorologist can and should recommend to the operator of the proposed facility that an air-tracer survey be conducted when necessary. The organizations that conduct air-tracer surveys can also take the routine meteorological observations if these cannot be obtained from Air Weather Service resources. The USAFETAC is familiar with tracer studies which have been conducted in the past and can provide assistance in defining objectives for contract meteorological programs.

Appendix

SUMMARY OF COMPUTATIONAL TECHNIQUES

In this Appendix the computational aids and graphs (full size) are assembled at the end for quick reference. Step-by-step procedures are given for several examples.

The systematic nature of these calculations can easily give the impression that air pollution concentrations can be accurately estimated. It should always be kept in mind that the concentrations calculated by these techniques apply to open, level terrain. For an area characterized by irregular terrain, the situation is severely complicated by the many local factors that were discussed in Chapter 2. The estimated concentrations should then be subjectively modified to account for local changes in the flow pattern and differences in the intensity of turbulent mixing.

1. General Form of Calculations.

The concentration of pollutants consists of the background level plus the contribution due to local sources. All of the methods discussed in Chapters 4 and 5 concern diffusion from local sources. For simplicity, the background concentration will be omitted in the examples which follow.

The contribution due to local sources is computed by evaluating certain factors in order. Each additional consideration can be accounted for by multiplying the result of the previous step by another factor. The complete equation for concentration from a single source can be represented as a series of products, thus

$$\overline{q} = [\text{Source Strength}] \times [\text{Along-Wind Dilution}] \times [\text{Cross-Section Dilution}] \times [\text{Vertical Term}] \times [\text{Lateral Term}] \times [\text{Depletion Term}].$$

Any time a factor can be neglected, the value of its term is unity. Since multiplying by one leaves the answer unchanged, the unneeded terms are simply omitted. The first three terms must always be used, and the vertical term is usually needed. Numerical values of the various factors can be obtained from Figures 21 through 34, 36, 37, 47, and 48 with use of Tables 1 and 2. The use of these values in the equation will now be illustrated.

a. Source Strength. If the source is continuous, it should be stated in grams per second. If the source is instantaneous, the source strength is simply the mass of contaminant release. All of the graphical aids in this report require metric units, i.e., meters, seconds, grams, etc. Thus, the mass should be converted to grams (one pound equals 453.6 grams).

b. Along-Wind Dilution.

(1) Continuous Source. Divide the source strength by the wind speed (meters per second) (1 kt = 0.515 m/sec). For smokestacks, the wind at release (stack) height can be estimated from Figure 49. For example, the wind at 66 feet would be 1.33 times the strength of the anemometer-level wind under neutral conditions.

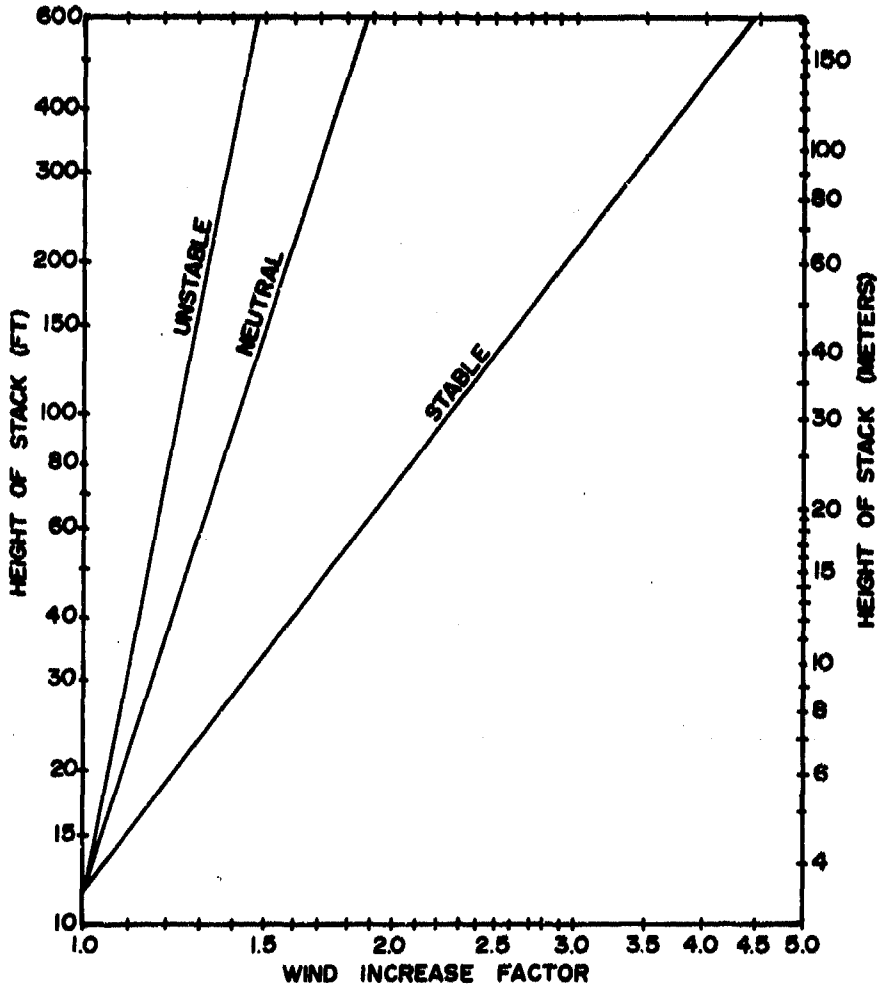

Figure 49. Graph for Determining Wind Speed at Release (stack) Height.

(2) Instantaneous Source. Select a value from the right-hand scale of Figure 32 according to the applicable stability category and the desired distance downwind of the release point. For example, at 1000 meters downwind in neutral conditions, the divisor would be about 280 on the logarithmic scale. Select the appropriate line as follows: If the stability category from Table 1 and Table 2 is A or B, use the line marked "unstable." The "neutral" line

corresponds to Category D and the "stable" line is equivalent to Category E or F. For Category C, use a value between the "unstable" and "neutral" values.

c. Cross-Section Dilution. The vertical and cross-wind dimensions of the plume or puff increase downwind. The same amount of material must occupy a larger and larger space, thus lowering the concentration at the center of the plume or puff. After this step the units will be grams per cubic meter. Proceed as follows:

(1) Continuous Source. Use the value on the ordinate of Figure 23 as a multiplier.

(2) Instantaneous Source. Use the value on the ordinate of Figure 34 as a multiplier. For example, at a downwind distance of 300 meters in unstable conditions, the factor would be about 5×10^{-4}. Selection of the three categories was explained in paragraph 1(b)(2) of this Appendix.

d. The Vertical Term. The vertical term is needed in most cases, even for concentrations measured at the height of the cloud center. In its most general form, the vertical term is

$$e^{-(z - h)^2/2\sigma_z^2} + e^{-(z + h)^2/2\sigma_z^2}$$

where h is the height of the cloud center above ground and z is the height above ground where the concentration is measured. This general form is given here only for the sake of completeness and is not used in the examples shown in this Appendix. An explanation of the equation and the reason for the second term is given by Sutton ([22] pp. 139-140) and in Meteorology and Atomic Energy 1968 ([20] p. 99).

When measuring at ground level, z becomes zero and the general equation reduces to

$$2e^{-h^2/2\sigma_z^2}$$

with h, the height of the cloud center above the ground. It is this reduced form of the equation that is used in the examples.

To aid in the calculations, Figure 24 was developed. It gives values of $e^{-a^2/2b^2}$ on the ordinate for any value of a on the abscissa. Values of the parameter b are shown as a family of sloping lines. To use the figures to evaluate the vertical term, use the value of h as the abscissa and proceed upward to the (interpolated) sloping line corresponding to σ_z and proceed across to the appropriate value of

$$e^{-h^2/2\sigma_z^2}$$

on the ordinate. Then double the result.

The vertical term must be modified if buoyant sources are involved, or if there is a significant elevated inversion. If the source is buoyant, the effective source height must be found. This modified value of h is then used to evaluate the vertical term in the usual way. Rules-of-thumb for estimating the effect of inversions are given in Chapter 4. The necessary steps for various situations can be summarized as follows:

(1) Non-Buoyant Sources without Elevated Inversions. For a given stability category and distance downwind, find σ_z from Figure 22. Evaluate the term

$$2e^{-h^2/2\sigma_z^2}$$

with the aid of Figure 24, as described above.

(2) Buoyant Sources without Elevated Inversions. Calculate Δh according to the Holland formula

$$\Delta h = \frac{3\ V_s\ d}{U}\left[1.5 + 2.68 \times 10^{-3}\ p\left(1 - \frac{T_a}{T_s}\right) d\right]$$

Next, compute the buoyancy flux $F = g\ V_s\ R^2\ (1 - T_a/T_s)$. (The definitions of the symbols were given in Chapter 5.) Again, all units should be in meters or meters per second. Enter Figure 47 with the buoyancy flux as the abscissa and proceed up to the sloping line corresponding to the wind speed. From this point, read across to the ordinate to find the value $2F^{1/3}\ U^{-1}$. Now, enter Figure 48 with downwind distance as the abscissa and proceed up to the sloping line corresponding to $2F^{1/3}\ U^{-1}$. From that point, proceed across to the ordinate to find a second value of Δh. Use whichever value of Δh is <u>smaller</u>. Add Δh to h and then proceed as in (1) above.

(3) Significant Inversion Aloft. First, use Figure 22 to find σ_z. There are three types of situations:

(a) For σ_z less than half the inversion height, neglect the inversion and proceed as in (1) above.

(b) For σ_z more than twice the inversion height, the vertical term is $2.56\ \sigma_z/H$, where H is the inversion height. By using this vertical term, we convert Equation (10) to Equation (17).

(c) For σ_z between half and twice the inversion height, proceed as follows. First evaluate the vertical term according to (1) or (2) above for σ_z equal to half the inversion height. Plot this value on a log-log plot (such as Figure 22 or 23) at the downwind distance where σ_z is half the inversion height. At the distance where σ_z is twice the inversion height, plot the value 5.12. The vertical term for any downwind distance in this range can be found by joining the two plotted points with a straight line. These steps are essentially equivalent to following the "rules of thumb" given in Chapter 4, paragraph 7. There would be a slight difference because the plot of σ_z on log-log

paper is not a straight line.

e. The Lateral Term. This term is not needed for calculating peak concentrations unless the peak is the result of the combined effect of several scattered sources. The value of the lateral term is always unity for peak concentrations from single sources. The form of the term is

$$e^{-y^2/2\sigma_y^2}$$

where y is the cross-wind distance in meters.

(1) Continuous Sources. Figure 21 gives values of σ_y as a function of downwind distances and stability category for the Pasquill-Gifford System. Use Figure 21 to get σ_y and then use Figure 24 to evaluate

$$e^{-y^2/2\sigma_y^2}$$

as explained for the vertical term. Isopleths of $\bar{q}$ U/Q for ground-level concentrations from ground-level sources are provided as Figure 25 through 30. The concentration, off axis, for any other values of z and h can be found by using half the vertical term as a multiplier for the values in Figures 25 through 30.

(2) Instantaneous Sources. Figure 33 gives values of σ_y for three stability categories: unstable, neutral, and stable. Select the stability category from Table 2 and the equivalence suggested for "along-wind dilution." Use these values of σ_y with Figure 24 to evaluate the lateral term.

f. The Depletion Term. Various depletion processes are discussed at the beginning of Chapter 5.

(1) Concentrations Remaining in Pollutant Cloud. Calculate depletion rate per meter (K/U where K is depletion per unit time). Be sure the same time units are used for U and K. Wind speeds in knots can be used with Figure 36 to find K/U if K is expressed in depletion per minute. Figure 37 gives the depletion term as a function of distance for a family of K/U values.

(2) Pollutants Deposited on the Ground. There are two general cases: dry deposition and washout due to rain. In the dry case, the deposit rate is proportional to the ground-level concentration. For washout, the deposit is proportional to the vertically-integrated depletion. Refer to Chapter 5 for details.

2. Illustrative Examples.

In this section we present some complicated problems which require evaluation of all terms except the depletion term and show the step-by-step solution of these problems.

Example 1. It is a summer afternoon at Edwards AFB and the surface wind is from 350° at 13 kts. A small experimental rocket motor containing 20 grams of

finely divided beryllium explodes on the top of a 15-ft test stand releasing a cloud of beryllium particles which, for this problem, is assumed to have no buoyancy. A group of engineers was standing 150 yards south of the test stand at the time of the explosion. What was the maximum concentration of beryllium that the engineers were exposed to?

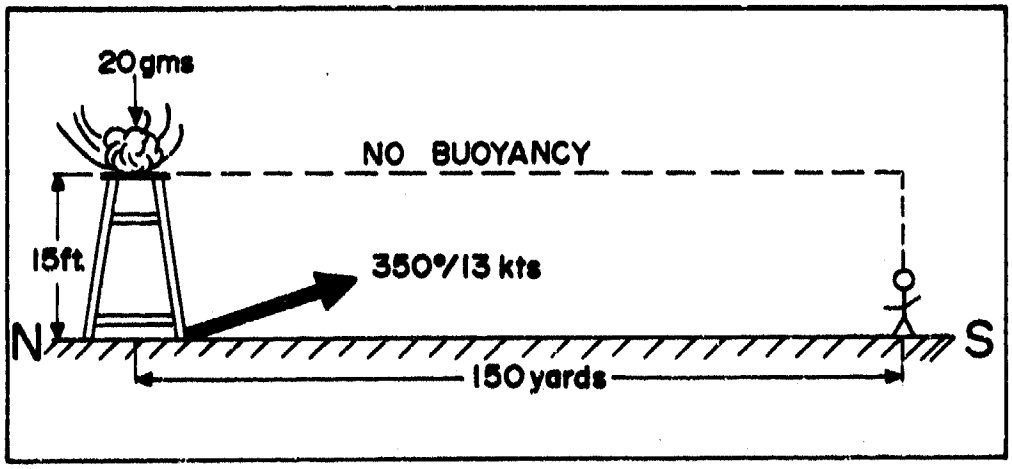

Figure 50. Diagram of Example 1.

Solution:

Step 1. Source strength: This is given as 20 grams; conversion to other units is not required in this case.

Step 2. Along-wind dilution factor: Using Figure 32 find the horizontal downwind distance, x (in meters).

$$x = 150 \text{ yds} \times \frac{3 \text{ ft/yd}}{3.28 \text{ ft/meter}} \times \text{cosine } (10^\circ) = 135 \text{ meters}$$

Using this distance, enter Figure 32 to get the downwind dilution factor. Table 2 gives the stability category as C. Interpolate between the "neutral" and "unstable" line to obtain 25 meters as the factor. Dividing 20 by 25 gives 0.80 grams/meter.

Step 3. Cross-section dilution: Go to Figure 34. For a downwind distance of 135 meters, interpolate between the "neutral" and "unstable" curves to obtain the factor 4.6×10^{-3} per square meter. Multiply this by the result of Step 2 to obtain $4.6 \times 10^{-3} \times 0.80 = 3.68 \times 10^{-3}$ grams per cubic meter on the centerline.

Step 4. Vertical term: The Pasquill stability category C has already been selected from Table 2. For this category, Figure 22 gives $\sigma_z = 10$m for the downwind distance 135 meters. There is no limiting inversion

and we are neglecting buoyancy, thus, the vertical term need not be modified. Convert h to meters, i.e., h = 15/3.28 = 4.57 m. Using Figure 24 with a = 4.57 and b = 10, the vertical term is 2 × 0.90 = 1.80. Thus, the concentration directly under the cloud would be $1.80 \times 3.68 \times 10^{-3} = 6.62 \times 10^{-3}$ g/m³.

Step 5. Lateral term: The lateral distance from the cloud trajectory is 150 yd × 3 yd/3.28 m × Sin (10°) = 24 meters. Enter Figure 33 with the downwind distance (135 m) and interpolate again between the "neutral" and "unstable" lines to obtain σ_y, which is 7.5 meters. Use Figure 24 with a = 24 and b = 7.5 to get the lateral term, which is 0.006. Multiplying this by the result of Step 4 gives the answer,

$$\overline{q} \approx 4 \times 10^{-8} \text{ grams/m}^3$$

Example 2. The base civil engineer proposes that a new base heating plant will have a 65-ft stack, four feet in diameter at the top. The stack temperature will be 600°F and stack velocity 10 ft/sec. Sulfur in the fuel oil is expected to produce 270 grams/sec of SO_2 as a combustion product. If the dining hall is 2000 feet northeast of the proposed heating plant, what would be the concentration of SO_2 on the ground at the dining hall at sunrise on a clear morning if the winds were southwest at 4 kts at anemometer level? Assume the air temperature at stack height is 50°F and the station pressure is 1000 mb.

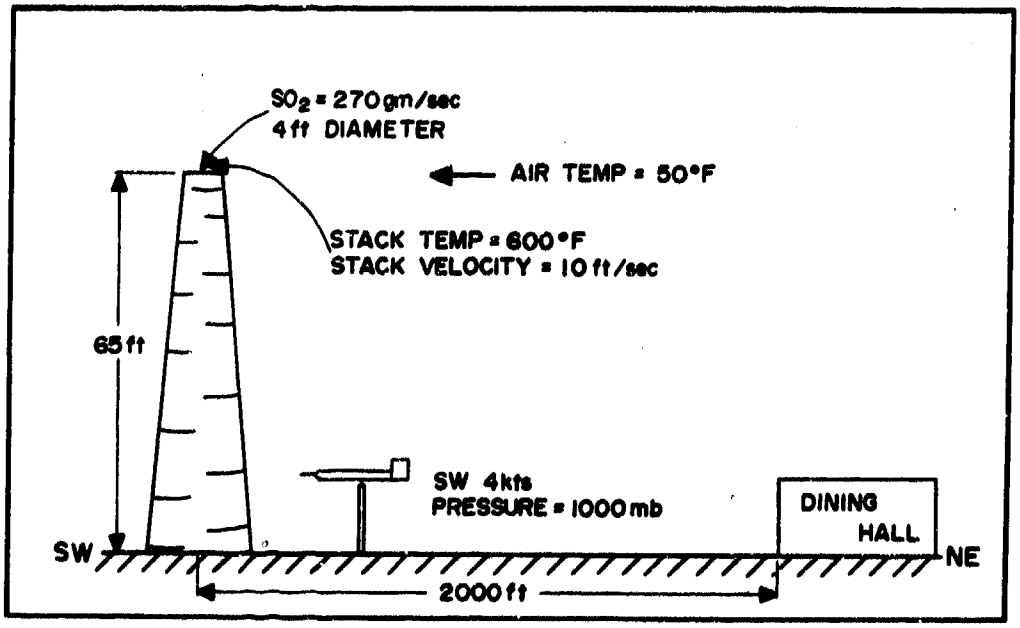

Figure 51. Diagram of Example 2.

Solution:

Step 1. Convert all units to metric. The stack height is 65/3.28 = 20 meters, the stack diameter = 1.22 meters, the stack velocity 3 m/sec, the stack temperature 316°C = 589°K, while the air temperature is 283°K. The surface (anemometer) wind is 2.06 m/sec and the downwind distance to the dining hall is 610 meters. The continuous source strength (270 gm/sec) is already in metric units, and the stability condition is stable (Category E).

Step 2. Along-wind dilution: First, find the wind at stack height. From Figure 49, the multiplier would be 1.95 under stable conditions, thus, the wind speed is 4 m/sec. Dividing the release rate (270 grams/sec) by 4 m/sec gives 67.5 grams/meter.

Step 3. Cross-section dilution: The stability category determined from Tables 1 and 2 is E. The dilution factor, Figure 23, for Category E and a downwind distance of 610 meters is 3.43×10^{-4}. Multiply this by 67.5 (the result of Step 2) to get 2.30×10^{-2} g/m³.

Step 4. Vertical term: This problem involves a buoyant source, so the first thing is to evaluate the additional rise, Δh, above the stack height. The Holland formula for Δh with a correction of 3 gives

$$\Delta h = \frac{3(3)(1.22)}{4}\left[1.5 + 2.68 \times 10^{-3} \times 1000 \left(1.0 - \frac{283}{589}\right)(1.22)\right]$$

$$= 2.74\ (1.5 + 1.71) = 8.8 \text{ m}$$

Compare this with the "transitional" plume rise given by Figures 47 and 48. The buoyancy flux, F, is

$$9.8 \times 3.0 \times (.61)^2 \left(1.0 - \frac{283}{589}\right) = 5.7$$

Enter Figure 47 with 5.7 on the abscissa and read up to the 4 m/sec (stack-height wind) line. The value from this graph (read from the ordinate) is 0.9. Enter Figure 48 at a downwind distance of 610 meters and proceed up to the (interpolated) sloping line corresponding to 0.9 from Figure 47. Reading across to the ordinate, find Δh = 64 meters. Use the lesser value for Δh. Add this to 20 m (the original stack height) to give an effective height of 29 meters. Next, find σ_z from Figure 22. In this case, σ_z is 14 meters. At ground level z = 0. Thus, $|z + h| = |z - h| = 29$. The vertical term (using Figure 24 with a = 29 and b = 14) becomes 0.1 + 0.1 = 0.2. Thus, the ground-level concentration is 4.6×10^{-3} grams/m³ or 4.6 milligrams per cubic meter.

Example 3. Suppose the heating plant of Example 2 continued to emit 270 grams/sec of SO_2 two hours after sunrise, at which time the ground-based inversion had lifted to 200 feet and the surface winds had increased to 9 knots. What would the SO_2 concentration at the dining hall be then?

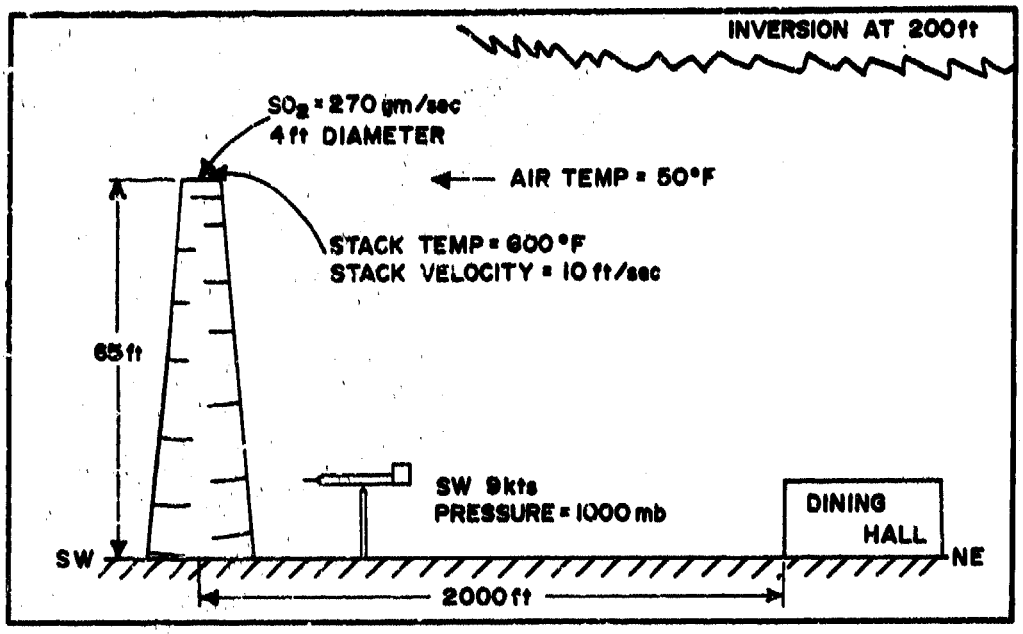

Figure 52. Diagram of Example 3.

Solution:

Step 1. All values are the same as in the last problem except the surface wind is 4.6 m/sec and the stability category is now C.

Step 2. The rate of increase of wind with height should now be interpolated between the "neutral" and "unstable" lines of Figure 49, giving us now an increase factor of 1.3, giving 6.0 m/sec. Dividing 270 by 6.0 gives 45.0 grams/meter.

Step 3. The cross-section dilution factor for 610 meters and C stability is 6.0×10^{-5}. Thus, the concentration on the centerline of the smoke plume is $45.0 \times 6.0 \times 10^{-5} = 2.7 \times 10^{-3}$ grams/m^3.

Step 4. Find the value of σ_z corresponding to 610 meters downwind for C stability. From Figure 22, σ_z is 37 meters. This is more than half the inversion height (61 meters), but less than twice the inversion height. Thus, the method given in paragraph 1d(3) of the Appendix must be used. The distance at which σ_z would be half the inversion height is 480 meters downwind for category C stability. Similarly, Figure 22 gives 2200 meters as the distance where σ_z would be twice the inversion height. First, evaluate the vertical term in the normal way for a σ_z of 30 meters. The effective source height is now somewhat lower because of the increased wind speed at stack height. Δh is now

$$\frac{3(3)(1.22)}{6.0}(1.50 + 1.71) = 5.87 \text{ m}$$

This added to the 20-meter stack height makes the effective height now 26 meters. Enter Figure 24 with a = 26 and b = 30, getting 0.72 for the exponential term. This term, in turn, is doubled to get the vertical term (= 1.44) at 480 meters downwind. Next, find any convenient log-log paper. (Figure 21 or Figure 22 would do.) At 480 meters downwind, plot a point with an ordinate value of 1.44. At 2.2 km downwind, plot a point with 5.12 as the ordinate. Join these two points with a straight line and read 1.75 as the vertical term for a downwind distance of 610 meters. Multiply 1.75 by the result of Step 3:

$$2.7 \times 10^{-3} \times 1.75 = 4.7 \times 10^{-3} \text{ grams/m}^3$$

Notice that this concentration is higher than the concentration calculated in Example 2, even though the surface wind is stronger and the lapse rate is unstable next to the ground.

3. Computational Tables and Graphs.

Tables 1 and 2 along with the figures appearing on the following pages are repeated from preceding chapters of this guide to allow easy access to the information required for the calculations within this Appendix. The larger size of these duplicated graphs will allow more accurate data to be read and their use in solving problems in the field will be enhanced.

TABLE 1

Net Radiation Classes

Cloud Cover	Night	Elevation of Sun			
		≤ 15°	> 15° but ≤ 35°	> 35° but ≤ 65°	> 65°
< 3/8	-2	-1	+1	+2	+3
3/8 or 4/8 at any hgt or broken abv 16000 ft (incl. -⊕)	-1	0	+1	+2	+3
⊕ abv 16000 ft or ⊙ between 7000 ft and 16000 ft	-1	0	0	+1	+1
⊙ below 7000 ft	0	0	0	0	+1
⊕ below 7000 ft	0	0	0	0	0

TABLE 2

Stability Category Based On Wind Speed and Net Radiation

Surface Wind Speed		Net Radiation Class (see Table 1)					
m/sec	knots	+3	+2	+1	0	-1	-2
< 2	< 4	A	A-B	B	D	E	F
2-3	4-6	A-B	B	C	D	E	F
3-5	6-10	B	B-C	C	D	D	E
5-6	10-12	C	C-D	D	D	D	D
> 6	> 12	C	D	D	D	D	D

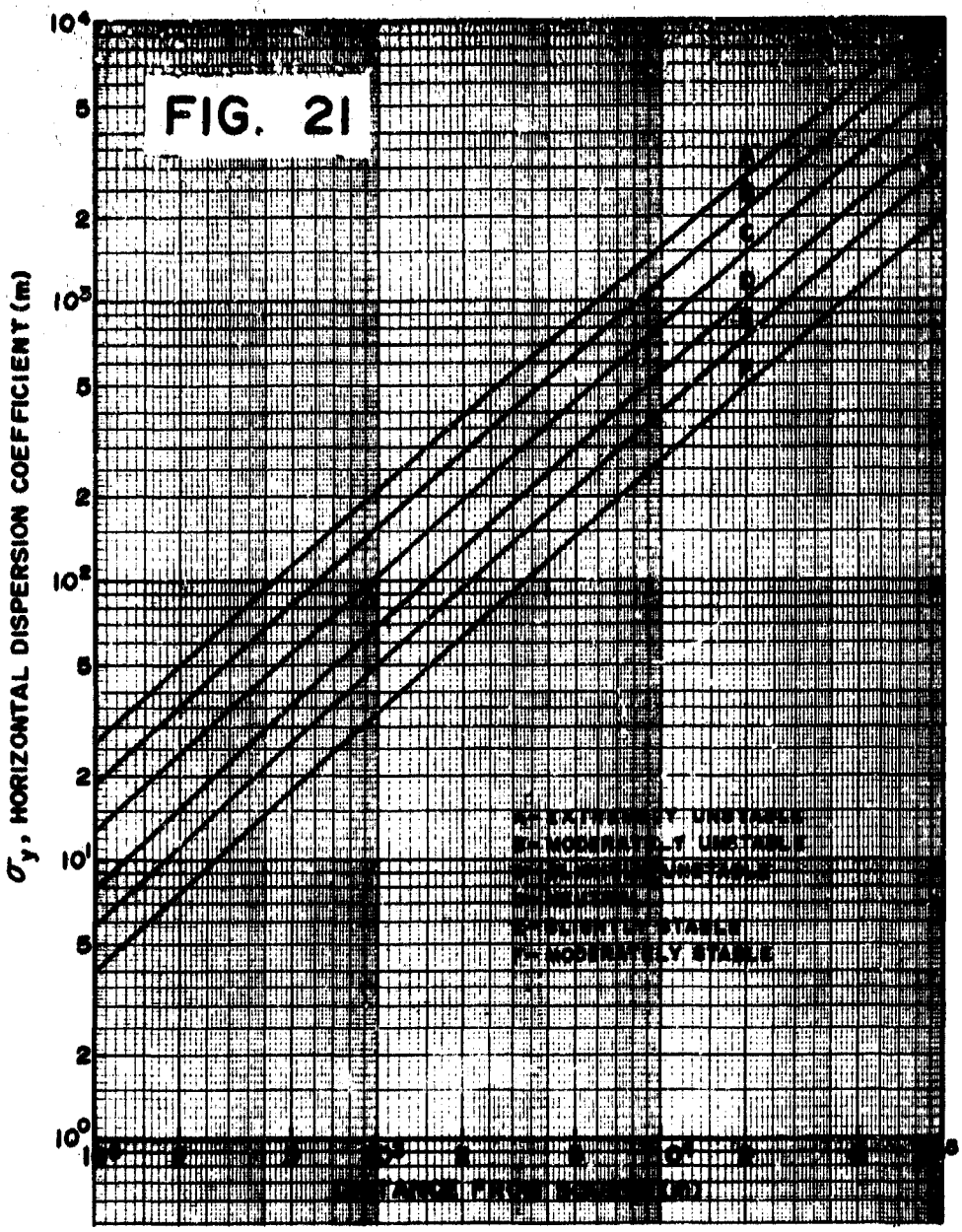

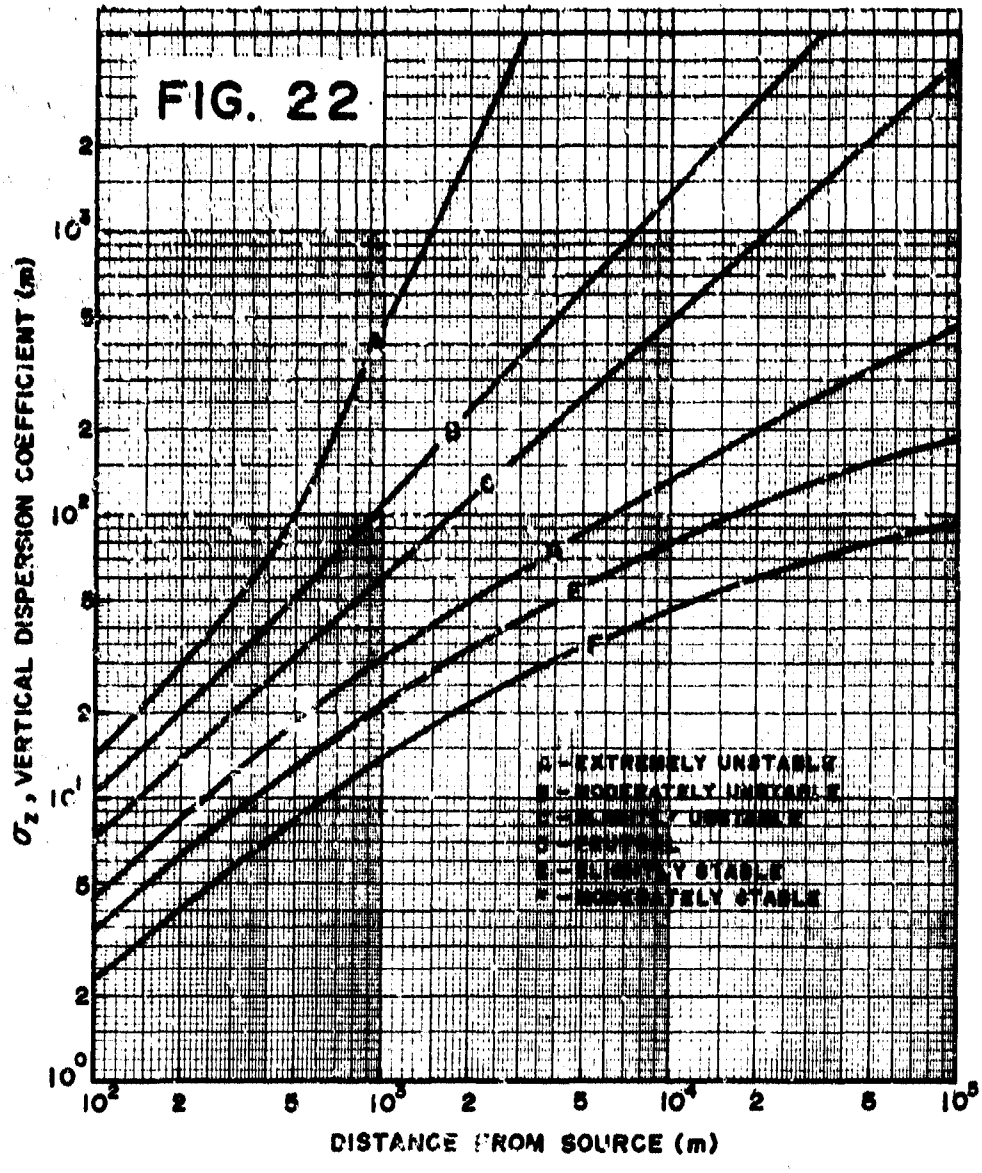
FIG. 22
σ_z, VERTICAL DISPERSION COEFFICIENT (m)
DISTANCE FROM SOURCE (m)
A - EXTREMELY UNSTABLE
B - MODERATELY UNSTABLE
C - SLIGHTLY UNSTABLE
D - NEUTRAL
E - SLIGHTLY STABLE
F - MODERATELY STABLE

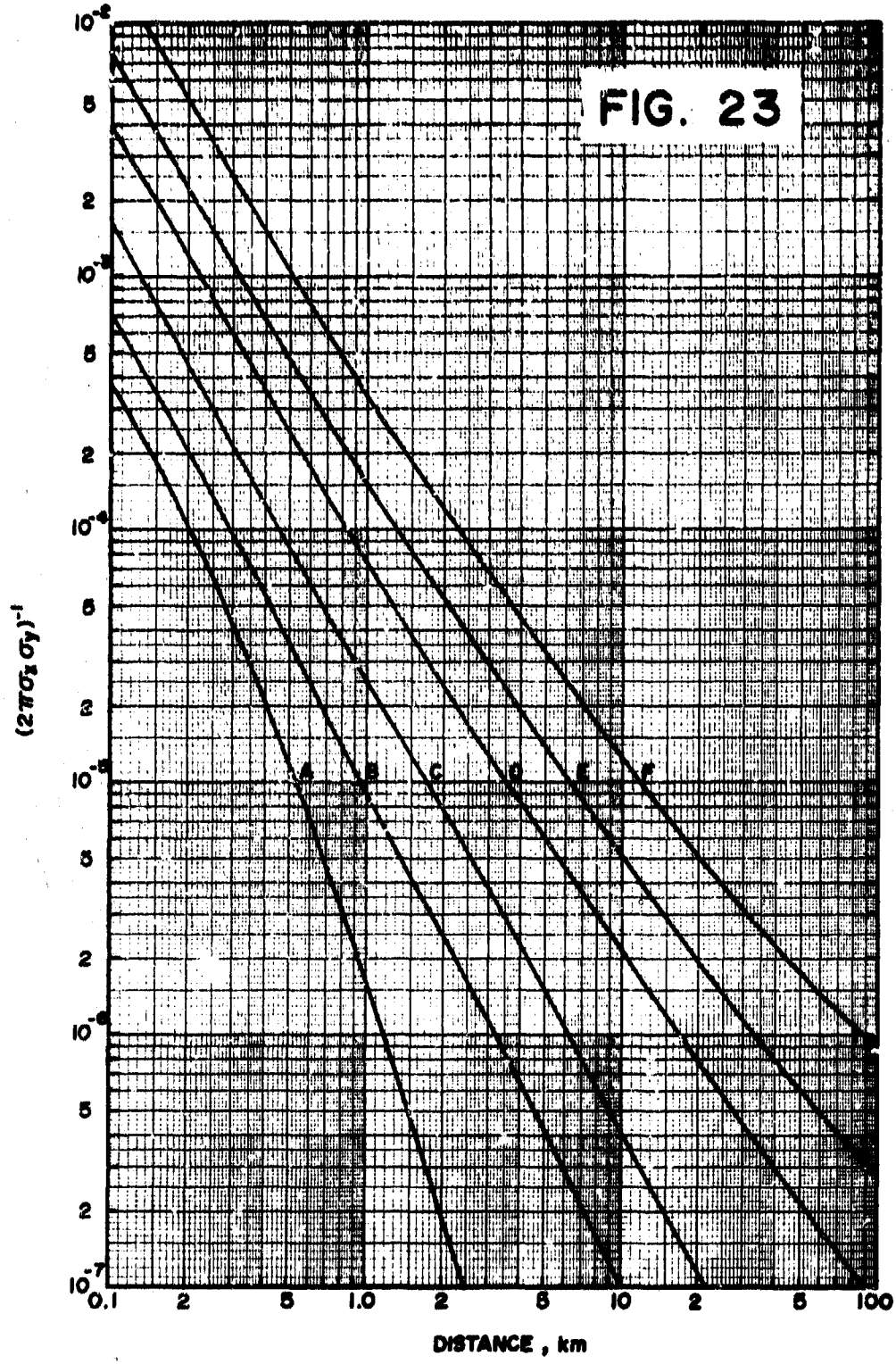
FIG. 23
10^{-2}
5
2
10^{-3}
5
2
10^{-4}
5
2
10^{-5}
5
2
10^{-6}
5
2
10^{-7}
$(2\pi\sigma_z\sigma_y)^{-1}$
A
B
C
D
E
F
0.1
2
5
1.0
2
5
10
2
5
100
DISTANCE , km

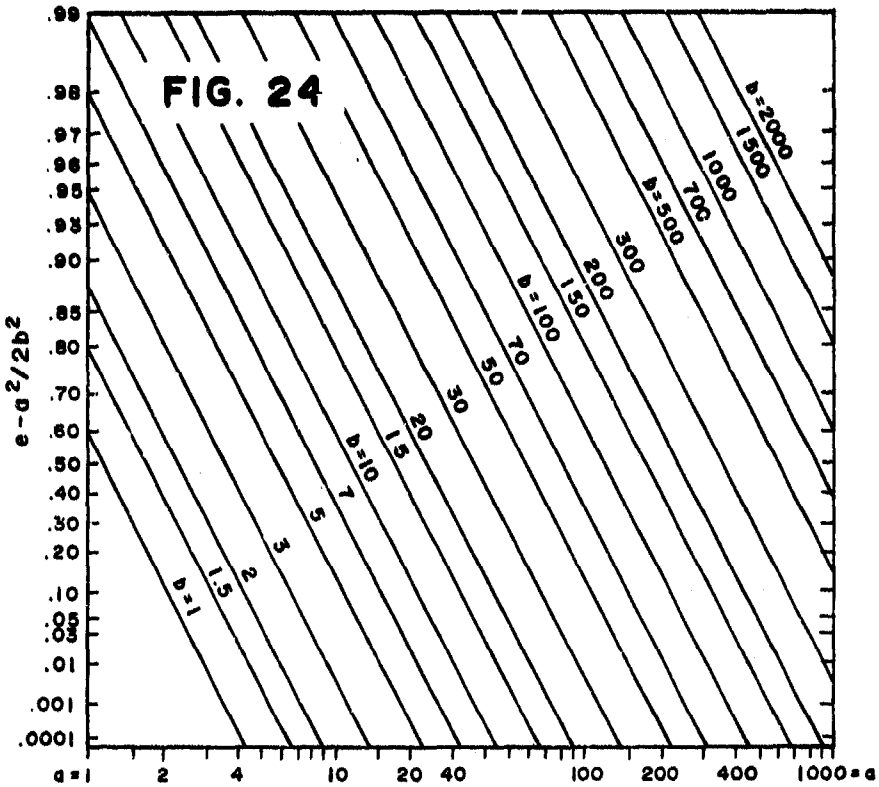
FIG. 24
$e^{-a^2/2b^2}$
.99
.98
.97
.96
.95
.93
.90
.85
.80
.70
.60
.50
.40
.30
.20
.10
.05
.03
.01
.001
.0001
b=1
1.5
2
3
5
7
b=10
15
20
30
50
70
b=100
150
200
300
b=500
700
1000
1500
b=2000
a=1
2
4
10
20
40
100
200
400
1000=a

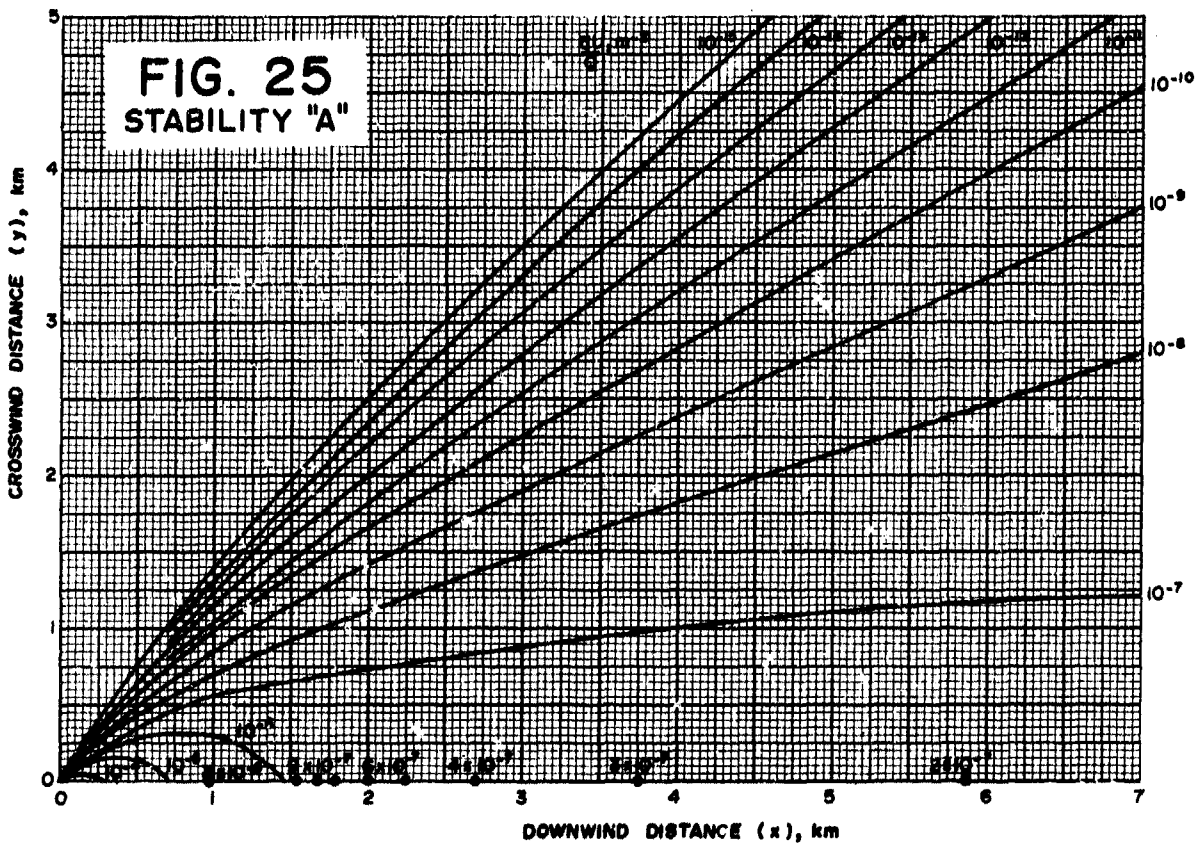
FIG. 25
STABILITY "A"
CROSSWIND DISTANCE (y), km
DOWNWIND DISTANCE (x), km
0
1
2
3
4
5
6
7
10^{-10}
10^{-9}
10^{-8}
10^{-7}

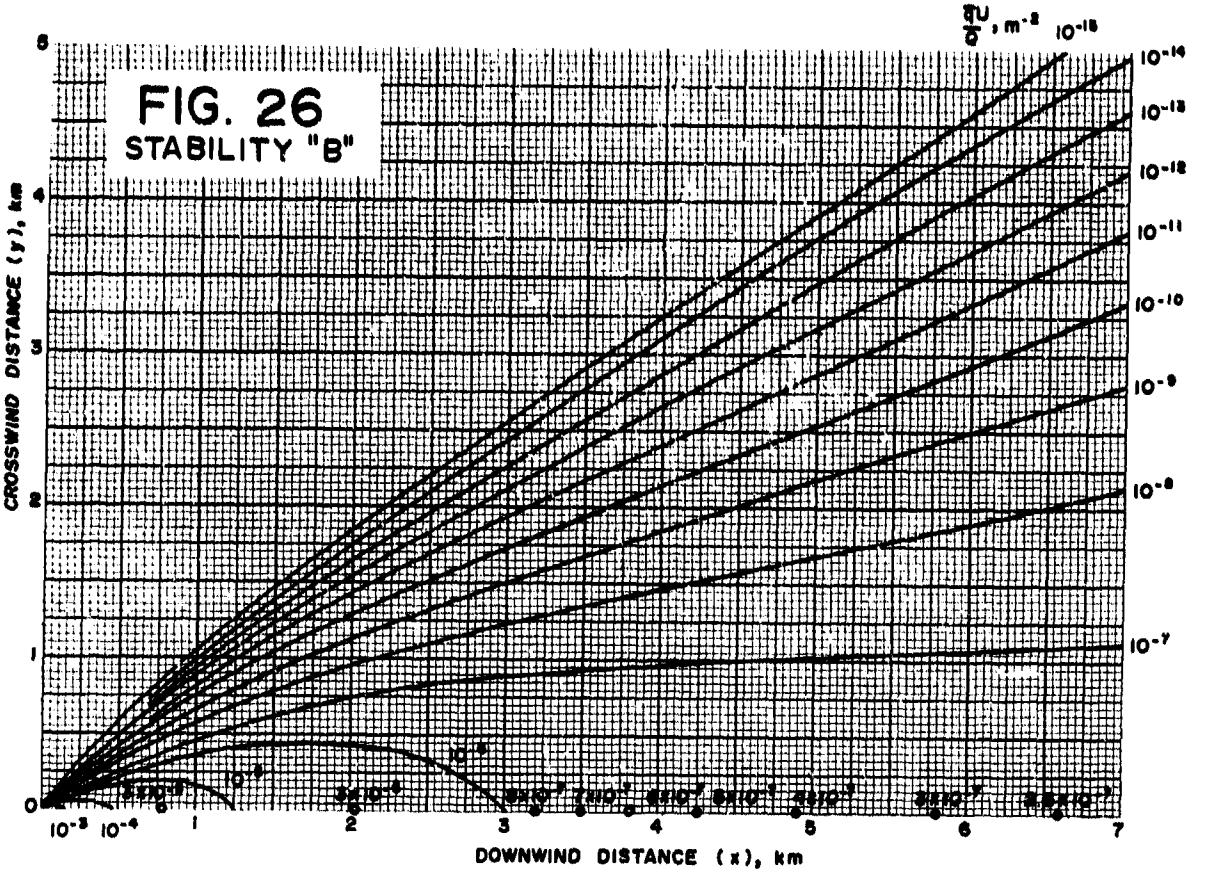
FIG. 26
STABILITY "B"
CROSSWIND DISTANCE (y), km
DOWNWIND DISTANCE (x), km
$\frac{qU}{Q}$, m^{-2}
10^{-15}
10^{-14}
10^{-13}
10^{-12}
10^{-11}
10^{-10}
10^{-9}
10^{-8}
10^{-7}

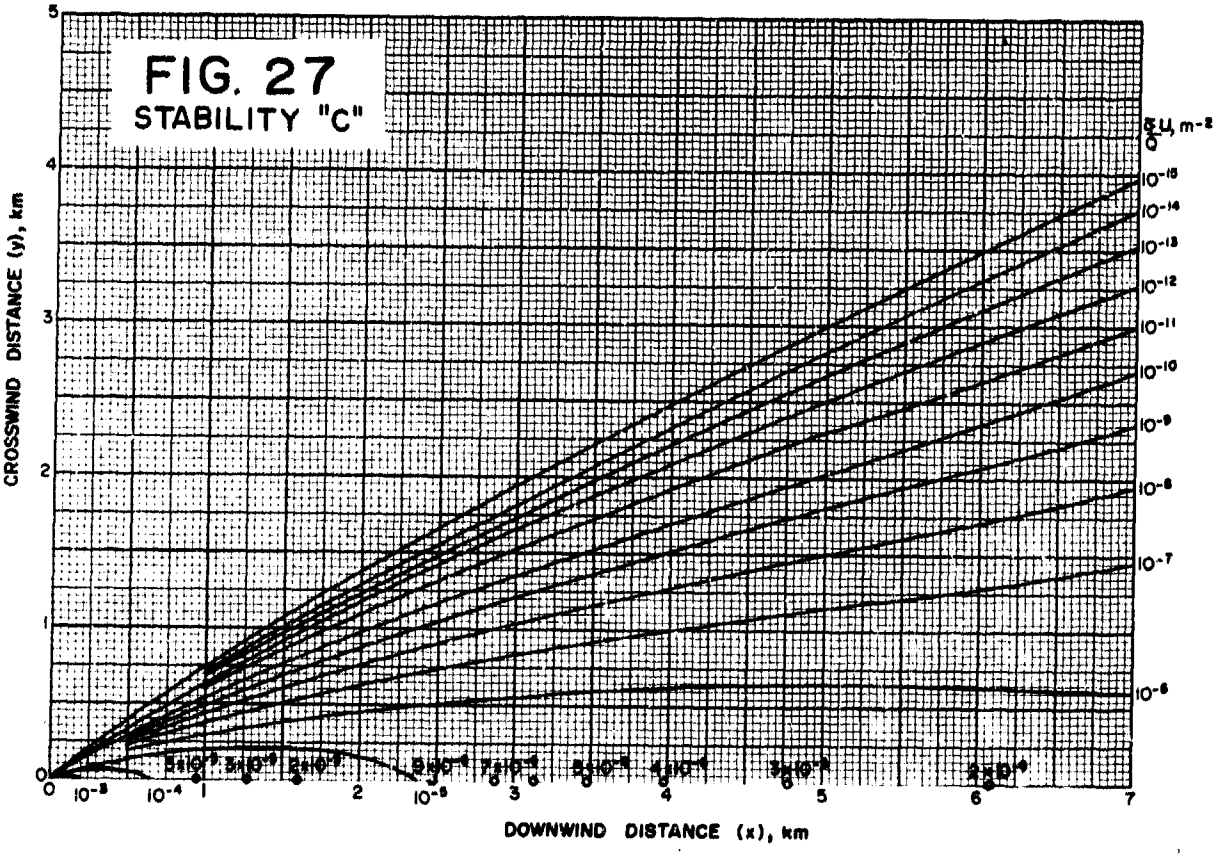
FIG. 27
STABILITY "C"
CROSSWIND DISTANCE (y), km
DOWNWIND DISTANCE (x), km
$\frac{qU}{Q}$, m^{-2}
10^{-15}
10^{-14}
10^{-13}
10^{-12}
10^{-11}
10^{-10}
10^{-9}
10^{-8}
10^{-7}
10^{-6}

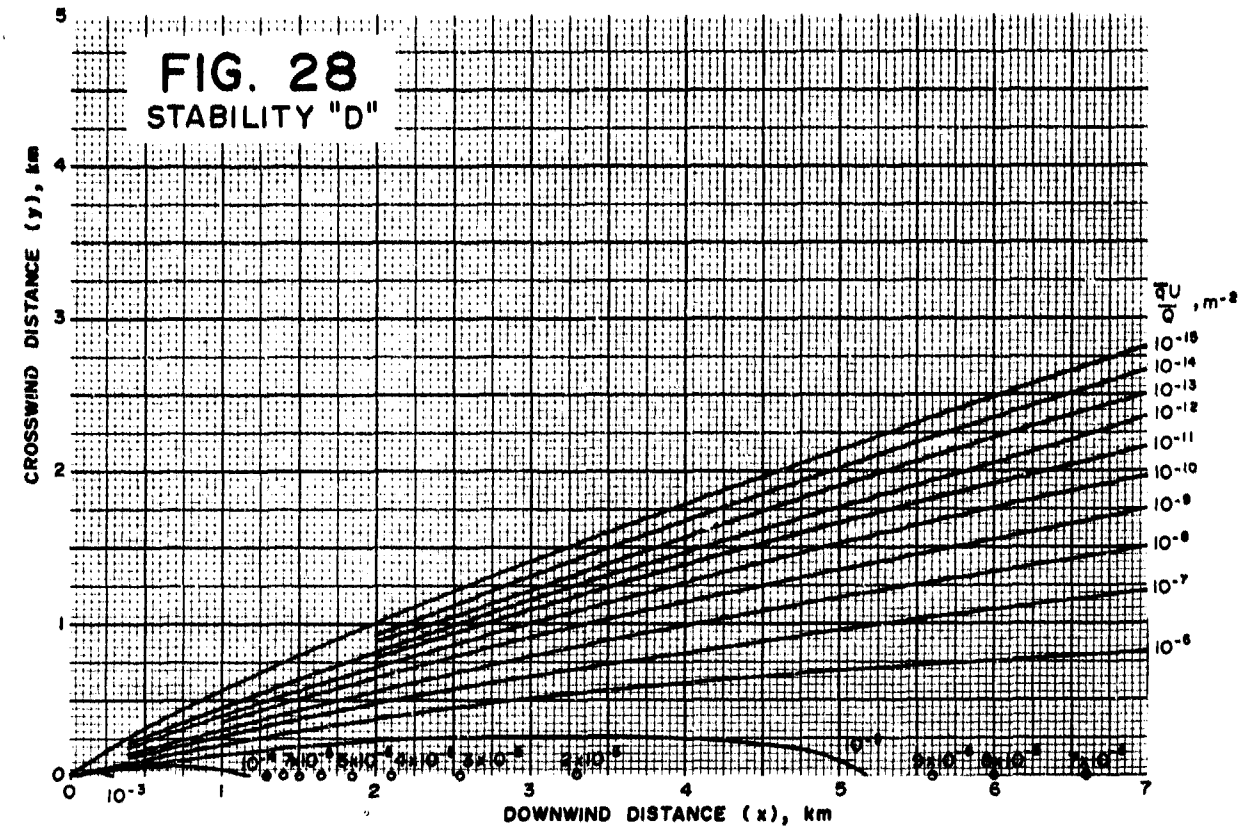
FIG. 28
STABILITY "D"
CROSSWIND DISTANCE (y), km
DOWNWIND DISTANCE (x), km
$\frac{Q}{\bar{q}U}$, m⁻²

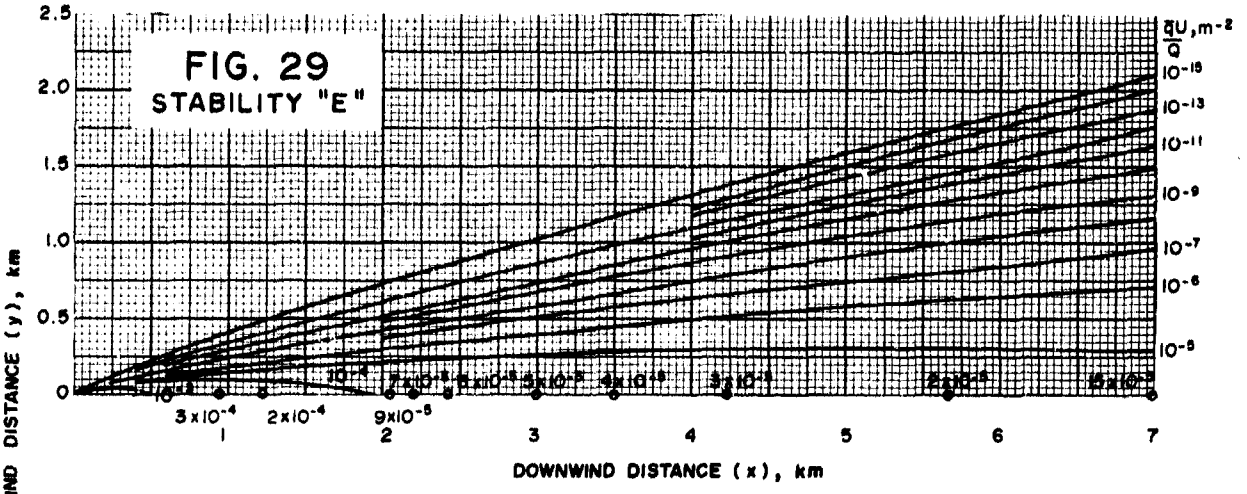
FIG. 29
STABILITY "E"
CROSSWIND DISTANCE (y), km
DOWNWIND DISTANCE (x), km
$\frac{Q}{\bar{q}U}$, m⁻²

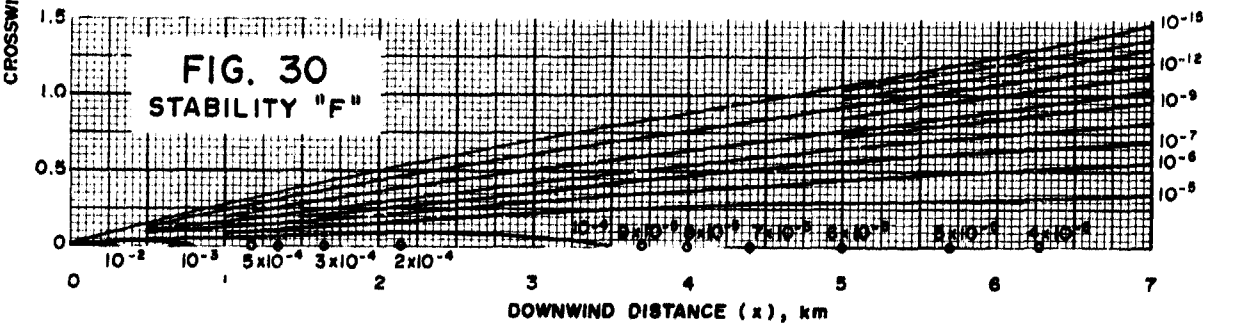
FIG. 30
STABILITY "F"
CROSSWIND DISTANCE (y), km
DOWNWIND DISTANCE (x), km

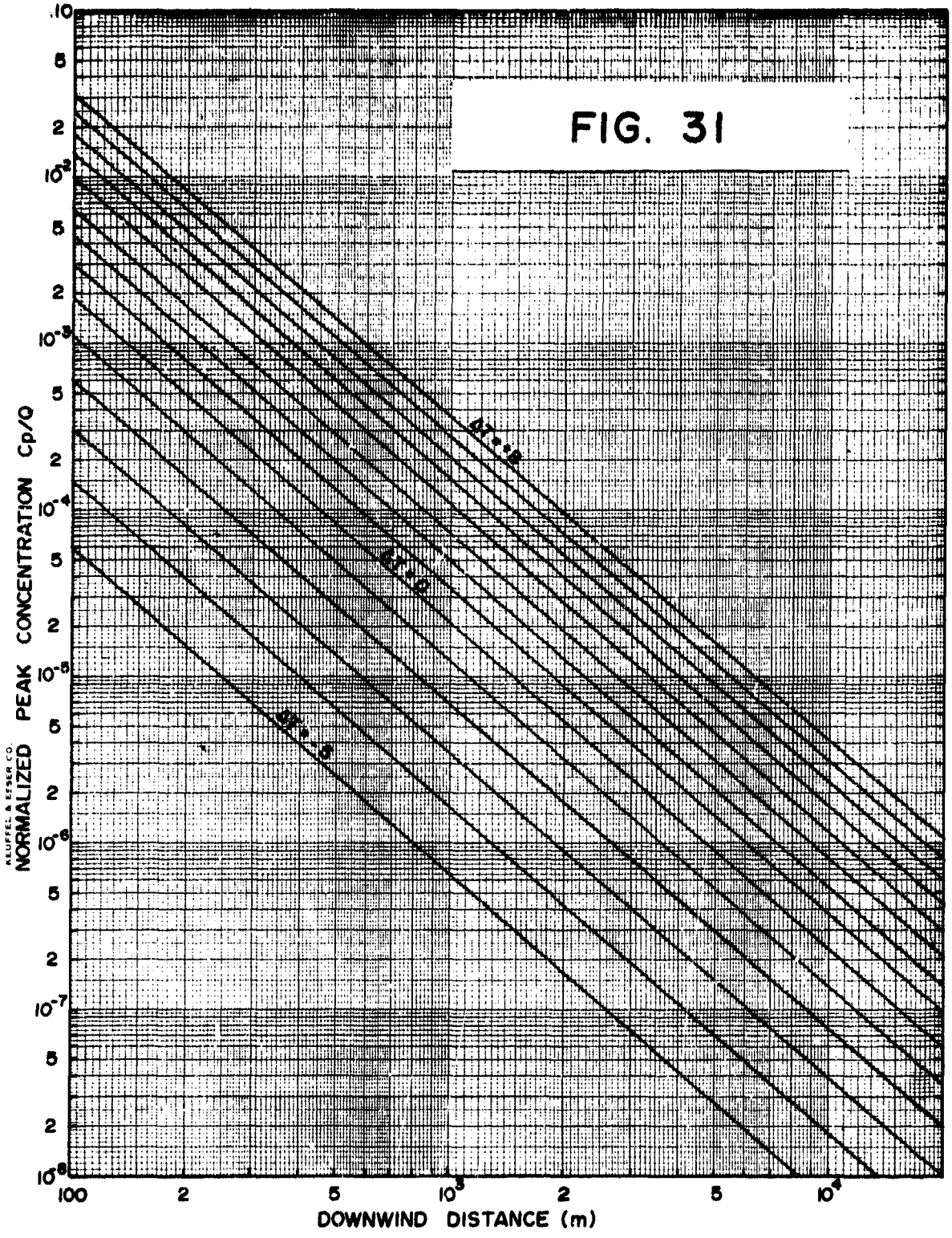
FIG. 31
NORMALIZED PEAK CONCENTRATION Cp/Q
KEUFFEL & ESSER CO.
.10
5
2
10^{-2}
5
2
10^{-3}
5
2
10^{-4}
5
2
10^{-5}
5
2
10^{-6}
5
2
10^{-7}
5
2
10^{-8}
100
2
5
10^{3}
2
5
10^{4}
DOWNWIND DISTANCE (m)

FIG. 32

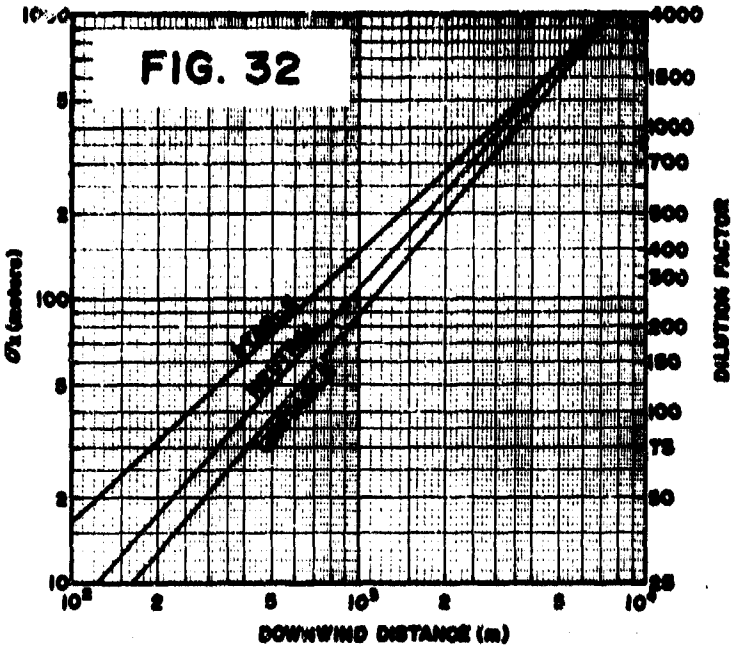
DOWNWIND DISTANCE (m)
DILUTION FACTOR

FIG. 33

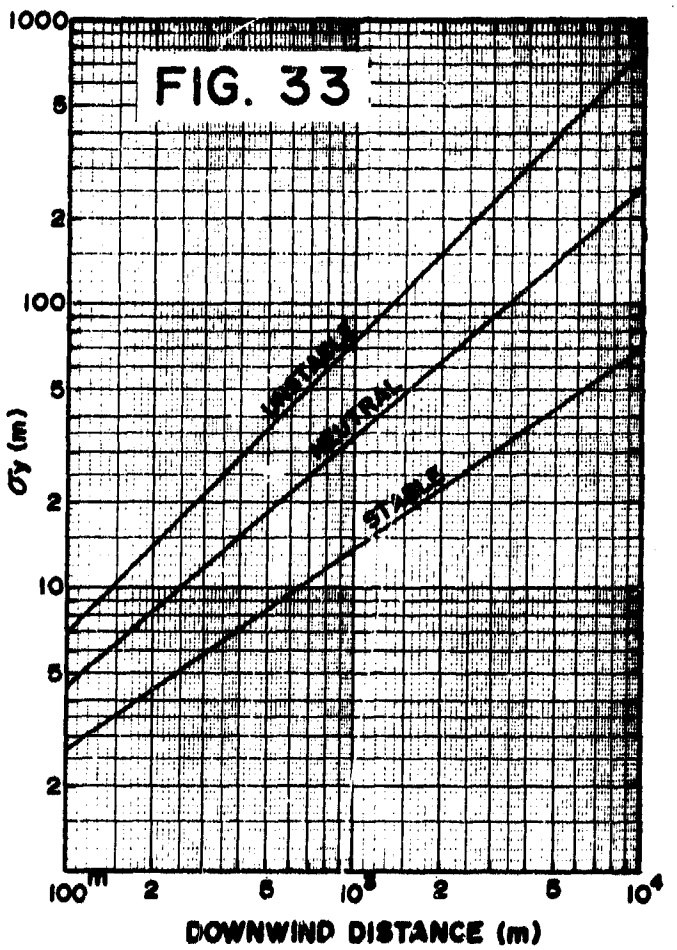
σy (m)
UNSTABLE
NEUTRAL
STABLE
DOWNWIND DISTANCE (m)

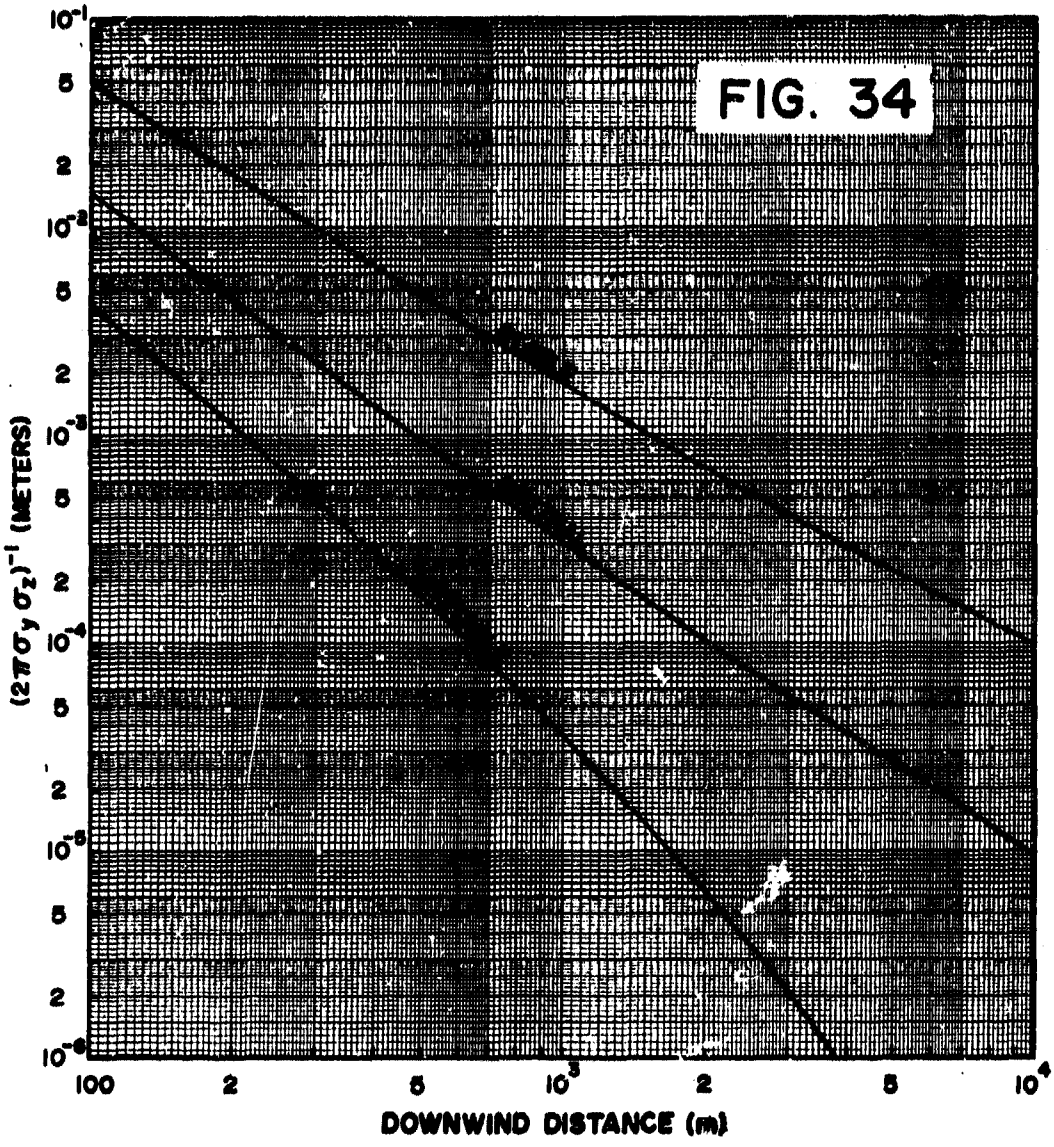
FIG. 34
10^{-1}
5
2
10^{-2}
5
2
10^{-3}
5
2
10^{-4}
5
2
10^{-5}
5
2
10^{-6}
$(2\pi\sigma_y\sigma_z)^{-1}$ (METERS)
100
2
5
10^3
2
5
10^4
DOWNWIND DISTANCE (m)

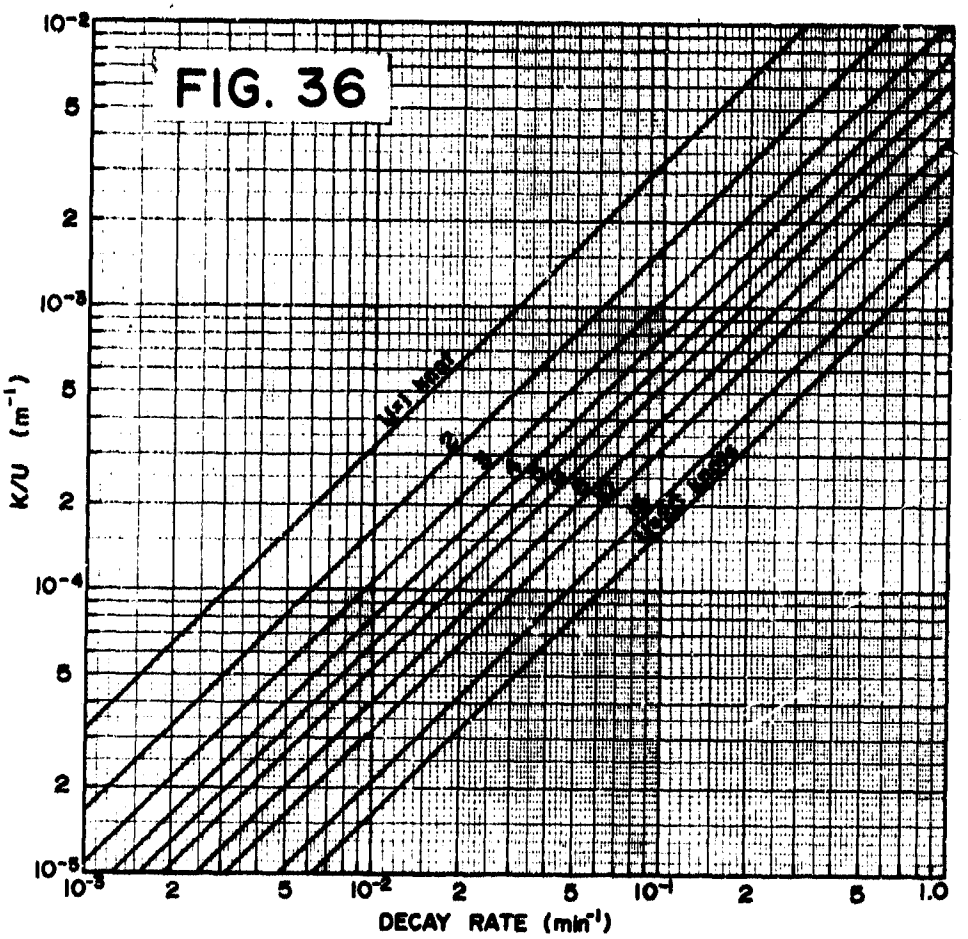
FIG. 36
K/U (m⁻¹)
DECAY RATE (min⁻¹)
10⁻²
5
2
10⁻³
5
2
10⁻⁴
5
2
10⁻⁵
10⁻³
2
5
10⁻²
2
5
10⁻¹
2
5
1.0

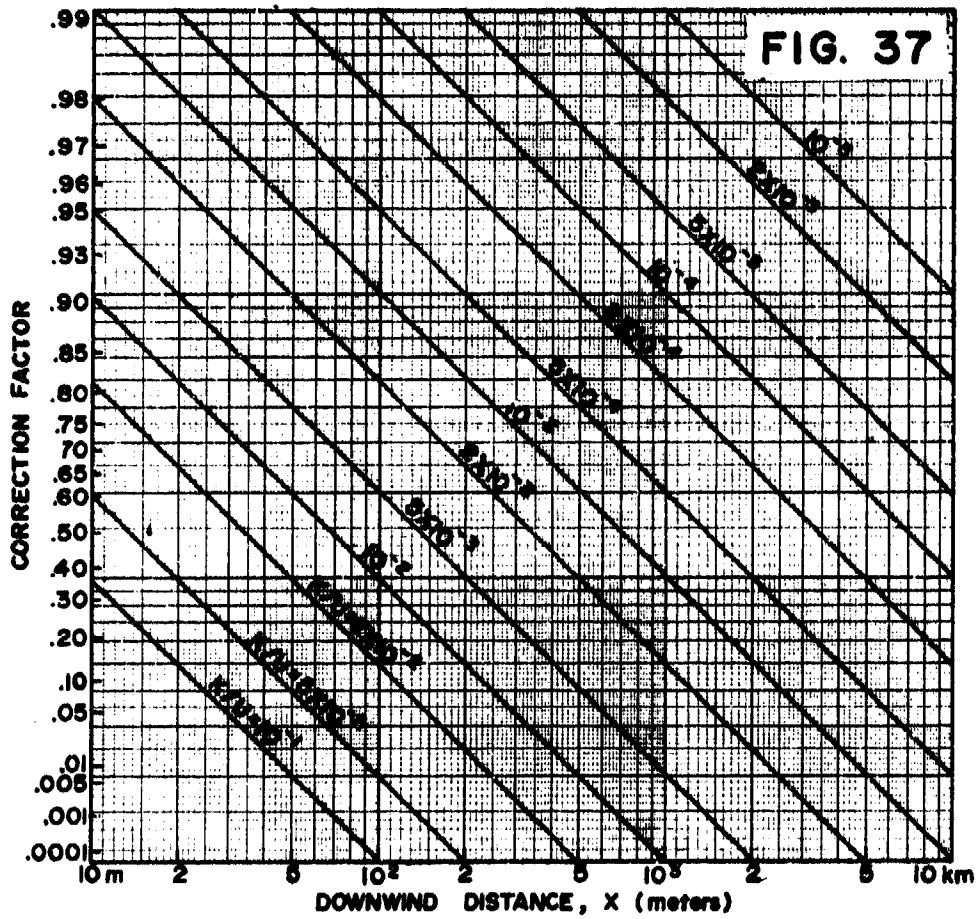
FIG. 37
CORRECTION FACTOR
.99
.98
.97
.96
.95
.93
.90
.85
.80
.75
.70
.65
.60
.50
.40
.30
.20
.10
.05
.01
.005
.001
.0001
10 m
2
5
10²
2
5
10³
2
5
10 km
DOWNWIND DISTANCE, X (meters)

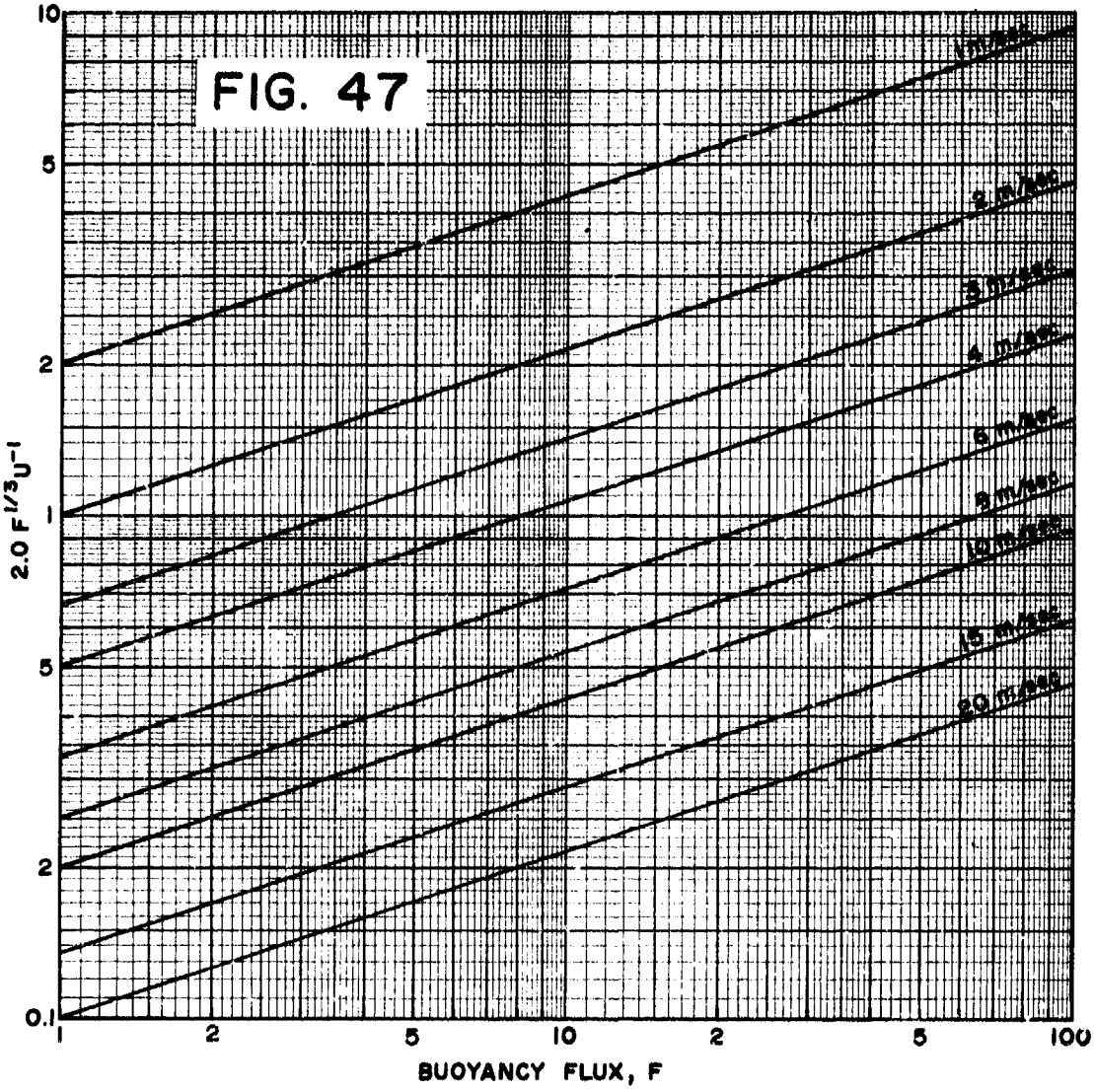
FIG. 47
10
5
2
1
5
2
0.1
$2.0\,F^{1/3}U^{-1}$
1
2
5
10
2
5
100
BUOYANCY FLUX, F
1 m/sec
2 m/sec
3 m/sec
4 m/sec
5 m/sec
8 m/sec
10 m/sec
15 m/sec
20 m/sec

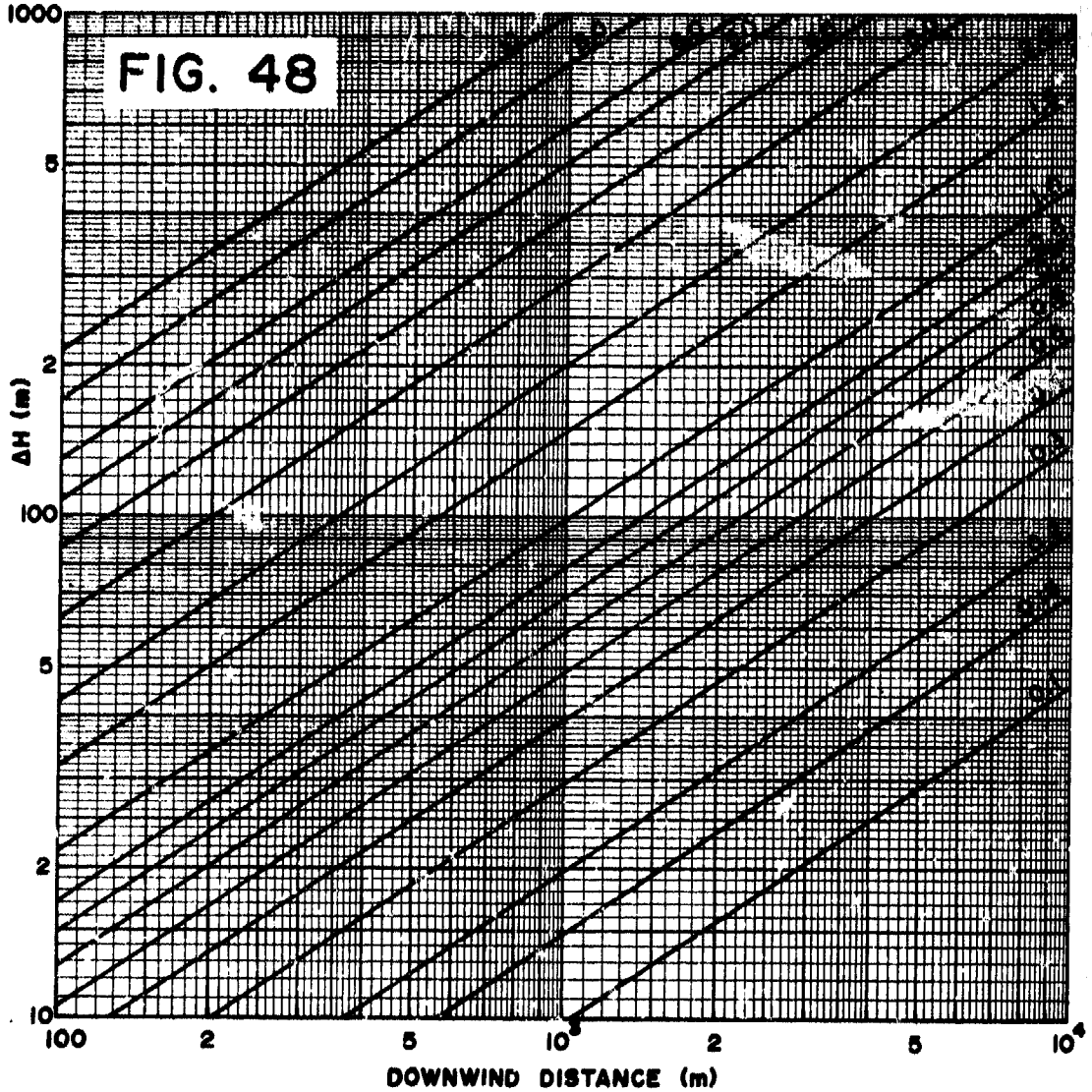
FIG. 48
1000
5
2
100
5
2
10
ΔH (m)
100
2
5
10³
2
5
10⁴
DOWNWIND DISTANCE (m)

REFERENCES

[1] Angell, J. K. and Pack, D. H.: "Mesoscale Diffusion from Tetroon Flights," in: Proceedings of the USAEC Meteorological Information Meeting, Chalk River, Ontario, Canada, September 11-14, 1967, pp. 241-251.

[2] Blackadar, A. K.: "A Single Layer Theory of the Vertical Distribution of Wind in a Baroclinic Neutral Atmospheric Boundary Layer," in: Flux of Heat and Momentum in the Planetary Boundary Layer of the Atmosphere, Report No. AFCRL-65-531, Air Force Cambridge Research Laboratories, Bedford, MA, 1965, pp. 1-22.

[3] Cramer, H. E.: "A Practical Method for Estimating the Dispersal of Atmospheric Contaminants," Proc. 1st National Conference on Applied Meteor., Amer. Meteorol. Soc., Hartford, CT, 1957, pp. C-33 to C-55.

[4] Davenport, A. G.: "The Relationship of Wind Structure to Wind Loading." Paper presented at Int. Conf. on The Wind Effects on Buildings and Structures, 26-28 June 1963, National Physical Laboratory, Teddington, Middlesex, England.

[5] DeMarrais, G. and Islitzer, N. F.: "Diffusion Climatology of the National Reactor Testing Station," USAEC Report IDO-12015, U.S. Weather Bureau, Idaho Falls, ID, 1960.

[6] Geiger, R.: The Climate Near the Ground, Harvard University Press, Cambridge, MA, 1950.

[7] Gifford, F.: "Use of Routine Meteorological Observations for Estimating Atmospheric Dispersion," Nuclear Safety, Vol. 2, No. 4, 1961, pp. 47-51.

[8] Hart, W. S.: "Predictions of the Terminal Altitude and Size of Large Buoyant Clouds Generated by Rocket Launches," Report No. TR-0066(5115-10)-1, The Aerospace Corporation, El Segundo, CA.

[9] Haug[illegible] and Taylor, J. (Eds.): The Ocean Breeze and Dry Gulch Diffusio[illegible] Vol. II, Report AFCRL-63-791, Air Force Cambridge Research Laboratori[illegible], December 1963, 100 p.

[10] Hilbers, C. E.: "Titan II Toxic Service Strength Studies (U)." Unpublished report prepared by Space Technology Laboratories, Inc. re: 6110-8141-MC-000. 15 February 1963 (CONFIDENTIAL).

[11] Hinds, W. T. and Nickola, P. W.: The Mountain Iron Diffusion Program: Phase 1, South Vandenberg: Vol. II, Air Force Western Test Range Technical Report 67-1, 1968.

[12] Holland, J. Z.: "A Meteorological Survey of the Oak Ridge Area," U.S. Atomic Energy Commission Report ORO-99, Washington, DC, 1953, p. 549.

[13] Howerton, A. E.: "Estimating the Area Affected by a Chlorine Release," Paper presented at the Symposium on Loss Prevention in the Process Industries, New Orleans, LA, 16-20 March 1969. American Institute of Chemical Engineers, New York, NY, 1969.

[14] Kaimal, J. C. and Haugen, D. A.: "Characteristics of Vertical Velocity Fluctuations Observed on a 430-Meter Tower," Quart. J. Roy. Meteorol. Soc., Vol. 93, 1967, pp. 305-317.

[15] Miller, R. L. and Miller, F. H.: "Diffusion Forecasting for Titan II Operations," AWS Technical Report 176, Hq Air Weather Service, Scott AFB, IL, 1964.

[16] Panofsky, A. A. and McCormick, R. A.: "Properties of Spectra of Atmospheric Turbulence at 100 Meters," Quart. J. Roy. Meteorol. Soc., Vol. 80, 1954, pp. 546-564.

[17] Pasquill, F.: "The Estimation of the Dispersion of Windborne Material," Meteorological Mag., Vol. 90, No. 1063, February 1961, pp. 33-49.

[18] Pasquill, F.: Atmospheric Diffusion, Van Nostrand, London, 1962.

[19] Singer, I. A. and Raynor, G. S.: "Analysis of Meteorological Tower Data April 1950-March 1952," USAEC Report BNL-461, Brookhaven National Laboratory, 1957.

[20] Slade, D. H. (Ed.): Meteorology and Atomic Energy, 1968, Atomic Energy Commission, Washington, DC, 1968.

[21] Smith, F. B.: "The Rule of Wind Shear in Horizontal Diffusion of Ambient Particles," Quart. J. Roy. Meteorol. Soc., Vol. 91, 1965, pp. 318-329.

[22] Sutton, O. G.: Micrometeorology, McGraw-Hill Book Co., Inc., New York, 1953, 297 p.

[23] Taylor, G. I.: "Diffusion by Continuous Movements," Proc. London Math. Soc., Vol. 20, 1921, pp. 196-202.

[24] Taylor, J. H. (Ed.): "Project Sand Storm, An Experimental Program in Atmospheric Diffusion," Environmental Research Papers, No. 134, Report AFCRL-65-649, Air Force Cambridge Research Laboratories, 1965.

[25] Thayer, S. D., Koch, R. C., and Milly, G. H.: Further Developments in Techniques for Dosage Prediction, Vol. I, 1968, Report TRC 315, The Travelers Research Center, Inc.

[26] Turner, D. B.: Workbook for Atmospheric Dispersion Estimates, U.S. Department of Health, Education and Welfare, Cincinnati, OH, Revised 1969.

[27] U.S. Army Munitions Command Operations Research Group. Unpublished memorandum.

[28] U.S Army Munitions Command Operations Research Group: CB Operations Technical Reference Handbook, Edgewood Arsenal, MD, May 1963.

[29] Vernot, E. H., et al.: "The Air Oxidation of Monomethyl Hydrazine," American Industrial Hygiene Assoc. Journal, Vol. 28, No. 5, 1967, pp. 343-347.

[30] Welker, J. R., Wesson, H. R., and Sliepcevich, C. M.: "LNG Spills: To Burn or Not to Burn!" Paper presented at the Distribution Conference (Operating Section), Philadelphia, PA, 12-15 May 1969. American Gas Association, Inc.

UNCLASSIFIED
Security Classification

DOCUMENT CONTROL DATA - R & D

(Security classification of title, body of abstract and indexing annotation must be entered when the overall report is classified)

1. ORIGINATING ACTIVITY *(Corporate author)*
Hq Air Weather Service
Scott Air Force Base, IL 62225

2a. REPORT SECURITY CLASSIFICATION
Unclassified

2b. GROUP
N/A

3. REPORT TITLE
A Guide to Local Dispersion of Air Pollutants

4. DESCRIPTIVE NOTES *(Type of report and inclusive dates)*
N/A

5. AUTHOR(S) *(First name, middle initial, last name)*
Gordon A. Beals, Major, USAF

6. REPORT DATE	7a. TOTAL NO. OF PAGES	7b. NO. OF REFS
April 1971	83	30

8a. CONTRACT OR GRANT NO.	9a. ORIGINATOR'S REPORT NUMBER(S)
N/A b. PROJECT NO.	Air Weather Service Technical Report 214
c.	9b. OTHER REPORT NO(S) *(Any other numbers that may be assigned this report)*
d.	

10. DISTRIBUTION STATEMENT
Approved for public release; distribution unlimited.

11. SUPPLEMENTARY NOTES	12. SPONSORING MILITARY ACTIVITY
N/A	Hq Air Weather Service (MAC) Scott AFB IL 62225

13. ABSTRACT

This report is intended as a guide on local air pollution for forecasters who have had no prior experience with diffusion. Certain fundamentals of micrometeorology and diffusion in the lower layers are expounded and their relation to the determination of air pollutant dispersion and concentration amounts is explained. Calculations of pollutant concentrations using accepted techniques are systematically discussed and solution of actual air pollution problems are shown in the Appendix. Graphs and nomograms used in solving air pollution problems are also furnished in the Appendix.

DD FORM 1 NOV 68 1473

UNCLASSIFIED
Security Classification

MAC-8 AFB, IL 71-18206